Experimental studies of Generalised Parton Distributions

Daria Sokhan
University of Glasgow, UK

26th International Symposium on Spin Physics (SPIN 2025)
Qingdao, China – 22nd September 2025

A constructivist view of the nucleon

Wigner distributions

$$\rho(x, \vec{k}_T, \vec{b}_T)$$

"phase space" distributions of partons in a nucleon

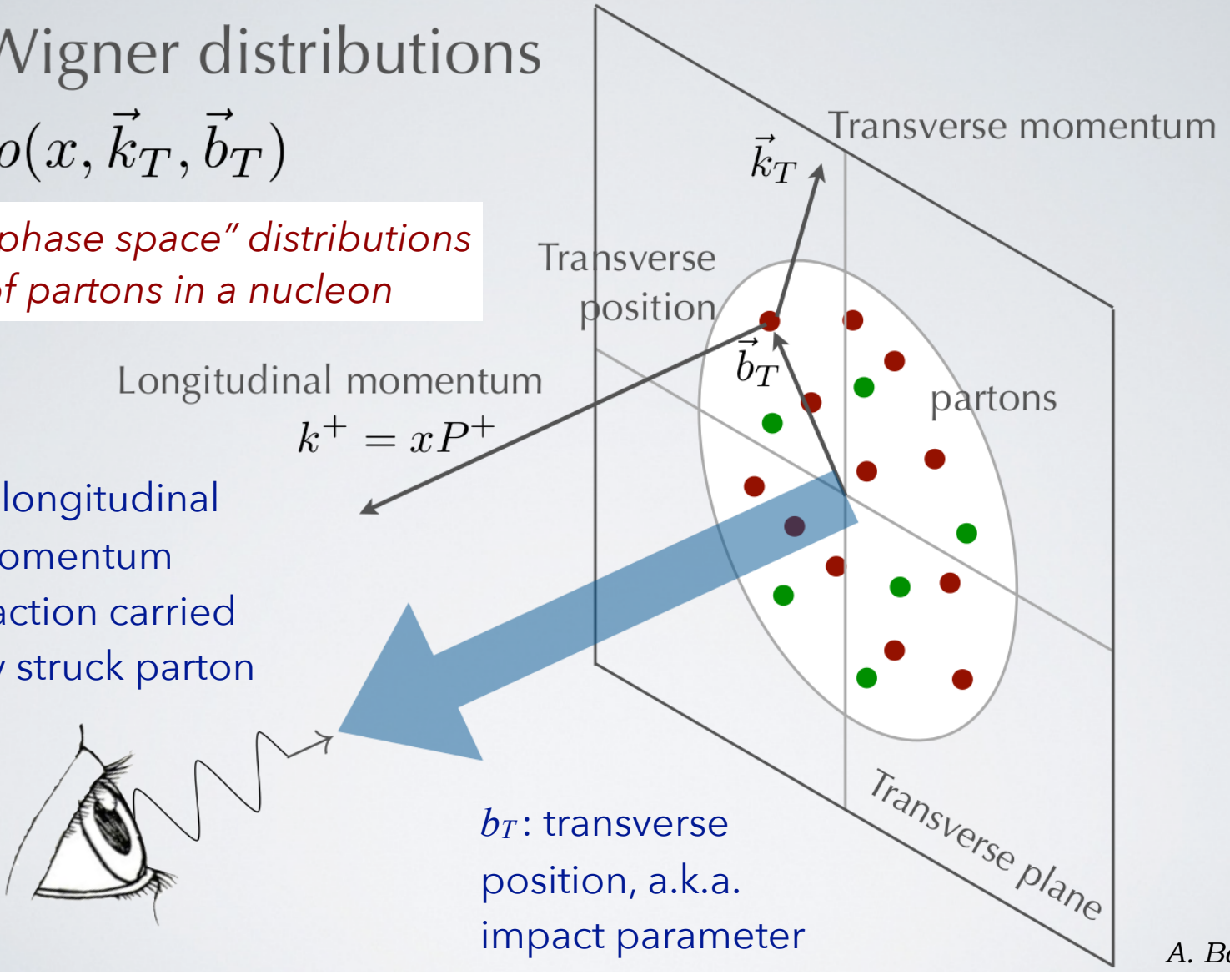

x: longitudinal momentum fraction carried by struck parton

b_T: transverse position, a.k.a. impact parameter

A. Bacchetta

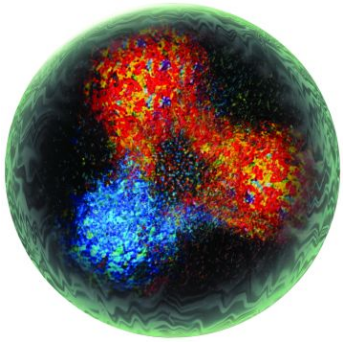

Wigner function: full phase space parton distribution of the nucleon

Generalised Transverse Momentum Distributions (GTMDs)

Possible access via exclusive di-jet production or exclusive π^0-production at high Q^2.

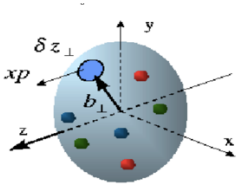

$$\int d^2k_T$$

$$\int d^2b_T$$

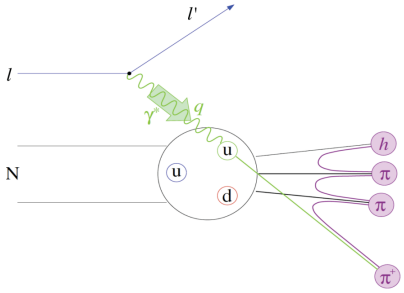

Generalised Parton Distributions (GPDs)

Exclusive processes

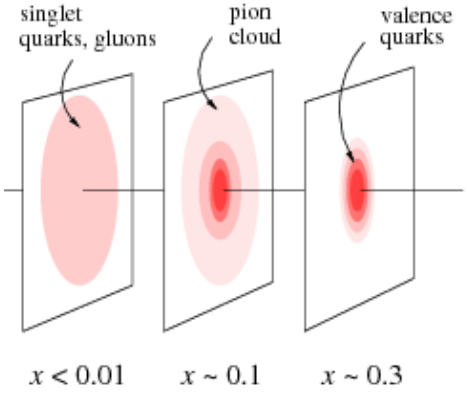

Transverse Momentum-Dependent distributions (TMDs)

Semi-inclusive DIS (SIDIS)

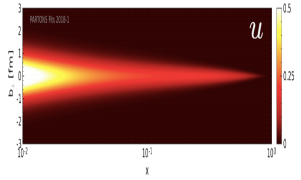

$$\int dx$$

$$\int d^2k_T$$

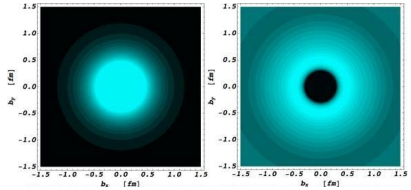

Form Factors

Elastic scattering

Parton Distribution Functions (PDFs)

Deep Inelastic Scattering (DIS)

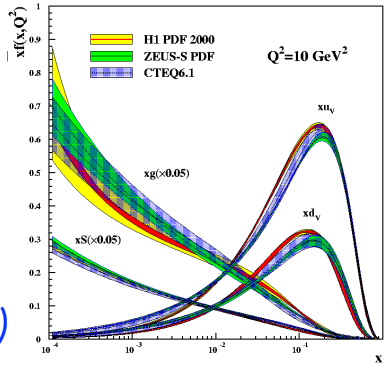

Generalised Parton Distributions

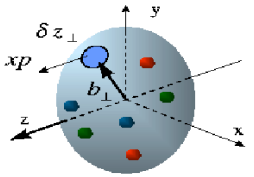

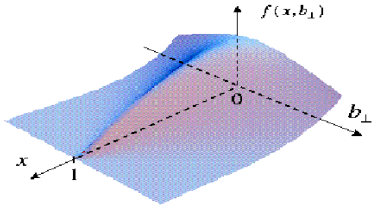

- proposed by Müller (1994), Radyushkin, Ji (1997).
- can be interpreted as relating, in the infinite momentum frame, transverse position of partons (impact parameter $b_\perp$) to longitudinal momentum fraction (x).

* **Tomography** of the nucleon: transverse spatial distributions of quarks and gluons in longitudinal momentum space.

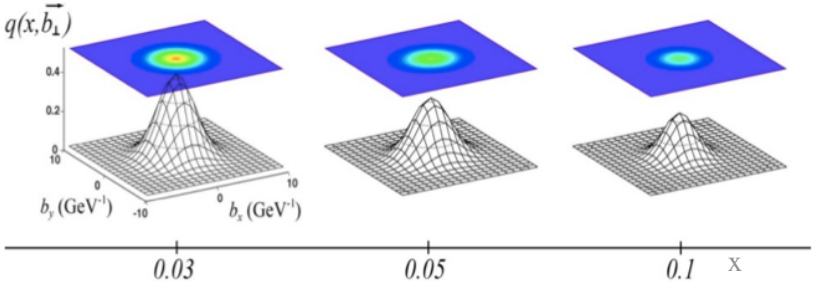

* Indirect access to mechanical properties of the nucleon: possibilities of extracting **pressure distributions** within the nucleon.

* Information on the orbital angular momentum contribution to nucleon spin: **the spin puzzle**.

$$J_N = \frac{1}{2} = \frac{1}{2}\Sigma_q + L_q + J_g$$

Ji's relation:

$$J^q = \frac{1}{2} - J^g$$

$$= \frac{1}{2}\int_{-1}^{1} x dx \left\{ H^q(x,\xi,0) + E^q(x,\xi,0) \right\}$$

GPDs

* Combine with Transverse Momentum Distributions (TMDs) to access **spin-orbit correlations** of quarks and gluons, study non-perturbative interactions of partons.

Generalised Parton Distributions

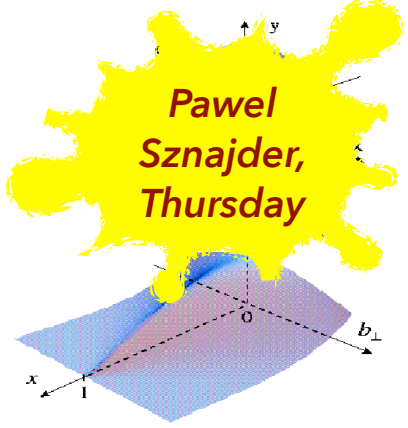

- proposed by Müller (1994), Radyushkin, Ji (1997).
- can be interpreted as relating, in the infinite momentum frame, transverse position of partons (impact parameter $b_\perp$) to longitudinal momentum fraction (x).

* **Tomography** of the nucleon: transverse spatial distributions of quarks and gluons in longitudinal momentum space.

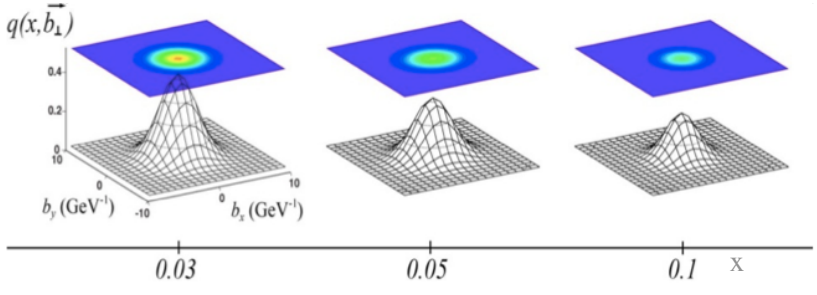

* Indirect access to mechanical properties of the nucleon: possibilities of extracting **pressure distributions** within the nucleon.

* Information on the orbital angular momentum contribution to nucleon spin: **the spin puzzle**.

$$J_N = \frac{1}{2} = \frac{1}{2}\Sigma_q + L_q + J_g$$

Ji's relation:

$$J^q = \frac{1}{2} - J^g$$

$$= \frac{1}{2}\int_{-1}^{1} x dx \left\{ H^q(x,\xi,0) + E^q(x,\xi,0) \right\}$$

GPDs

* Combine with Transverse Momentum Distributions (TMDs) to access **spin-orbit correlations** of quarks and gluons, study non-perturbative interactions of partons.

Experimental access to GPDs

Accessible in *exclusive* processes, where all final state particles are determined, *eg*:

- Deeply Virtual Compton Scattering (DVCS)
- Time-like Compton Scattering (TCS)
- Hard Exclusive Meson Production (HEMP) – a.k.a. Deeply Virtual Meson Production (DVMP)
- Double DVCS
- Certain diffractive processes, eg: diffractive ρ-production with the emission of a meson or virtual photon from the nucleon
- Hard exclusive production of a meson-photon or photon-photon pair
- Charged-current meson production, eg: $ep \to \nu_e \pi^- p$

Relies on *factorisation* of the process amplitude into a hard, perturbative part and the soft non-perturbative part containing GPD information.

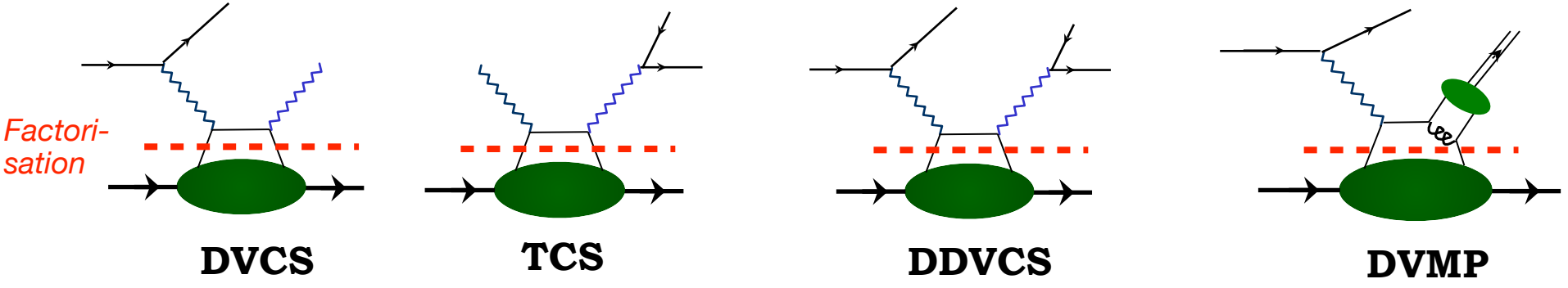

Experimental access to GPDs

Tuesday Rm 9, session 3

Accessible in *exclusive* processes, where all final state particles are detern

- Deeply Virtual Compton Scattering (DVCS)
- Time-like Compton Scattering (TCS)
- Hard Exclusive Meson Production (HEMP) – a.k.a. Deeply Virtual Meson Production (DVMP)
- Double DVCS
- Certain diffractive processes, eg: diffractive ρ-production with the emission of a meson or virtual photon from the nucleon
- Hard exclusive production of a meson-photon or photon-photon pair
- Charged-current meson production, eg: $ep \to \nu_e \pi^- p$

Relies on *factorisation* of the process amplitude into a hard, perturbative part and the soft non-perturbative part containing GPD information.

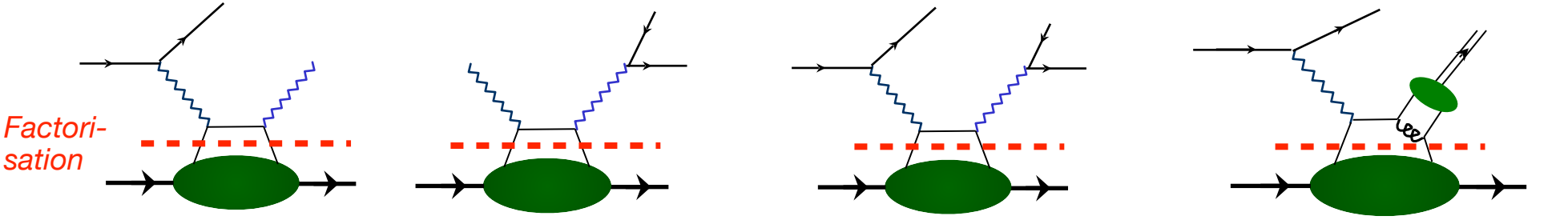

DVCS

Virtual photon space-like

TCS

Virtual photon time-like

DDVCS

One time-like, one space-like virtual photon

DVMP

Virtual photon space-like

Deeply Virtual Compton Scattering

the "golden channel" for GPD extraction

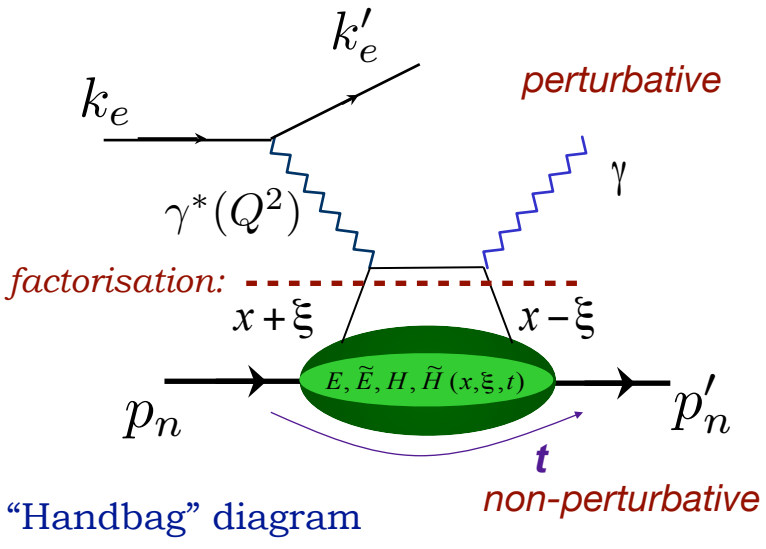

"Handbag" diagram

$$Q^2 = -(\mathbf{k} - \mathbf{k}')^2 \qquad t = (\mathbf{p'_n} - \mathbf{p_n})^2$$

Bjorken variable: $x_B = \dfrac{Q^2}{2\mathbf{p_n}\cdot\mathbf{q}}$

$x \pm \xi$ *longitudinal momentum fractions of the struck parton*

Skewness: $\xi \cong \dfrac{x_B}{2 - x_B}$

- At high exchanged Q^2 and low t access to four parton helicity-conserving, chiral-even GPDs:

$$E^q, \tilde{E}^q, H^q, \tilde{H}^q(x, \xi, t)$$

- Can be related to PDFs:

$$H(x,0,0) = q(x) \qquad \tilde{H}(x,0,0) = \Delta q(x)$$

and form factors:

$$\int_{-1}^{+1} H dx = F_1 \qquad \int_{-1}^{+1} \tilde{H}\, dx = G_A$$

(Dirac and Pauli)

$$\int_{-1}^{+1} E\, dx = F_2 \qquad \int_{-1}^{+1} \tilde{E}\, dx = G_P$$

(axial and pseudo-scalar)

- Small changes in nucleon transverse momentum allows mapping of transverse structure at large distances.

Measuring DVCS

- Process measured in experiment:

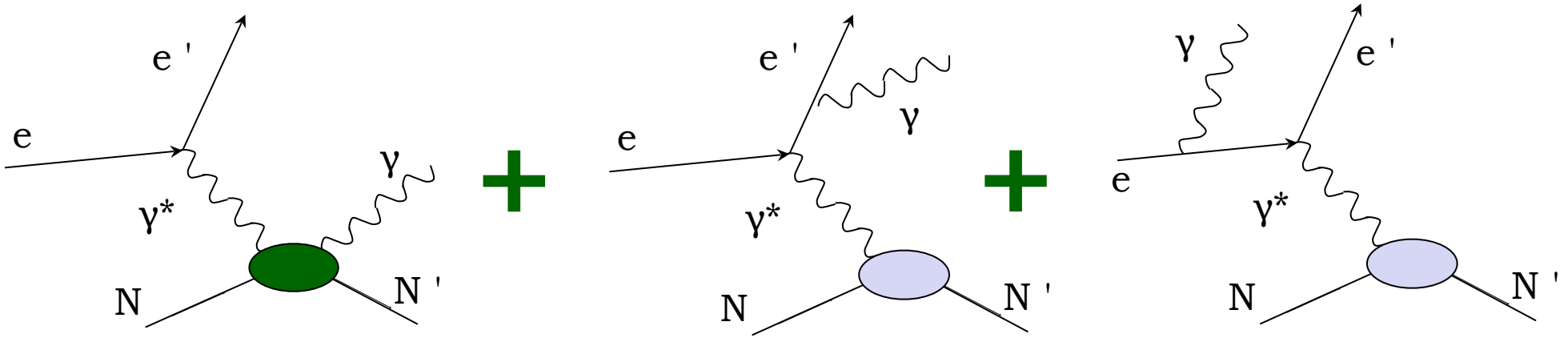

DVCS

Bethe - Heitler

$$d\sigma \propto \left|T_{DVCS}\right|^2 + \left|T_{BH}\right|^2 + T_{BH}T^*_{DVCS} + T_{DVCS}T^*_{BH}$$

Amplitude parameterised in terms of Compton Form Factors

Amplitude calculable from elastic Form Factors and QED

Interference term

$$\left|T_{DVCS}\right|^2 << \left|T_{BH}\right|^2$$

Compton Form Factors in DVCS

Experimentally accessible in DVCS cross-sections and spin or charge asymmetries, eg:

$$A_{LU} = \frac{d\vec{\sigma} - d\overleftarrow{\sigma}}{d\vec{\sigma} + d\overleftarrow{\sigma}} = \frac{\Delta\sigma_{LU}}{d\vec{\sigma} + d\overleftarrow{\sigma}}$$

cross-sections, beam-charge and double polarisation asymmetries

single-spin asymmetries

At leading twist, leading order:

$$T^{DVCS} \sim \int_{-1}^{+1} \frac{GPDs\ (x,\xi,t)}{x \pm \xi + i\varepsilon} dx + \ldots \sim P\int_{-1}^{+1} \frac{GPDs\ (x,\xi,t)}{x \pm \xi} dx \pm i\pi GPDs\ (\pm\xi,\xi,t) + \ldots$$

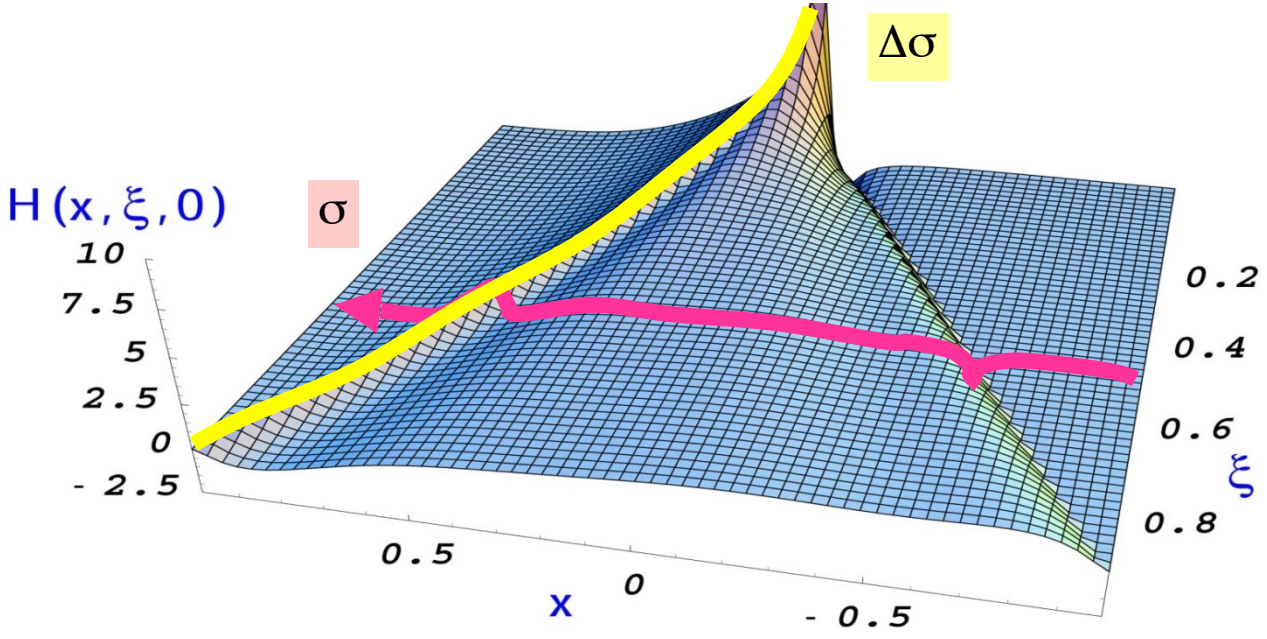

Only ξ and t are accessible experimentally!

To get information on x need extensive measurements in Q^2.

Need measurements off proton and neutron to get flavour separation of CFFs in DVCS.

Nucleon at different resolutions

Nucleon at different scales

Valence quarks

Jefferson Lab: fixed-target electron scattering

$0.1 < x_B < 0.7$

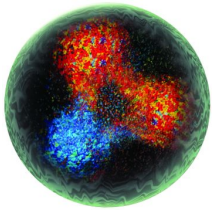

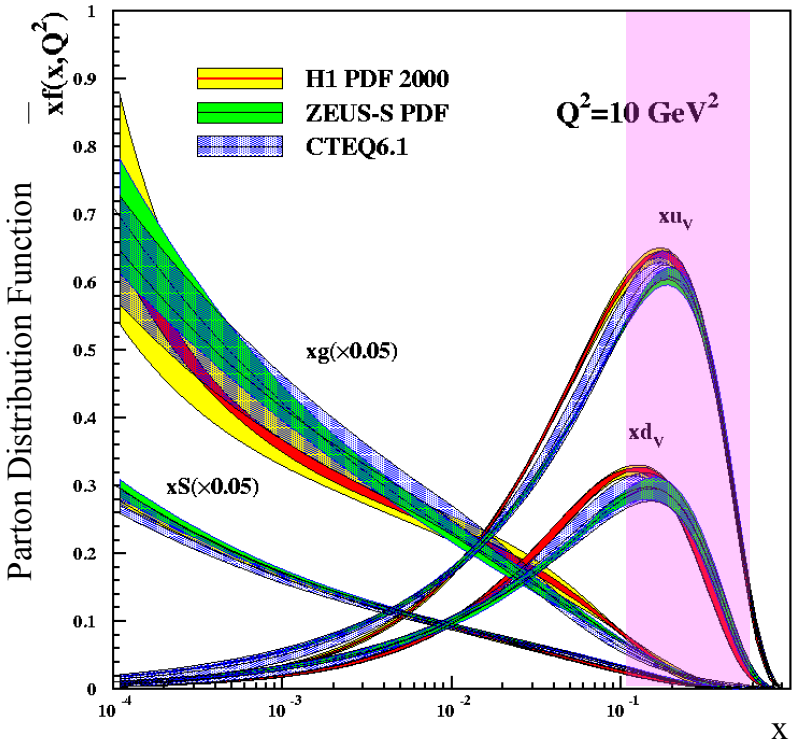

Nucleon at different scales

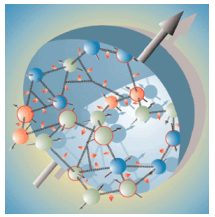

Valence quarks

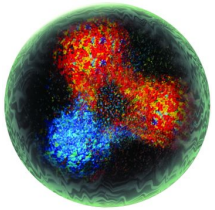

Jefferson Lab: fixed-target electron scattering

$0.1 < x_B < 0.7$

Sea quarks

HERMES: fixed gas-target electron/positron scattering

$0.02 < x_B < 0.3$

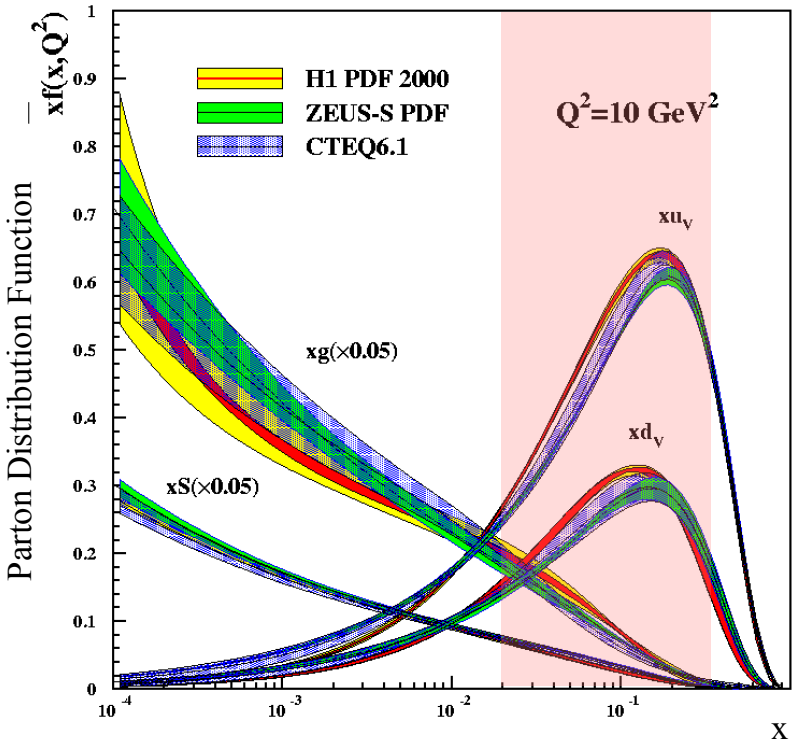

Nucleon at different scales

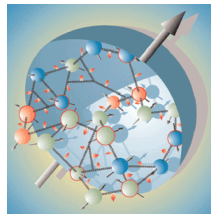

Valence quarks

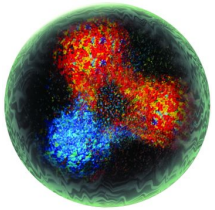

Jefferson Lab: fixed-target electron scattering

$0.1 < x_B < 0.7$

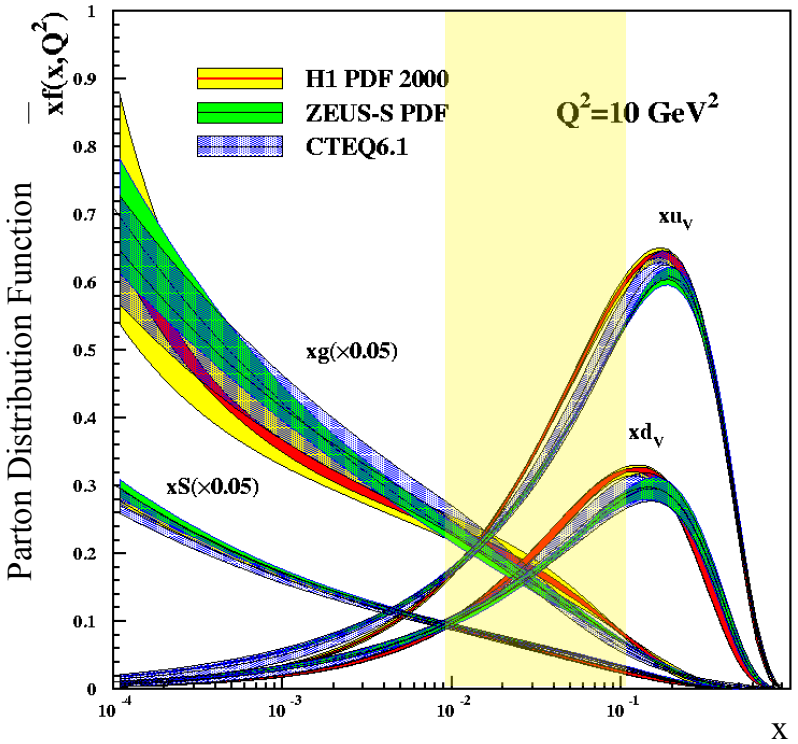

Sea quarks

HERMES: fixed gas-target electron/positron scattering

$0.02 < x_B < 0.3$

COMPASS: fixed-target muon scattering

$0.01 < x_B < 0.1$

Nucleon at different scales

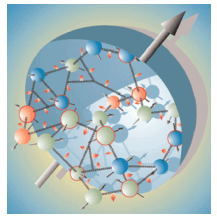

Valence quarks

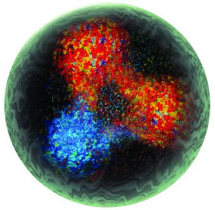

Jefferson Lab: fixed-target electron scattering

$0.1 < x_B < 0.7$

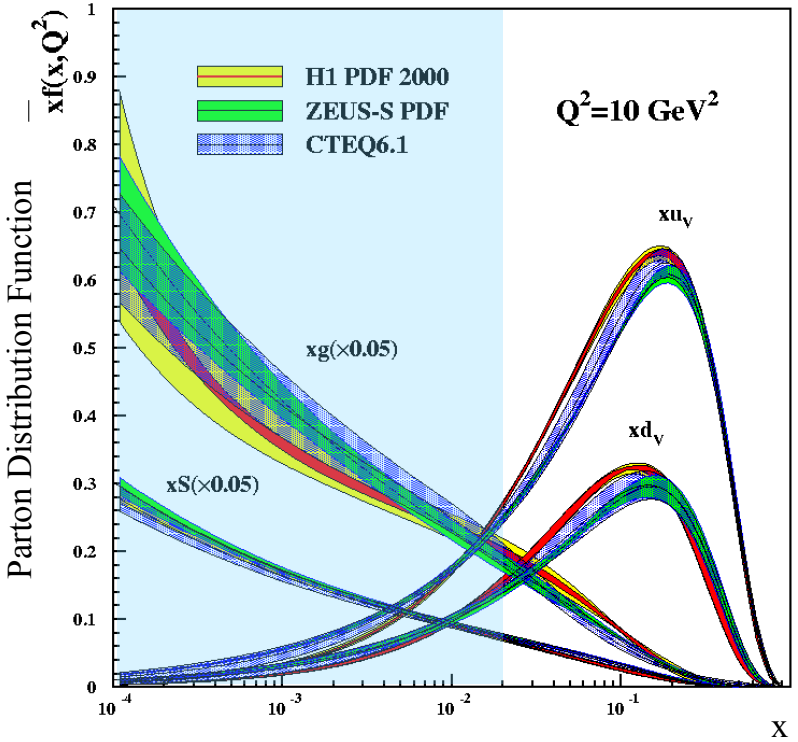

Sea quarks

HERMES: fixed gas-target electron/positron scattering

$0.02 < x_B < 0.3$

COMPASS: fixed-target muon scattering

$0.01 < x_B < 0.1$

The glue

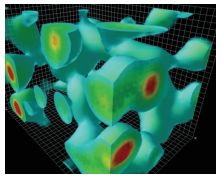

Derek Leinweber

ZEUS/H1: electron/positron-proton collider

$10^{-4} < x_B < 0.02$

Nucleon at different scales

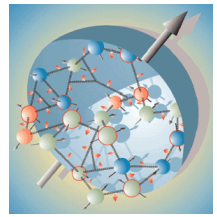

Valence quarks

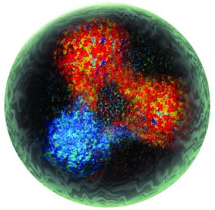

Jefferson Lab: fixed-target electron scattering

$0.1 < x_B < 0.7$

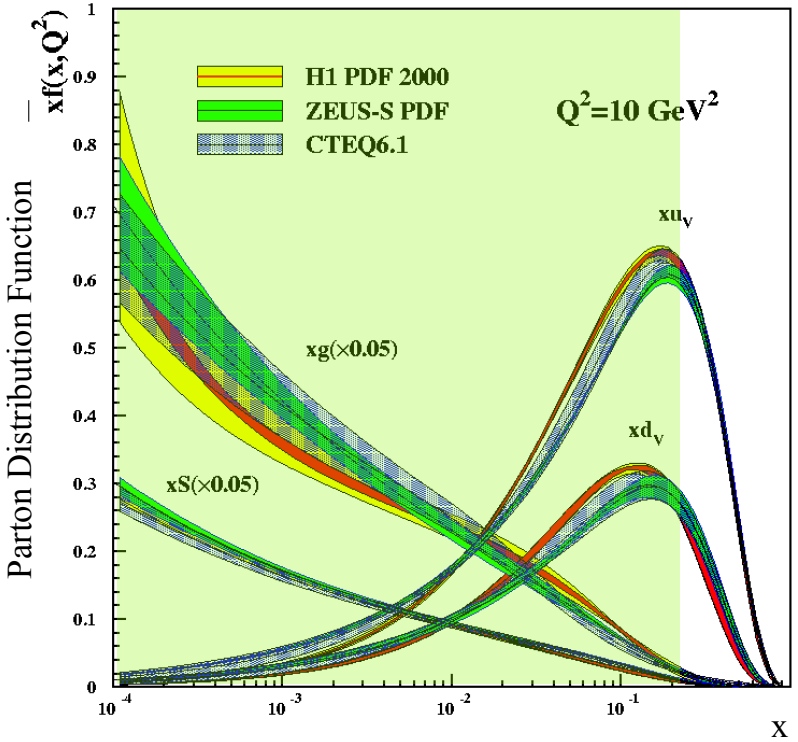

Sea quarks

HERMES: fixed gas-target electron/positron scattering

$0.02 < x_B < 0.3$

COMPASS: fixed-target muon scattering

$0.01 < x_B < 0.1$

The glue

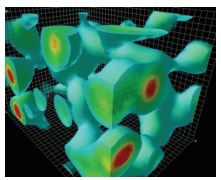

Derek Leinweber

ZEUS/H1: electron/positron-proton collider

$10^{-4} < x_B < 0.02$

EIC: $10^{-4} < x_B < 0.2$

Luminosity 100 - 1000 times that of HERA

Jefferson Lab: valence quarks

JLab @ 12 GeV

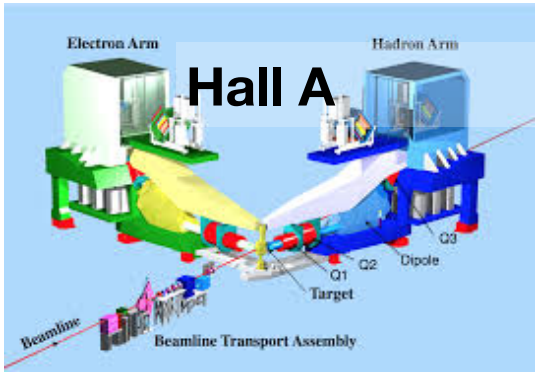

High resolution($\delta p/p = 10^{-4}$) spectrometers, very high luminosity, large installation experiments.

SBS: Super-BigBite Spectrometer

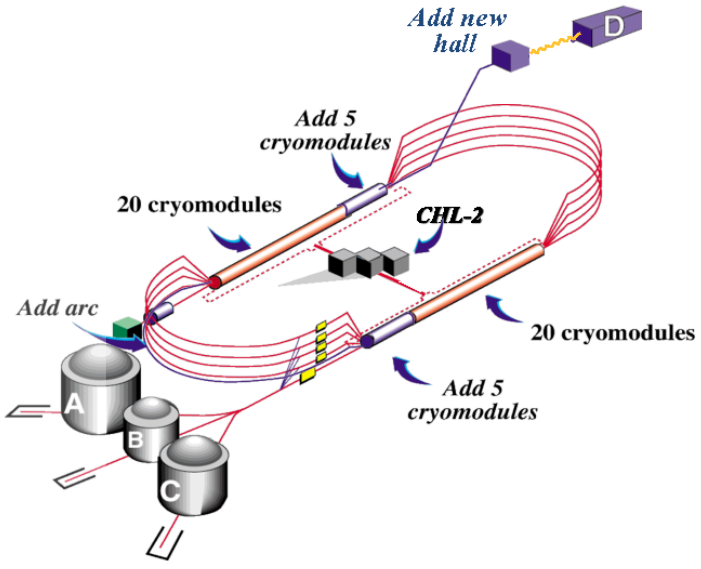

Hall C

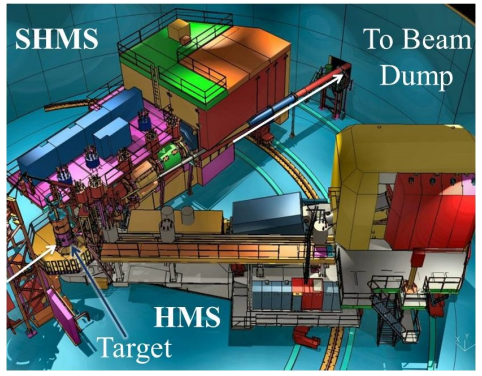

Two movable high momentum spectrometers, well-defined acceptance, very high luminosity.

NPS: Neutral Particle Spectrometer

GlueX

Hall D

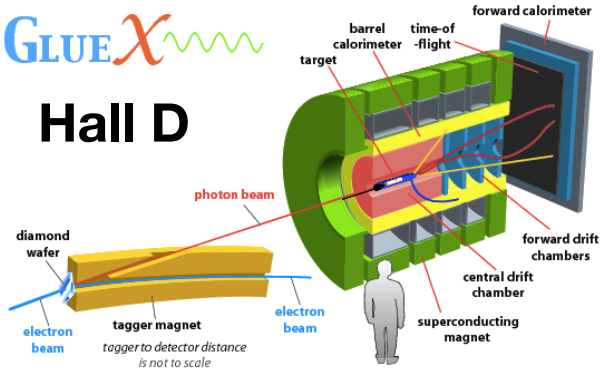

9 GeV tagged polarised photons, full acceptance

Hall B: CLAS12

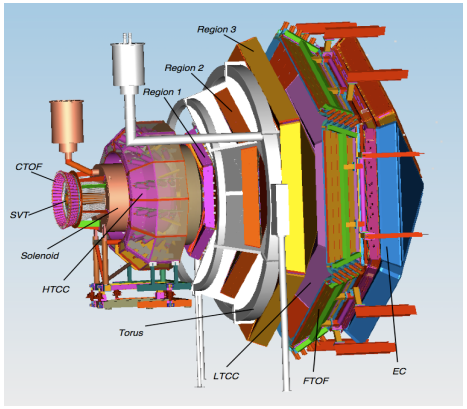

Very large acceptance, high luminosity.

JLab @ 12 GeV

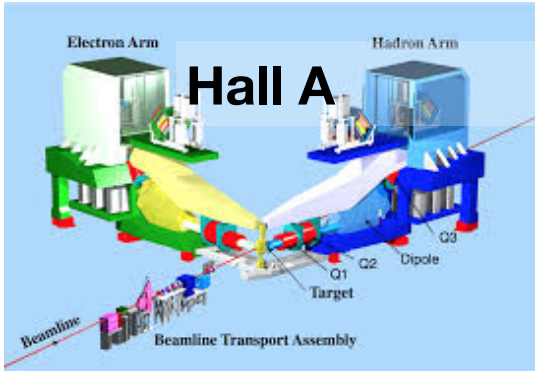

High resolution($\delta p/p = 10^{-4}$) spectrometers, very high luminosity, large installation experiments.

SBS: Super-BigBite Spectrometer

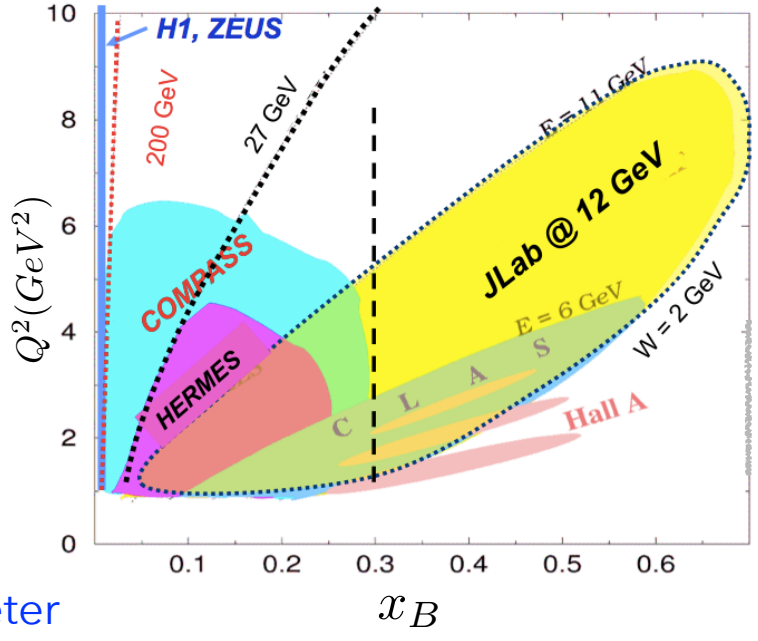

Hall C

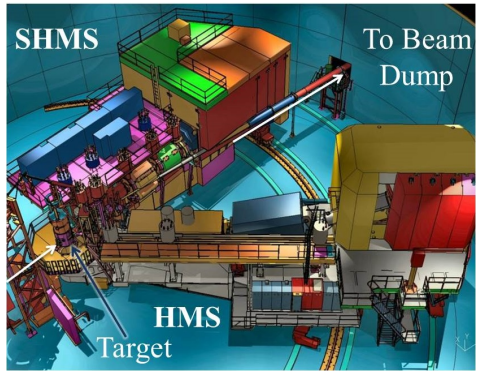

Two movable high momentum spectrometers, well-defined acceptance, very high luminosity.

NPS: Neutral Particle Spectrometer

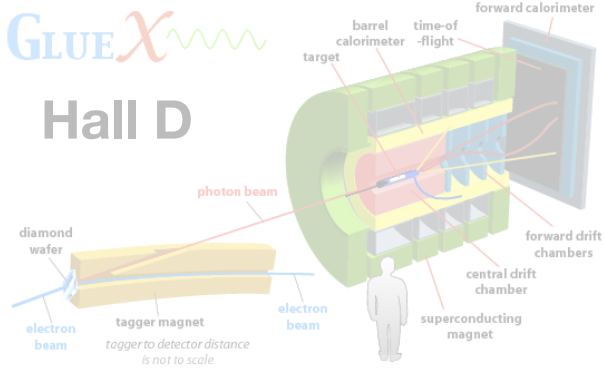

9 GeV tagged polarised photons, full acceptance

Hall B: CLAS12

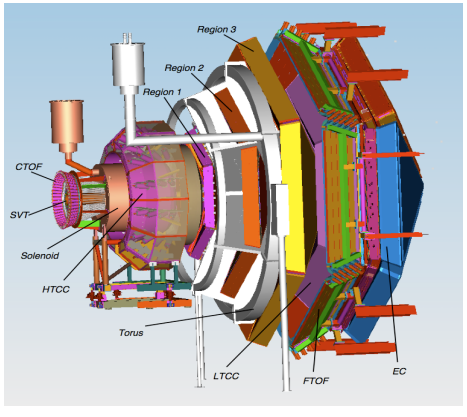

Very large acceptance, high luminosity.

DVCS beam-spin asymmetry

First experiment with CLAS12

Data taken 2018 - 2019

Electron beam energies: 10.2 - 10.6 GeV

Beam polarisation ~ 86%

Liquid H_2 target

Beam-spin asymmetry (BSA)

64 bins in Q^2, x_B and t.

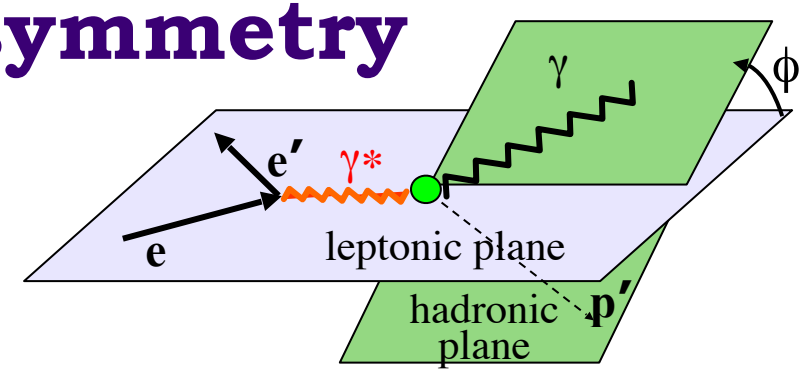

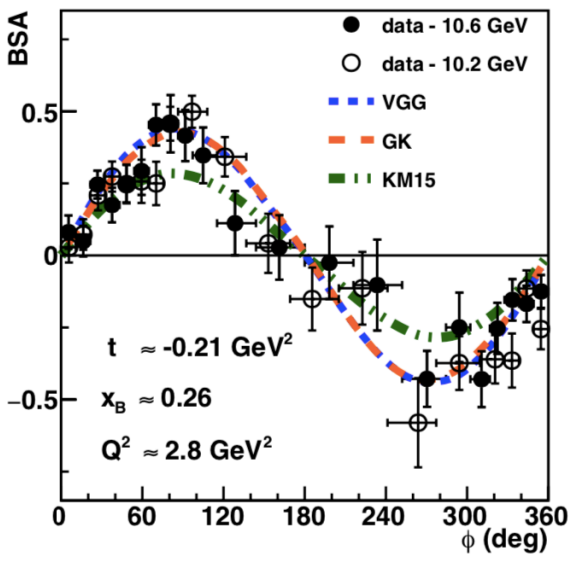

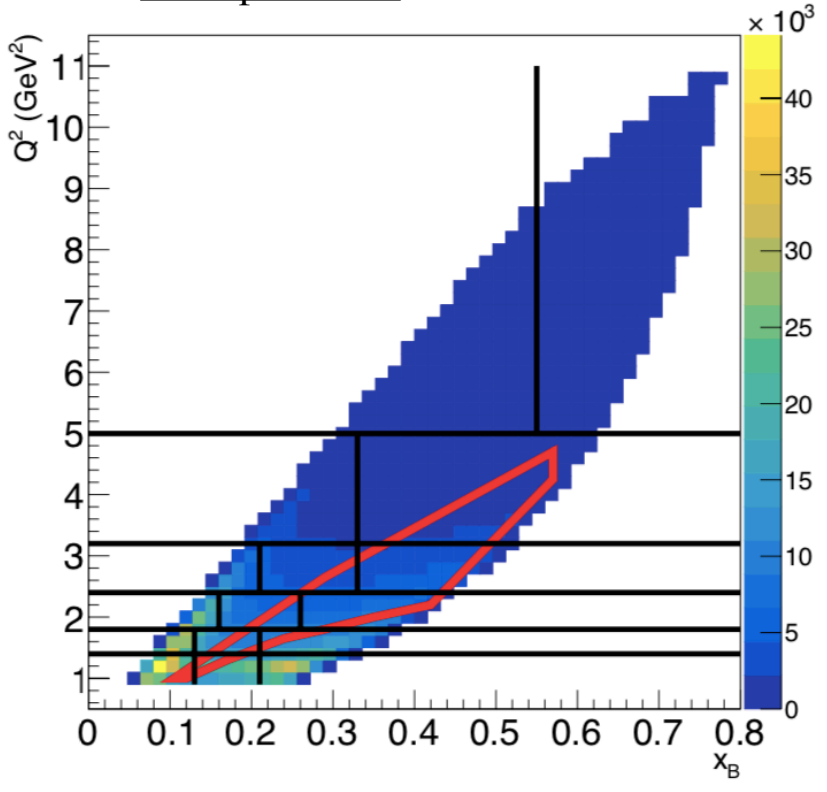

A_{LU} characterised by imaginary parts of CFFs via: $F_1 H + \xi G_M \tilde{H} - \frac{t}{4M^2} E$ → ***Im(H$_p$)***

G. Christiaens *et al.* (CLAS), PRL 130, 211902 (2023)

DVCS Cross-sections: Hall A

Amplitude sensitive to *Re* part of CFF H_p

Rosenbluth-like separation of pure DVCS and Interference terms:

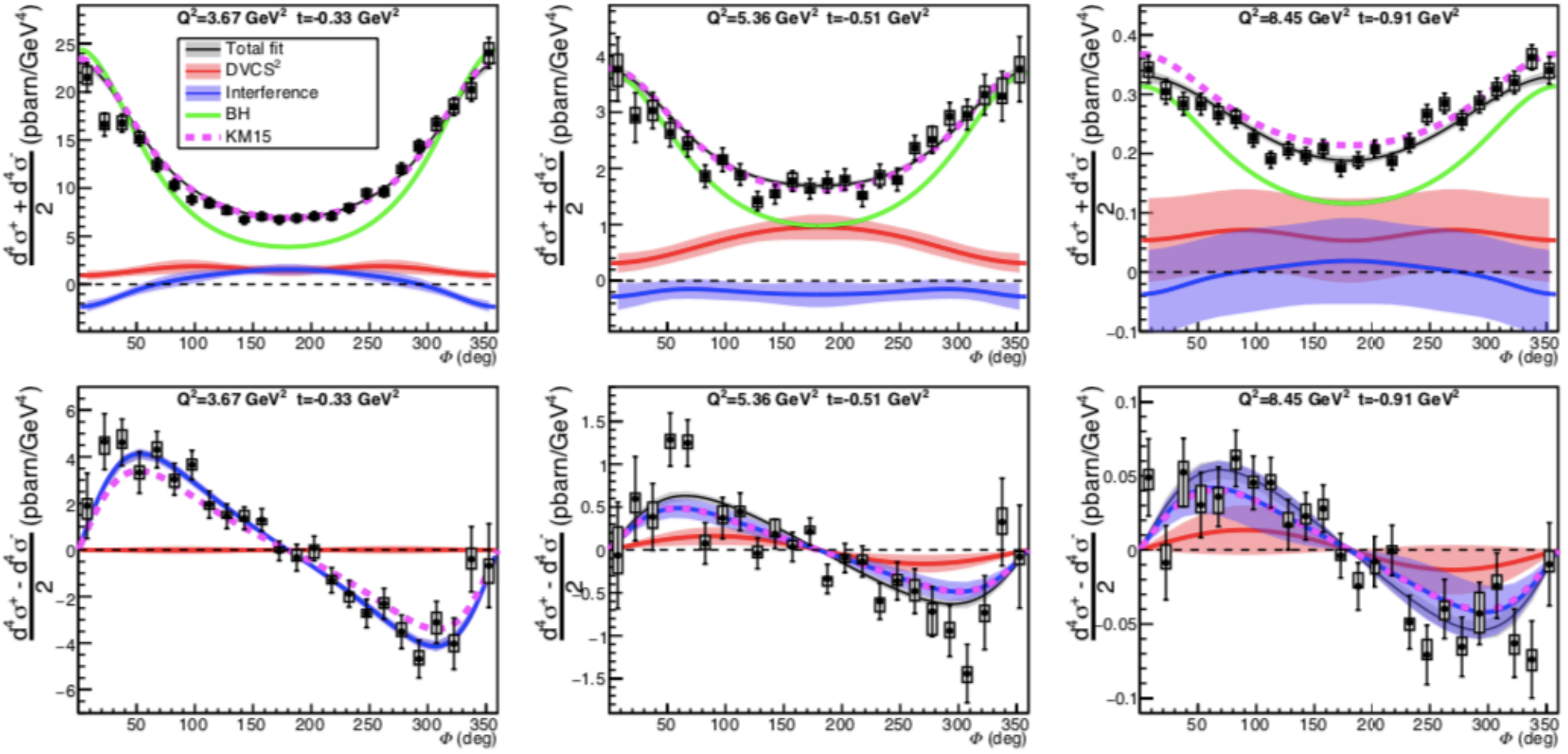

F. Georges *et al.* (Hall A Collaboration), PRL 128, 252002 (2022).

Data: 2014 - 2016

Beam E: 4.5 - 11 GeV

Neutron DVCS beam-spin asymmetry

$$J_N = \frac{1}{2} = \frac{1}{2}\Sigma_q + L_q + J_g$$

Ji's relation: $$J^q = \frac{1}{2} - J^g = \frac{1}{2}\int_{-1}^{1} x dx \left\{ H^q(x,\xi,0) + E^q(x,\xi,0) \right\}$$

Beam-spin asymmetry sensitive to ***Im*(E$_n$):**

$$\Delta\sigma_{LU} \sim \sin\phi\ \mathbf{Im}\{F_1 H + \xi(F_1+F_2)H - kF_2 E\}d\phi$$

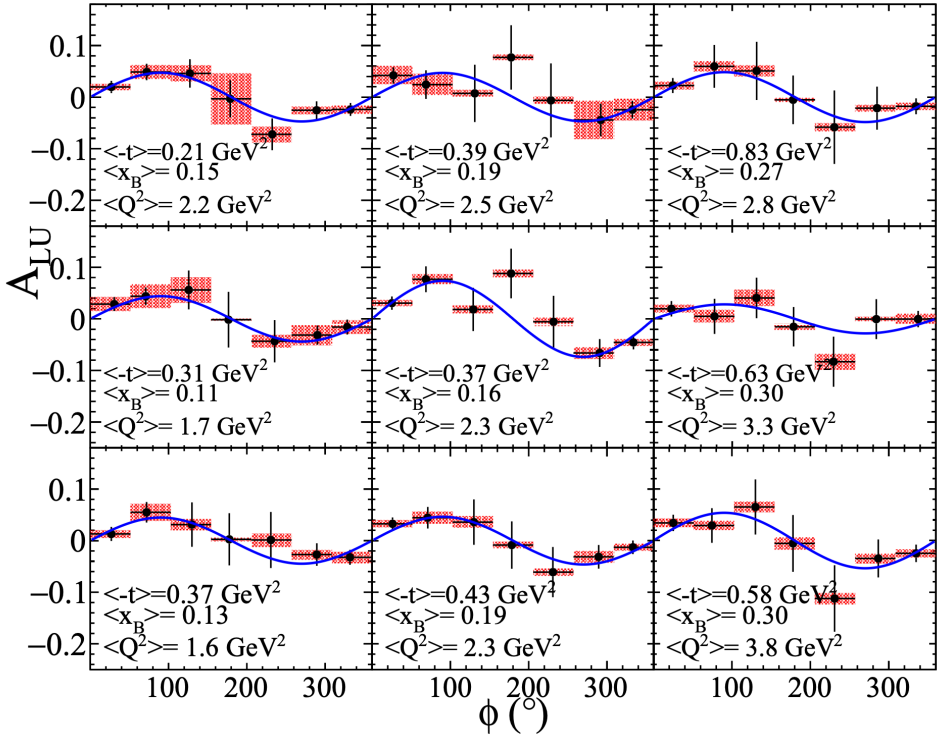

Dedicated detector added to CLAS12:
Central Neutron Detector

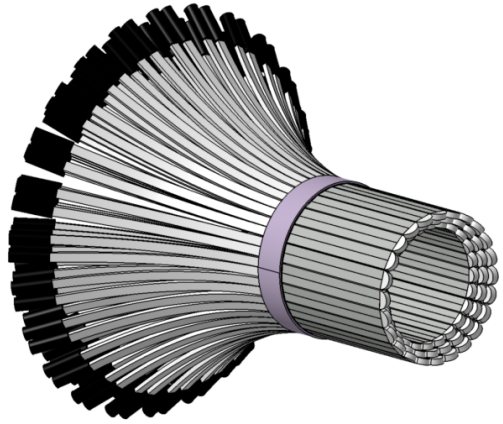

A. Hobart *et al.* (CLAS), PRL 133, 211903 (2024)

Neutron DVCS beam-spin asymmetry

Constraints on the flavour-separated values of angular momentum J_u, J_d

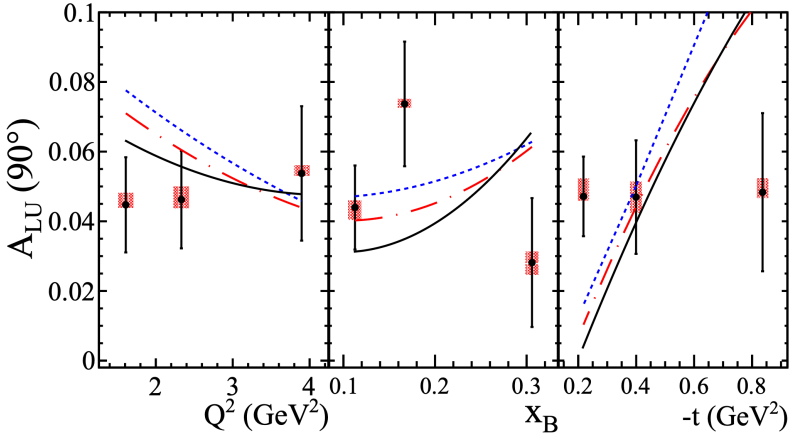

VGG, J_u = 0.35, J_d = 0.05

VGG, J_u = -0.2, J_d = 0.15

VGG, J_u = -0.45, J_d = 0.2

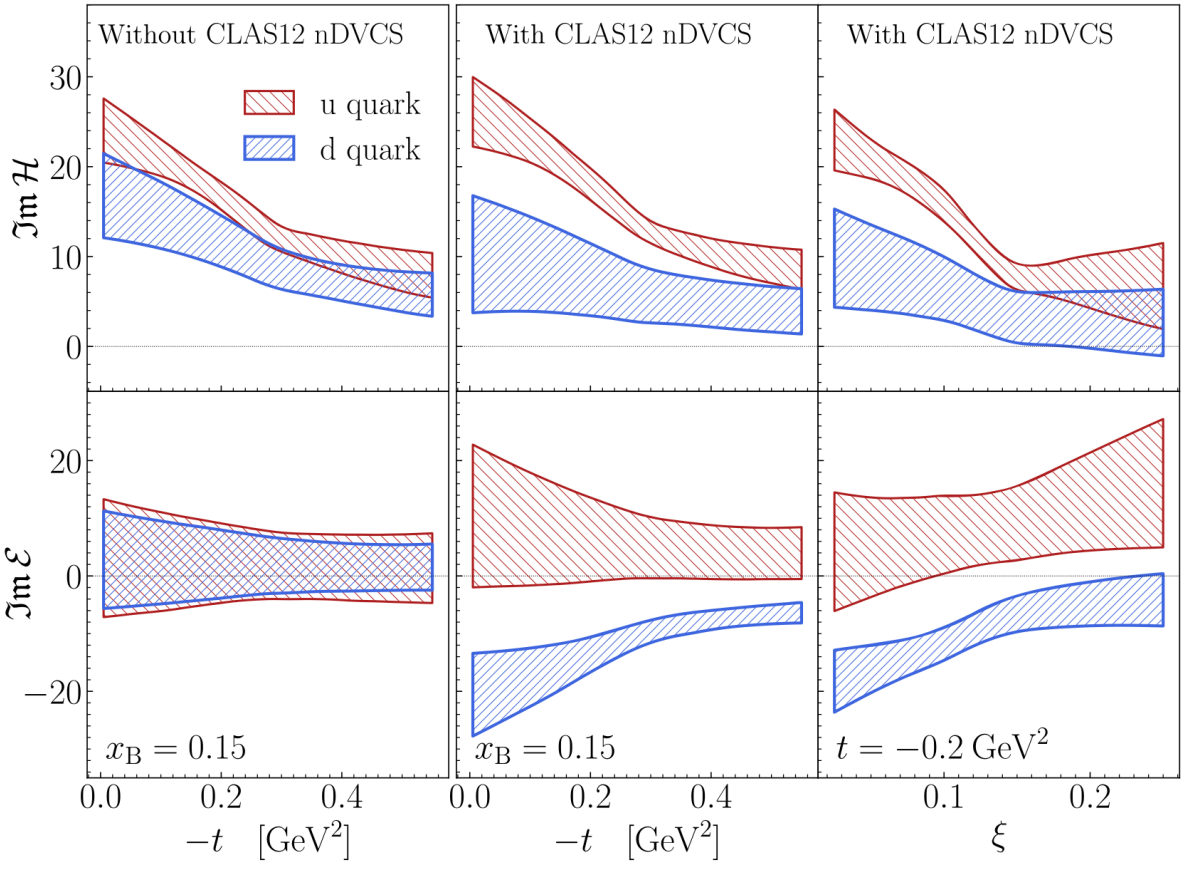

A. Hobart *et al.* (CLAS), PRL 133, 211903 (2024)

Neutron DVCS cross-sections

Hall A

Rosenbluth separation of interference & DVCS terms.

LD_2 target $\langle Q^2 \rangle = 1.75$ GeV^2 $\langle x_B \rangle = 0.36$

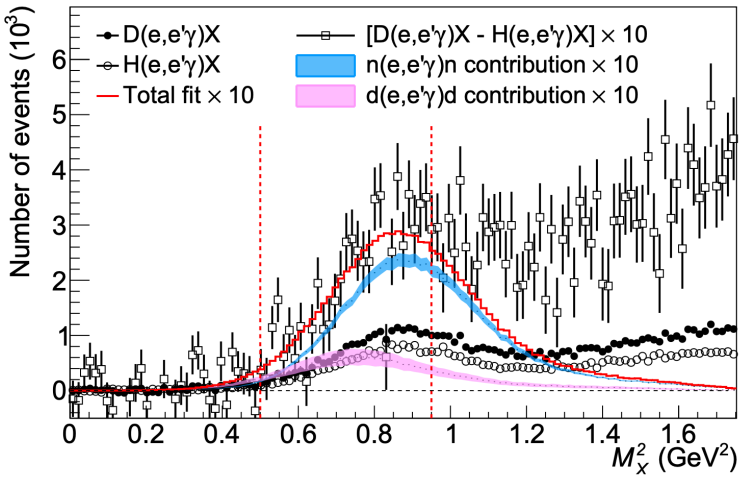

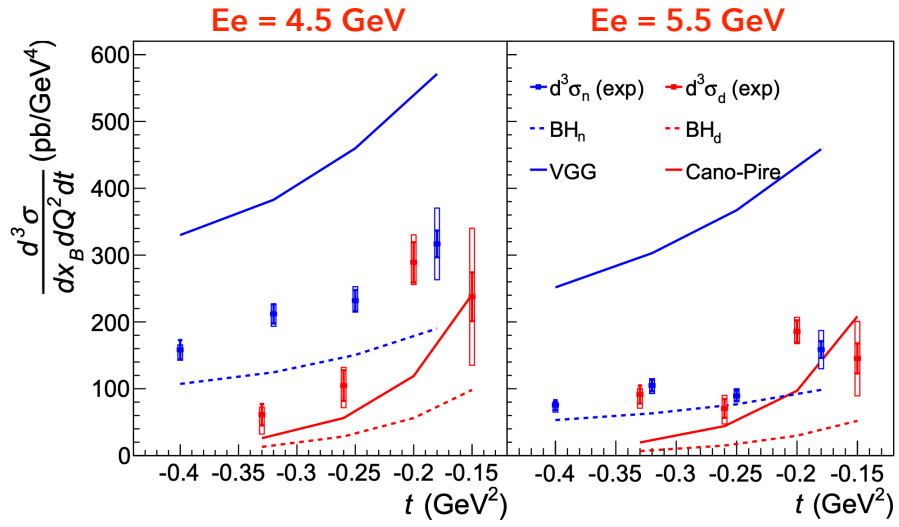

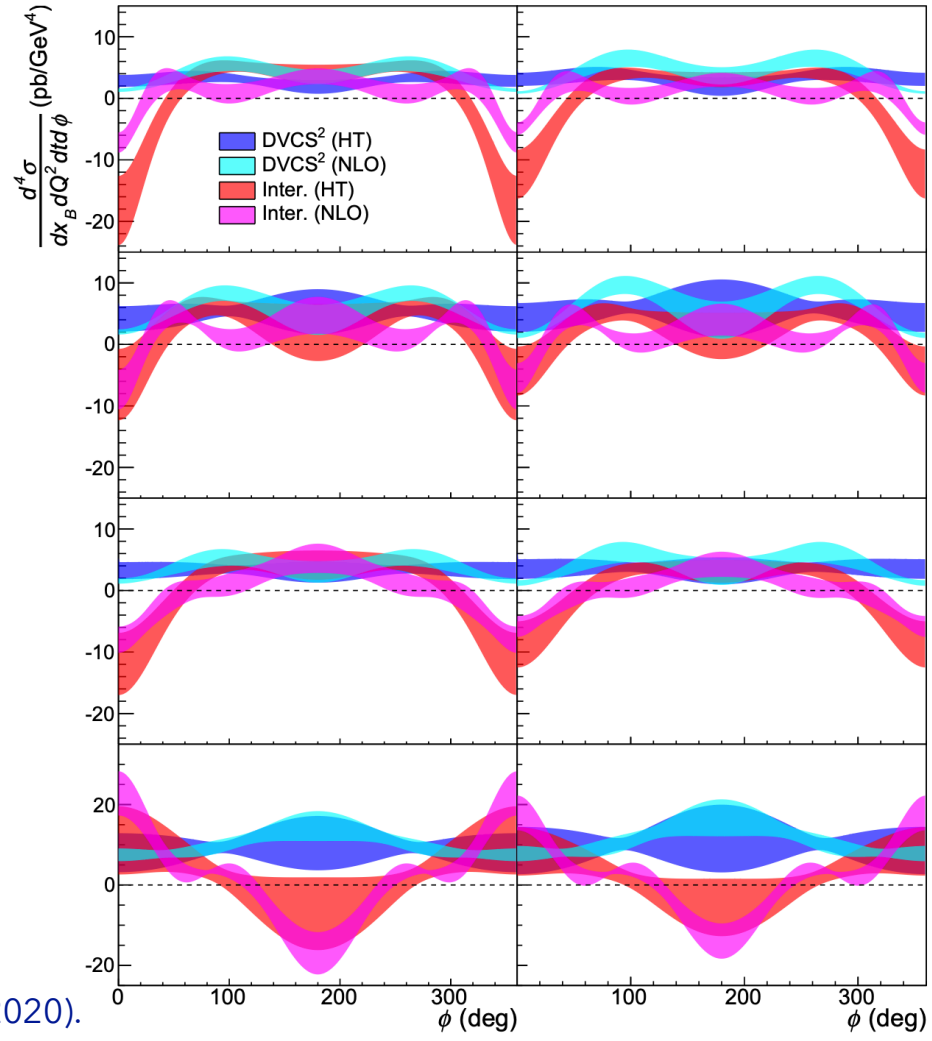

M. Benali *et al.* (Hall A Collab.), Nature Physics 16, 191 - 198 (2020).

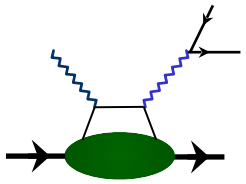

First TCS measurement

$$\frac{d^4\sigma_{INT}}{dQ'^2 dt d\Omega} = A\frac{1+\cos^2\theta}{\sin\theta}[\cos\phi\ \mathrm{Re}\tilde{M}^{--} - \nu\cdot\sin\phi\ \mathrm{Im}\tilde{M}^{--}]$$

$$\tilde{M}^{--} = \left[F_1\mathcal{H} - \xi(F_1+F_2)\tilde{\mathcal{H}} - \frac{t}{4m_p^2}F_2\mathcal{E}\right]$$

suppressed

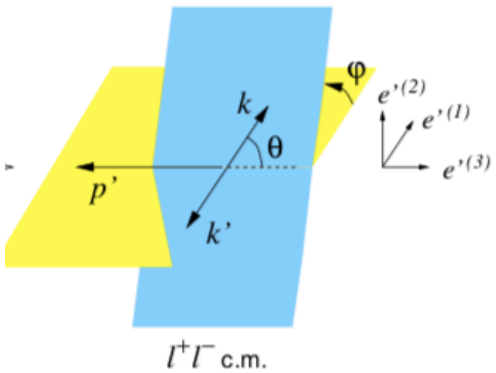

- Circularly-polarised photon cross-section: access to $\mathcal{Im}\ \mathcal{H}$

P. Chatagnon et al. (CLAS), Phys. Rev. Lett. 127, 262501 (2021).

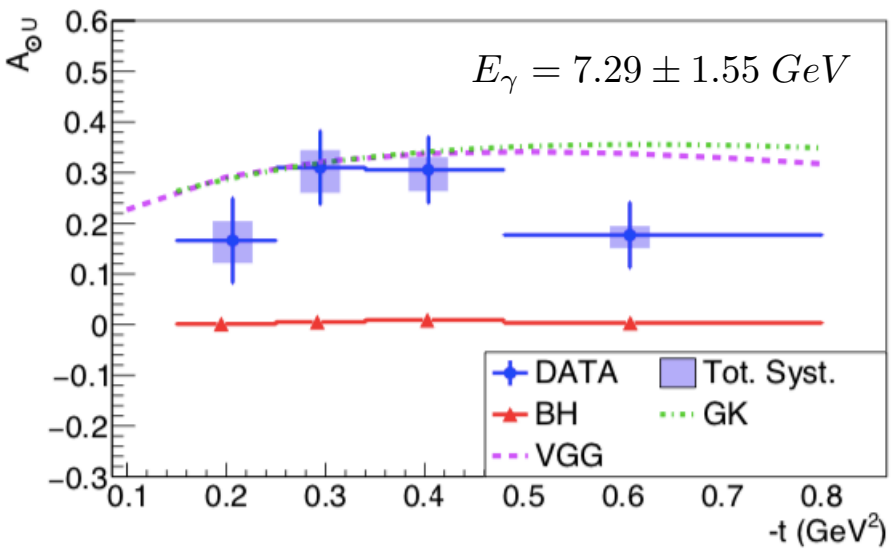

Photon-polarisation asymmetry:

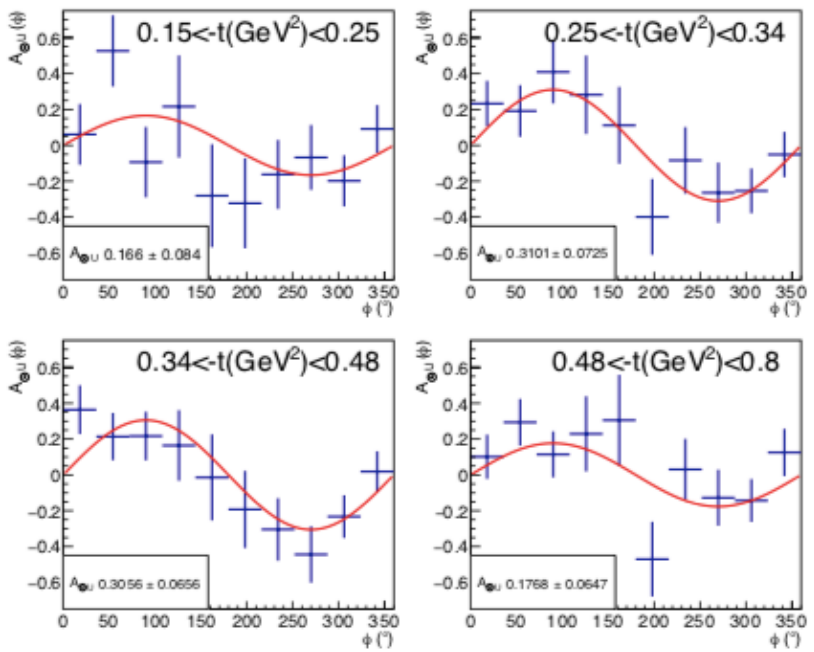

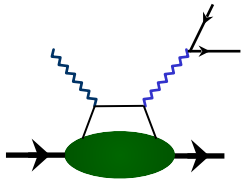

First TCS measurement

- Forward-backward asymmetry: $A_{FB}(\theta,\phi) = \dfrac{d\sigma(\theta,\phi) - d\sigma(180^\circ-\theta, 180^\circ+\phi)}{d\sigma(\theta,\phi) + d\sigma(180^\circ-\theta, 180^\circ+\phi)}$

access to $\mathcal{Re}\,\mathcal{H}$

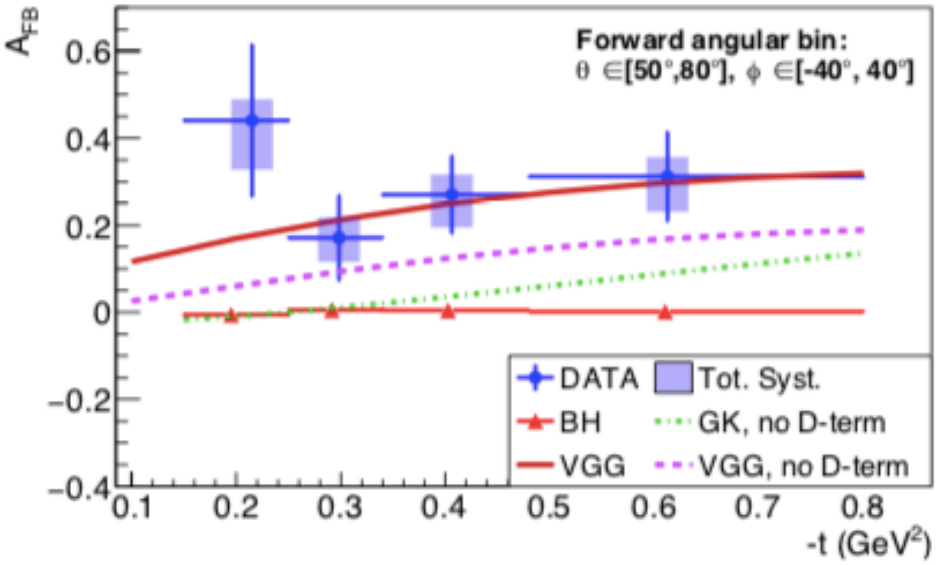

$E_\gamma = 7.23 \pm 1.61\ GeV$

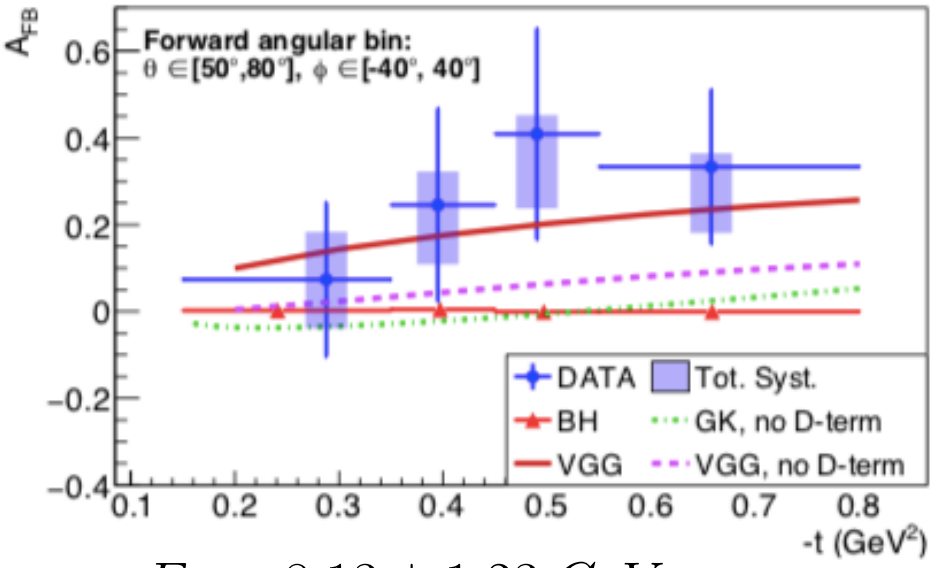

$E_\gamma = 8.13 \pm 1.23\ GeV$

P. Chatagnon et al. (CLAS), Phys. Rev. Lett. 127, 262501 (2021).

Hard exclusive production of π⁺

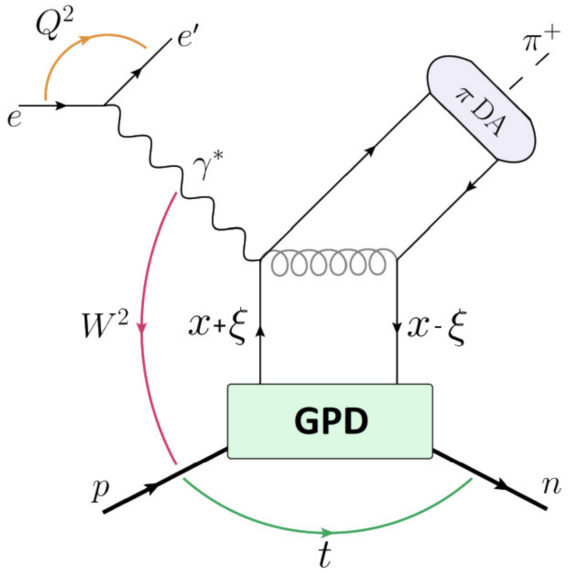

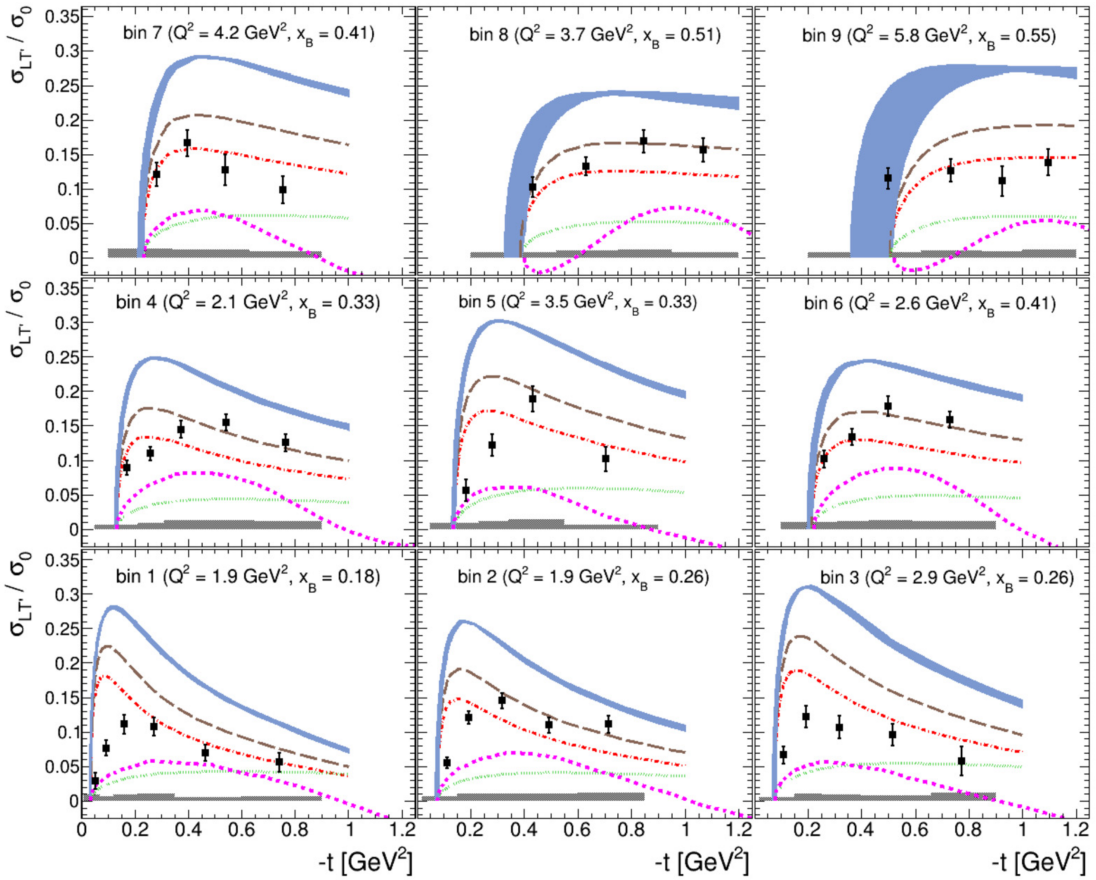

Sensitivity to chiral odd transversity GPDs: tensor charge of the nucleon.

$$\sigma_{LT'} \sim \frac{\sqrt{-t'}}{2m} Im[\langle \overline{E}_{T-eff} \rangle^* \langle \widetilde{H}_{eff} \rangle + \langle H_{T-eff} \rangle^* \langle \widetilde{E}_{eff} \rangle]$$

GK model (GPD-based)

JML model (Regge-based)

S. Diehl et al. (CLAS), PLB 839, 137761 (2023)

Hard exclusive production of π^0

Hall A

$$\frac{d^4\sigma}{dQ^2 dx_B dt d\phi} = \frac{1}{2\pi}\frac{d^2\,\Gamma_\gamma}{dQ^2 dx_B}(Q^2, x_B, E)$$

$$\left[\frac{d\sigma_T}{dt} + \epsilon\frac{d\sigma_L}{dt} + \sqrt{2\epsilon(1+\epsilon)}\frac{d\sigma_{LT}}{dt}\cos(\phi) + \epsilon\frac{d\sigma_{TT}}{dt}\cos(2\phi)\right.$$

$$\left. + h\sqrt{2\epsilon(1-\epsilon)}\frac{d\sigma_{LT'}}{dt}\sin(\phi)\right]$$

interference

transverse photon polarisation

longitudinal photon polarisation

Separation of structure functions and constraints on GPD $\tilde{E}$

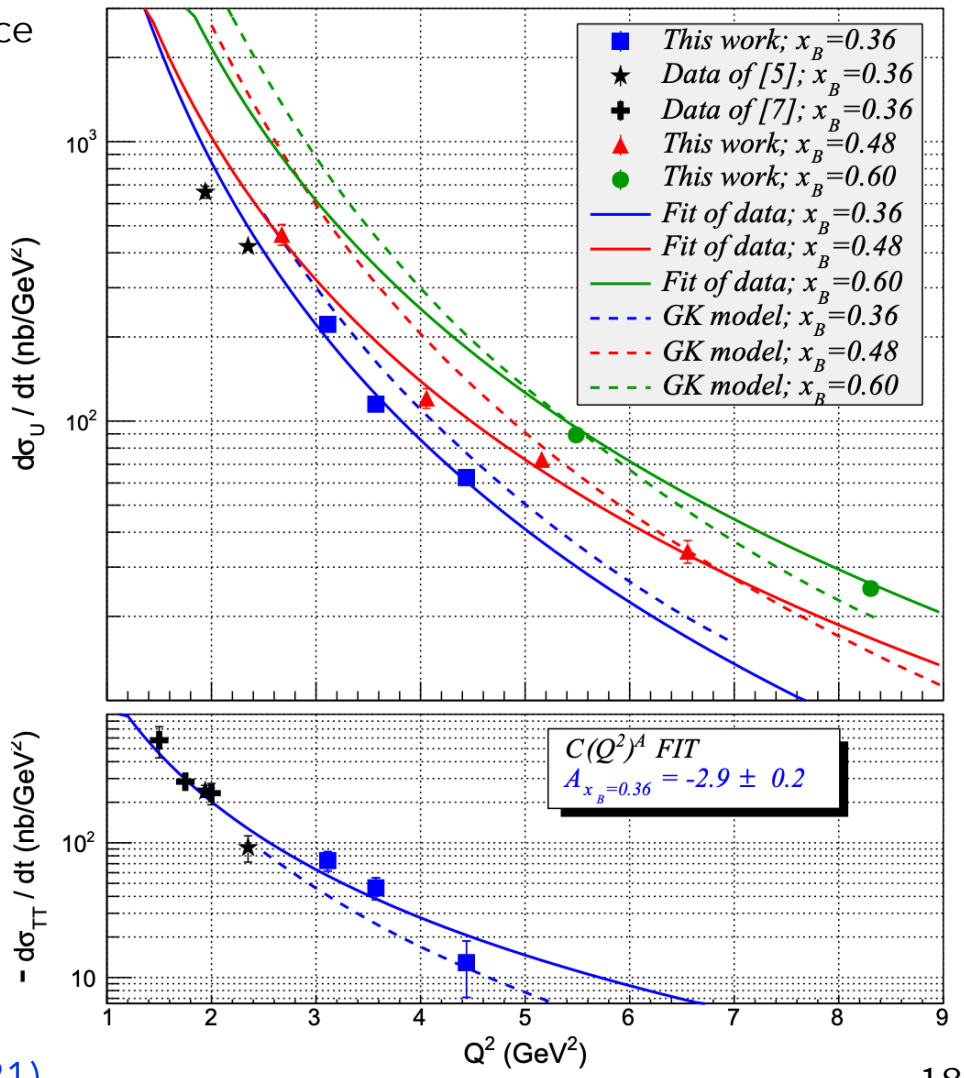

M. Dlamini et al. (Hall A Collab.), PRL 127, 152301 (2021)

Hard exclusive production of π^0

$$BSA = \frac{\sqrt{2\epsilon(1-\epsilon)}\frac{\sigma_{LT'}}{\sigma_0}\sin\phi}{1+\sqrt{2\epsilon(1+\epsilon)}\frac{\sigma_{LT}}{\sigma_0}\cos\phi+\epsilon\frac{\sigma_{TT}}{\sigma_0}\cos 2\phi}$$

Highly sensitive to

$$\bar{E}_T = 2\tilde{H}_T + E_T$$

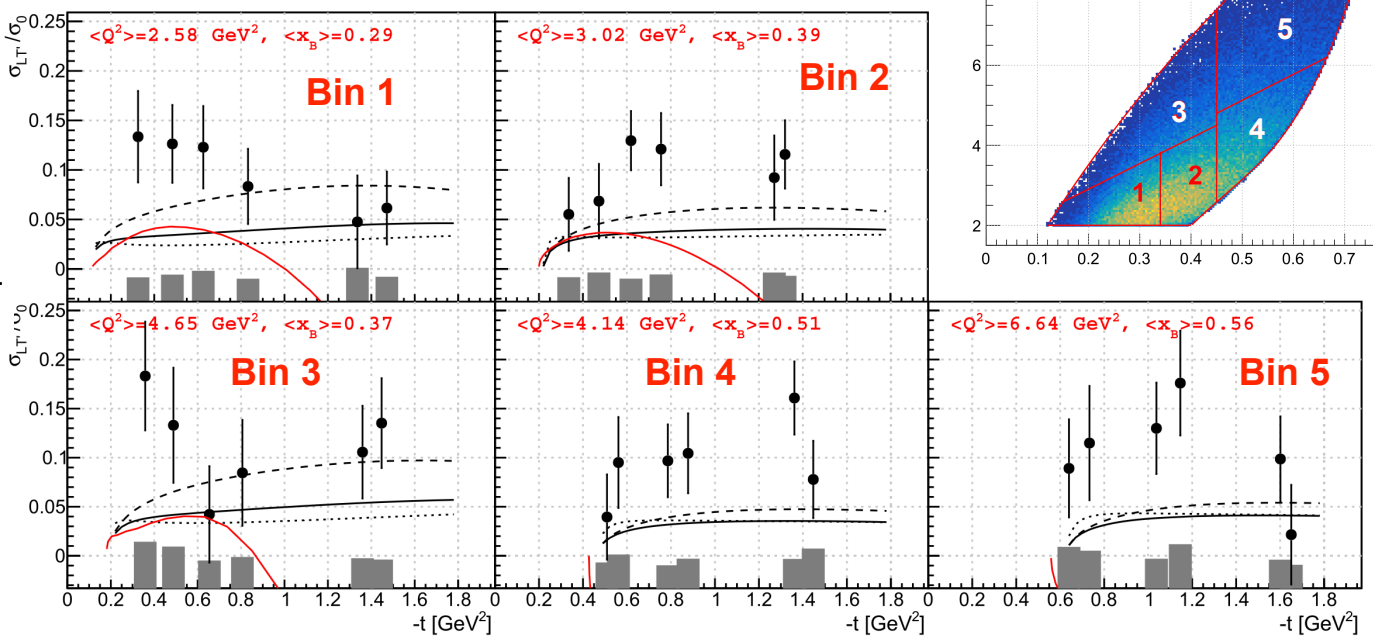

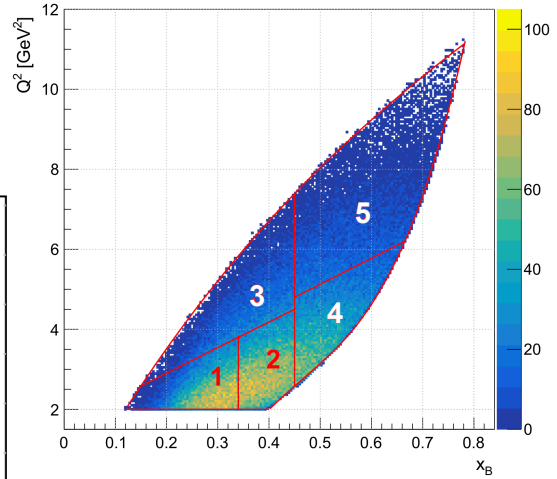

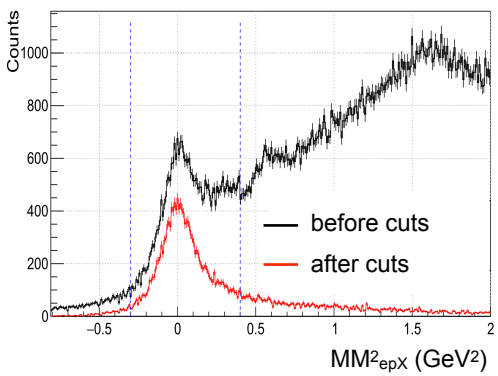

$$k_T^{u,d} = \int dx \bar{E}_T^{u,d}(x,\xi,t=0)$$

GK model (GPD-based)
GK model, 0.5 $\bar{E}_T$
GK model, 0.5 H_T
JML model (Regge-based)

A. Kim et al. (CLAS), PLB 849, 138459 (2024)

BSA in $\pi^-\Delta^{++}$ electroproduction

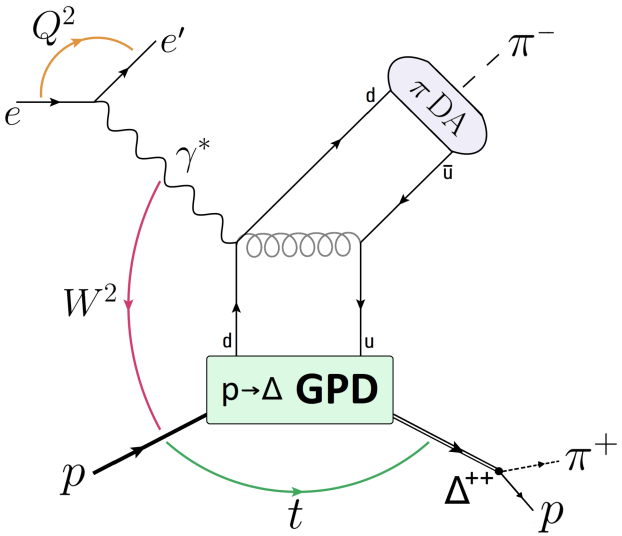

First measurement.

Probes the $p \rightarrow \Delta^{++}$ transition GPDs

Access to d-quark content of the nucleon.

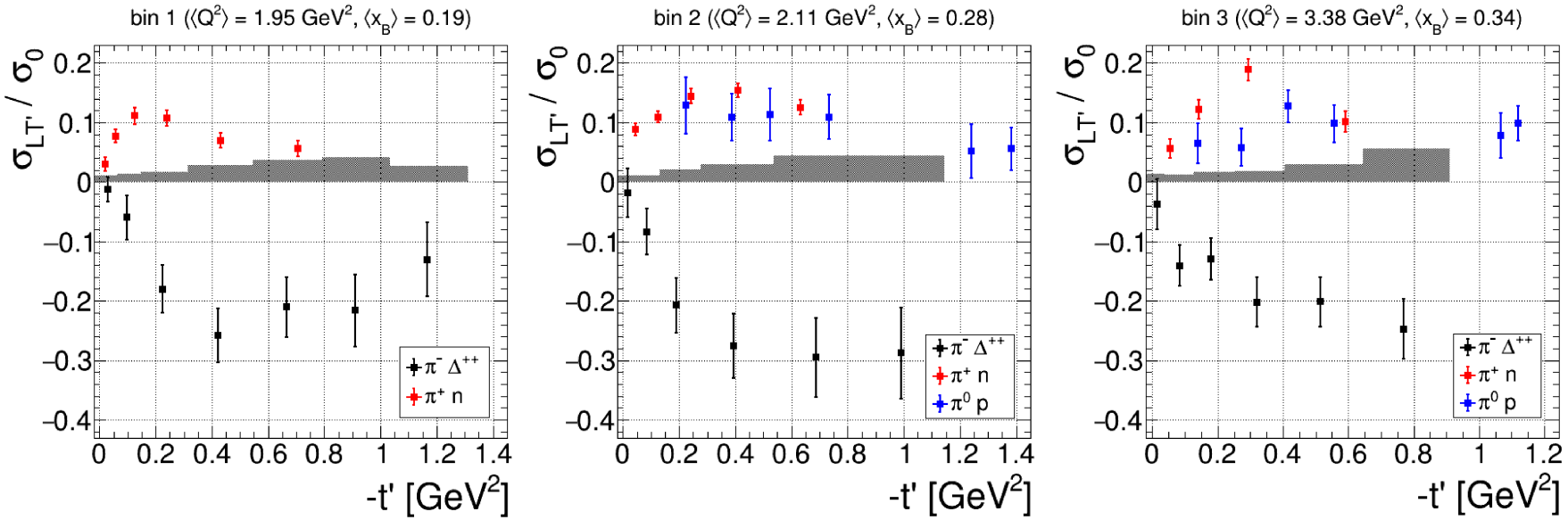

S. Diehl et al. (CLAS), PRL 131, 021901 (2023)

Proton & neutron DVCS with a longitudinally polarised target

Experiments: E12-06-119
E12-06-109A

A_{UL} characterised by imaginary parts of CFFs via:

$$F_1\tilde{H} + \xi G_M(H + \frac{x_B}{2}E) - \frac{\xi t}{4M^2}F_2\tilde{E} + \ldots$$

→ $Im(\tilde{H}_p)$
$Im(H_n)$

Longitudinally polarised NH_3 and ND_3 targets:

- Dynamic Nuclear Polarisation (DNP) of target material, cooled to 1K in a *He* evaporation cryostat.
- P_{proton} > 80%
- $P_{deuteron}$ up to 50%

Run Group C: 2022-23
Data under analysis

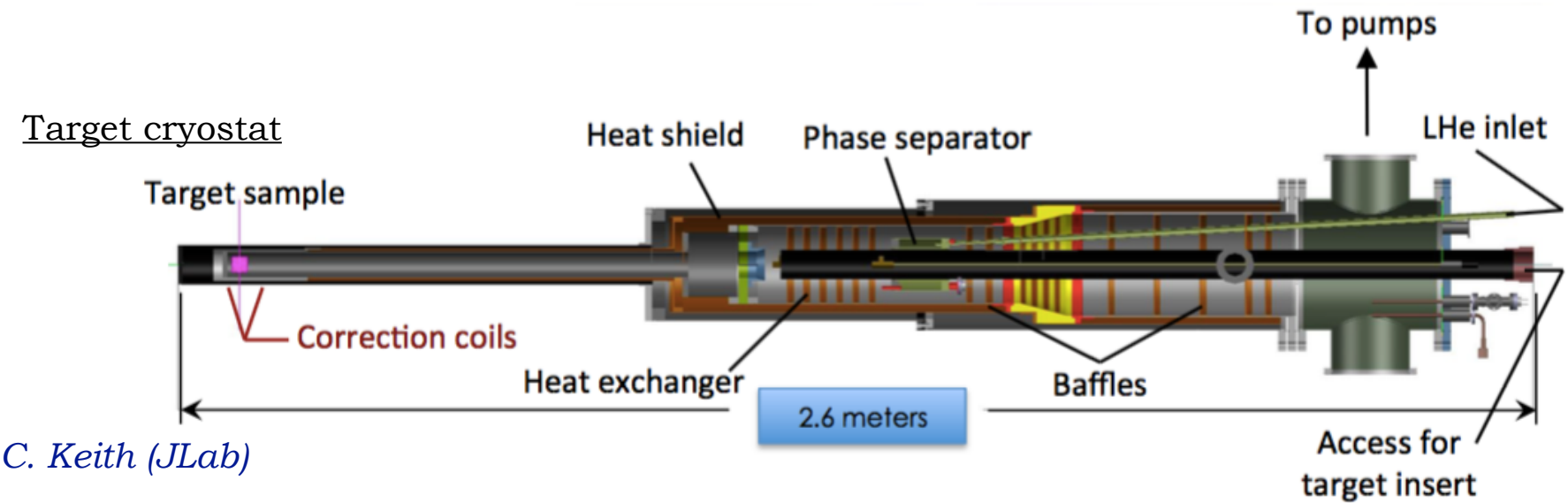

C. Keith (JLab)

Measurements on the way

In **Hall B (CLAS12)**, data has also been taken with:

- LH_2 target at lower energies (6.5 GeV, 7.5 GeV; 8.8 GeV planned): Rosenbluth separation of DVCS-BH cross-section to access directly the DVCS term.

- ALERT: DVCS, meson-production on ^{4}He target. Run has just completed.

  ^{4}He: spin-0. Only one leading-twist GPD! Fully bound nucleus – access to medium-modification effects.

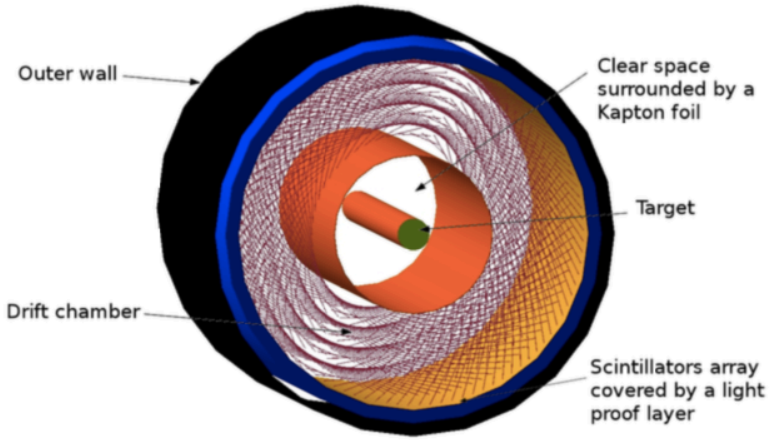

Hall C: Addition of a Neutral Particle Spectrometer (NPS) calorimeter for measurements of DVCS off proton and neutron, π^0-production off proton. Data taken 2023 - 24, under analysis.

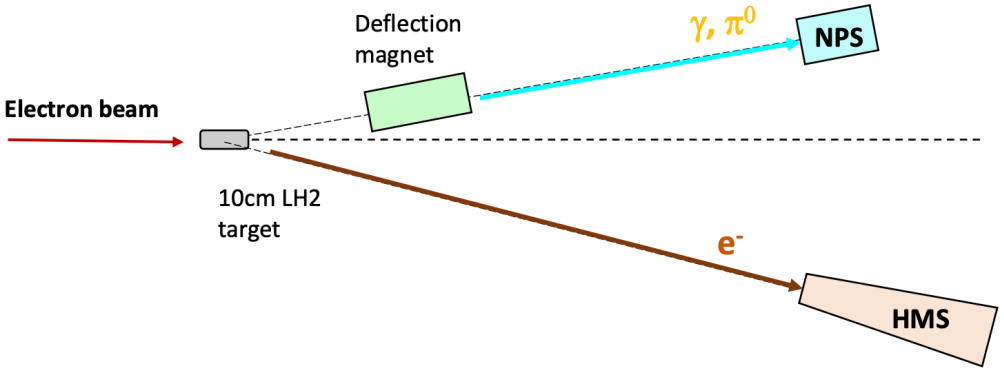

COMPASS: sea quarks

COMPASS @ Cern (SPS)

Compact **M**uon and **P**roton **A**pparatus for **S**tructure and **S**pectroscopy

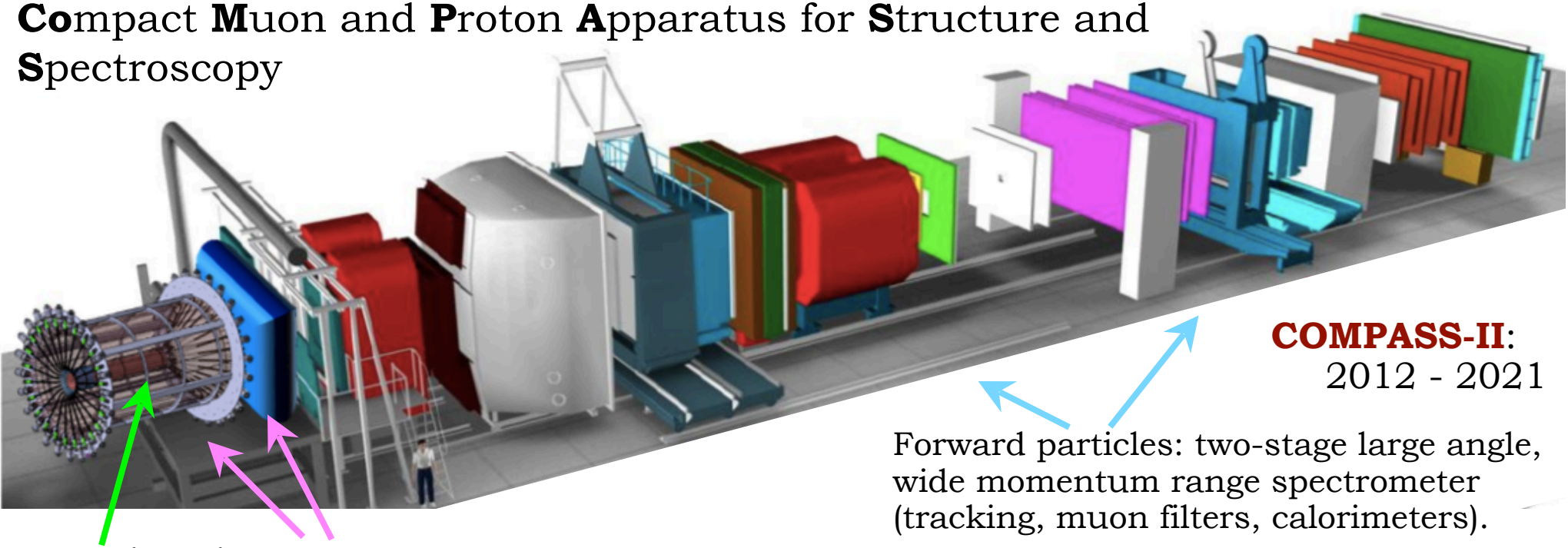

COMPASS-II:
2012 - 2021

Forward particles: two-stage large angle, wide momentum range spectrometer (tracking, muon filters, calorimeters).

2.5m liquid H_2 target

Upgrades: new scintillator ToF CAMERA for recoil proton detection & new EM calorimeter.

DVCS : μ p → μ' p γ

Full exclusive reconstruction

- 160 GeV 80% polarised μ^+/μ^-
- $\sim 4 \times 10^8 \mu/spill$, 9.6s/40s duty cycle

Data:

- 2008 & 2009: two v. short test runs, 40 cm LH_2 target.
- COMPASS-II: 1 month in 2012, 6 months in 2016 & 2017 each (GPD **H**).
- 2022+: transversely pol. NH_3 target (GPD **E**). LOI stage…

DVCS @ COMPASS (2016 run)

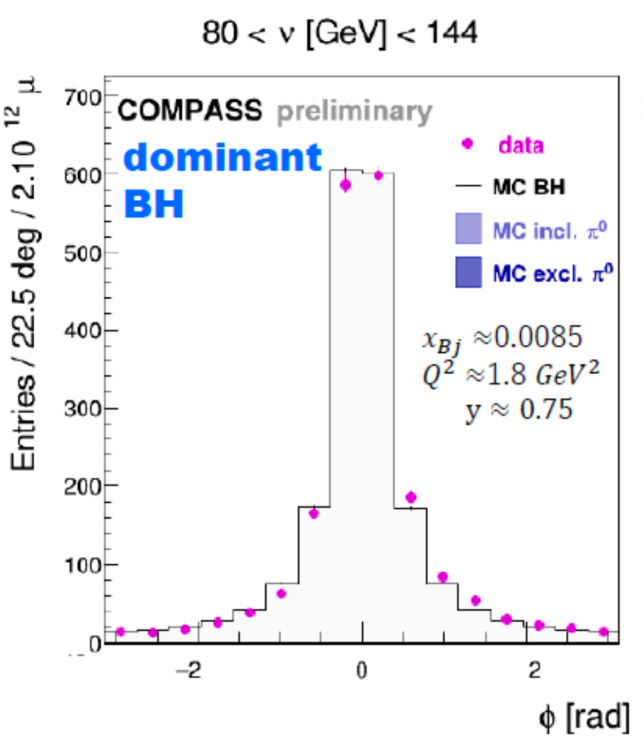

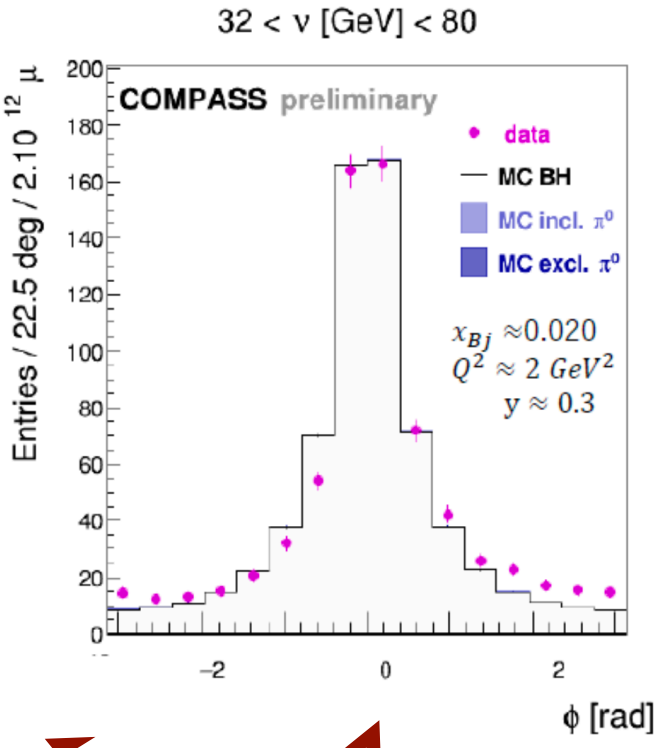

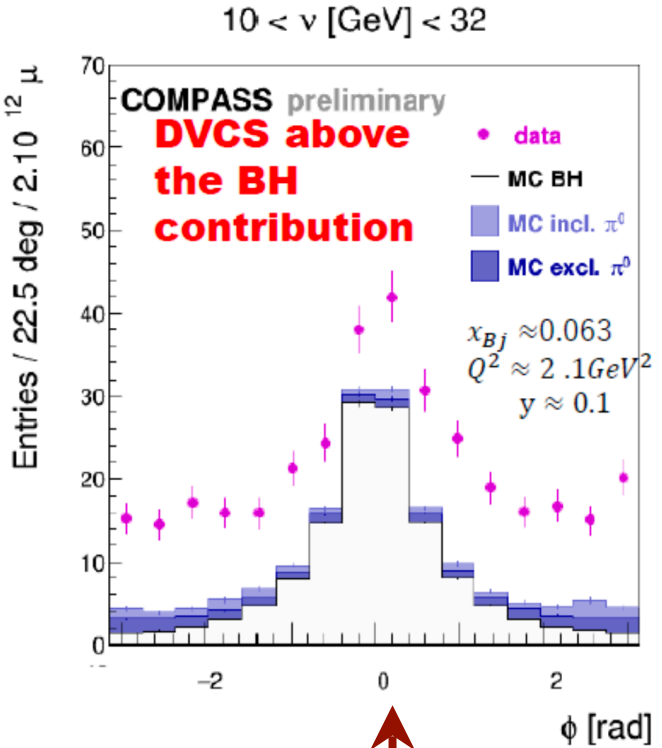

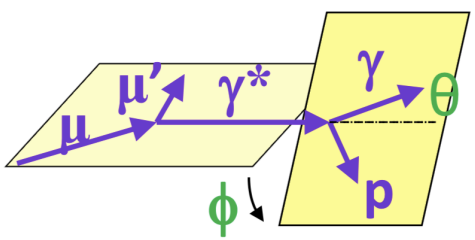

Bethe-Heitler dominates at very low x_B

DVCS dominates at these kinematics

See also π^0 publication with separation of structure functions:
G. Alexeev *et al.* (COMPASS), PLB 139832 (2025)

Transverse size of the nucleon

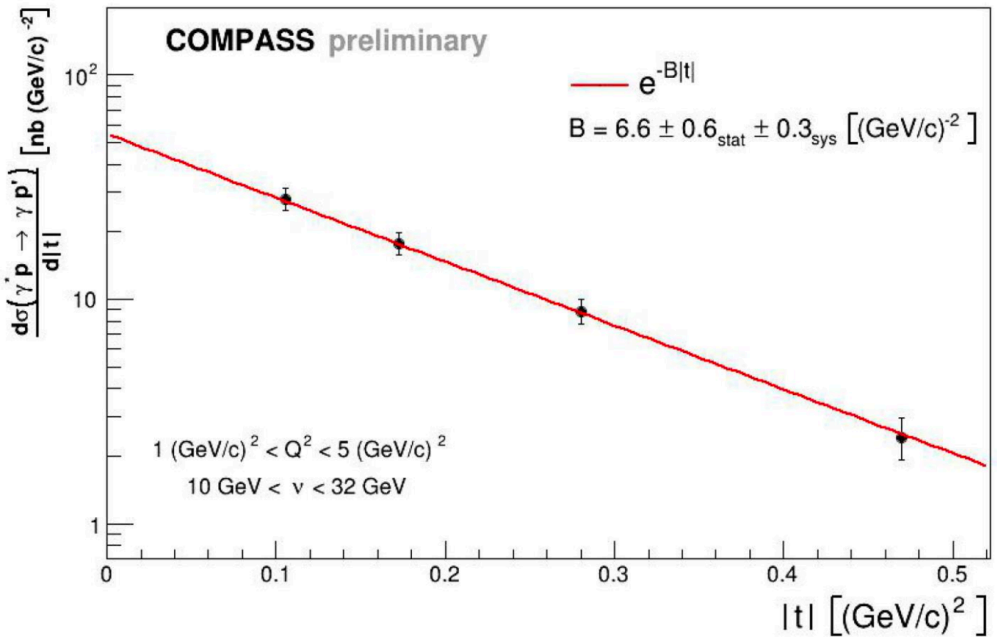

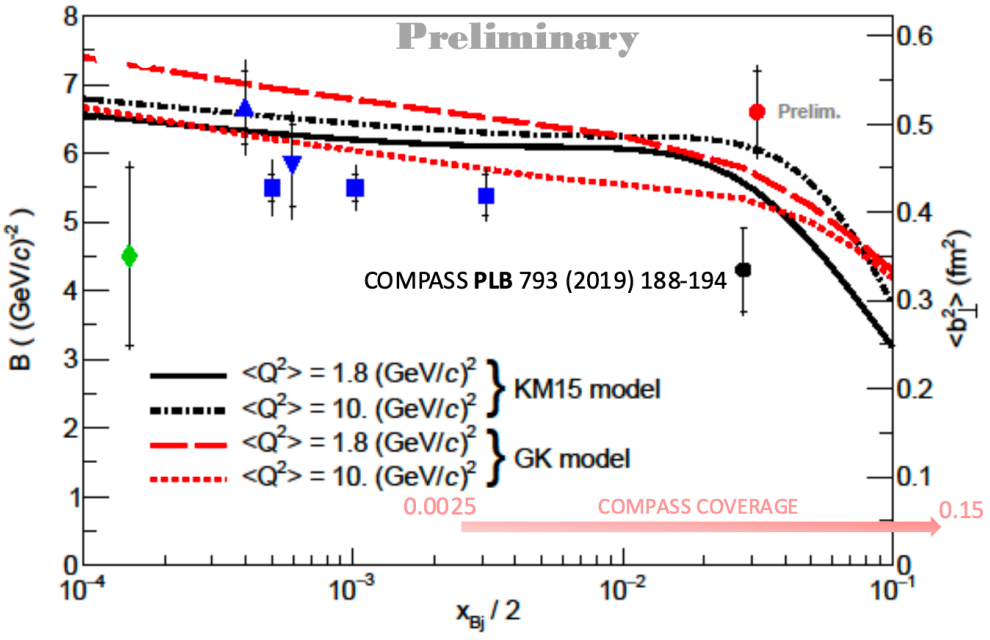

Expect at least 3 bins in x_B from 2026-27 data

- COMPASS: <Q^2> = 1.8 (GeV/c)^2
- ZEUS: <Q^2> = 3.2 (GeV/c)^2
- H1: <Q^2> = 4.0 (GeV/c)^2
- H1: <Q^2> = 8.0 (GeV/c)^2
- H1: <Q^2> = 10. (GeV/c)^2

Electron-Ion Collider

Electron-Ion Collider

World's first polarized electron - proton / light ion and electron - nucleus collider.

- Widely variable CoM energy: 30 - 140 GeV
- High luminosity $L_{ep} \sim 10^{33\text{-}34}$ $cm^{-2}s^{-1}$
- Wide range of nuclei up to Uranium

Starting construction at Brookhaven National Lab in 2026.

Dedicated studies of EIC physics and design:

EIC White Paper, Eur. Phy. J. A 52, 9 (2016)
EIC Yellow Report, Nuc. Phys. A 1026, 122447 (2022)

Plus numerous ePIC technical reports, impact studies, etc.

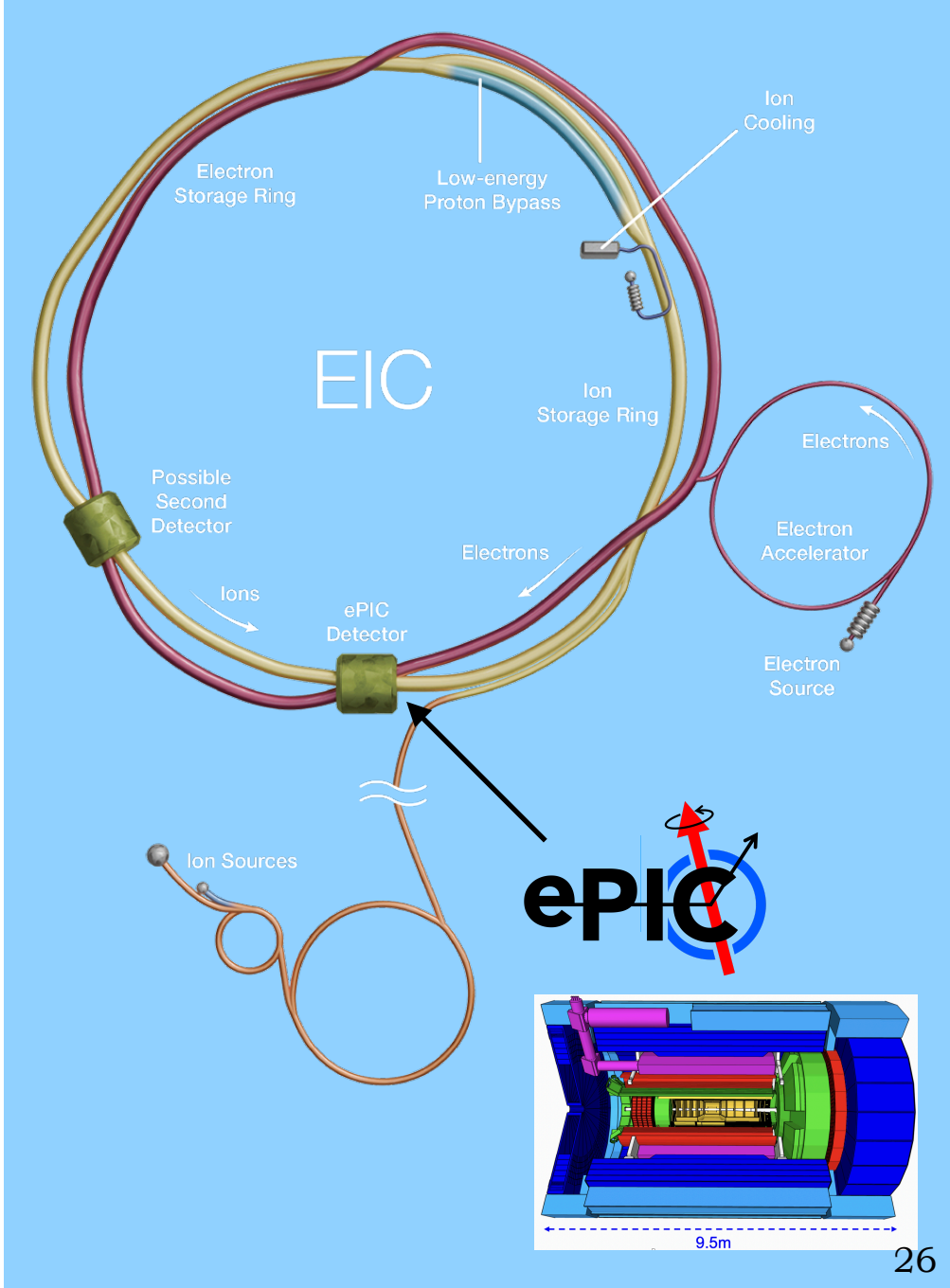

Electron-Ion Collider

World's first polarized electron - proton / light ion and electron - nucleus collider.

- Widely variable CoM energy: 30 - 140 GeV
- High luminosity $L_{ep} \sim 10^{33\text{-}34}$ cm^{-2}s^{-1}
- Wide range of nuclei up to Uranium

Starting construction at Brookhaven National Lab in 2026.

Dedicated studies of EIC physics and design:

EIC White Paper, Eur. Phy. J. A 52, 9 (2016)
EIC Yellow Report, Nuc. Phys. A 1026, 122447 (2022)

Plus numerous ePIC technical reports, impact studies, etc.

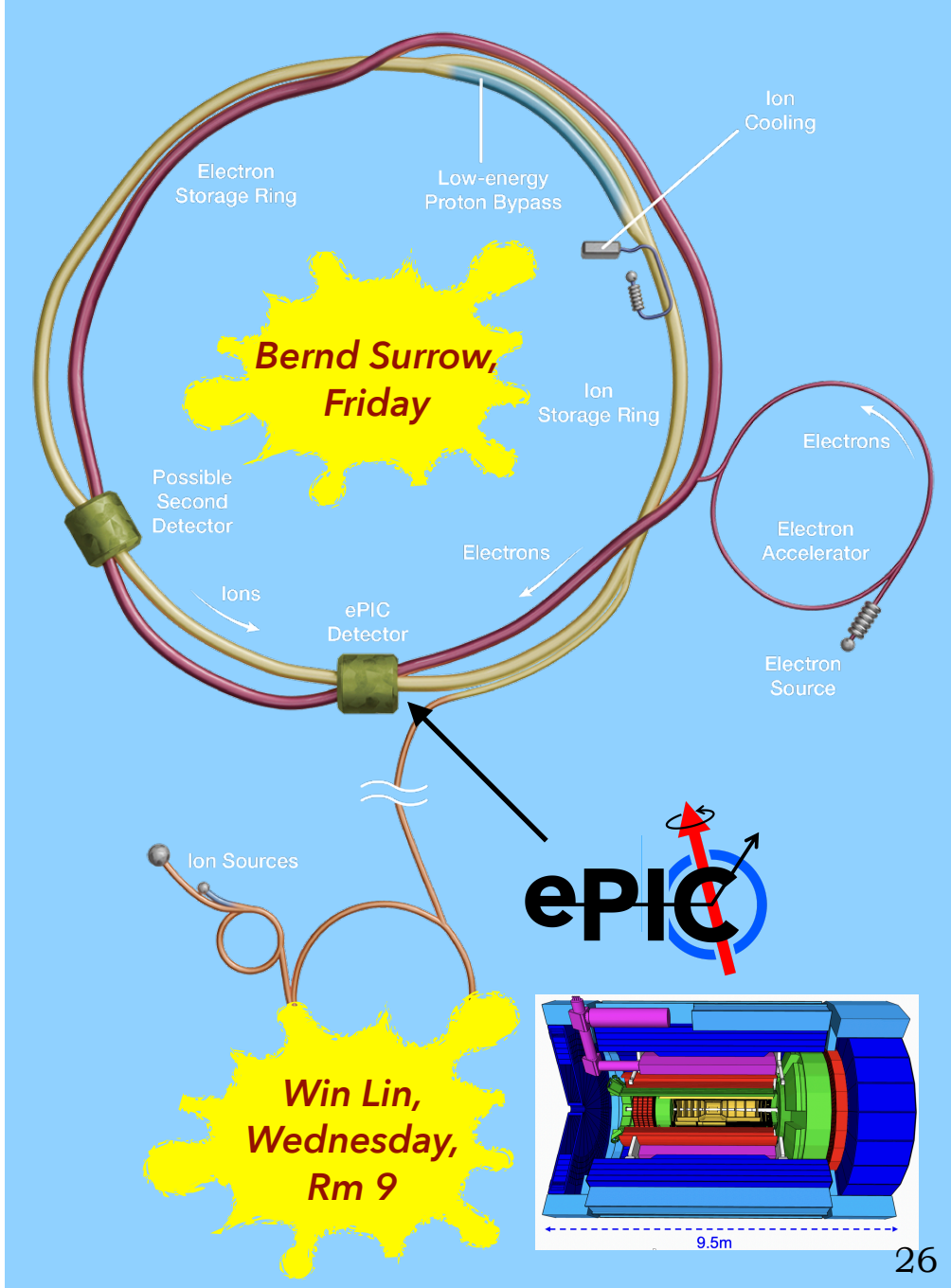

Detector configuration

Very asymmetric beams

Hermetic detectors within a central solenoid

Very far-forward and far-backward instrumentation for lowest scattering angles.

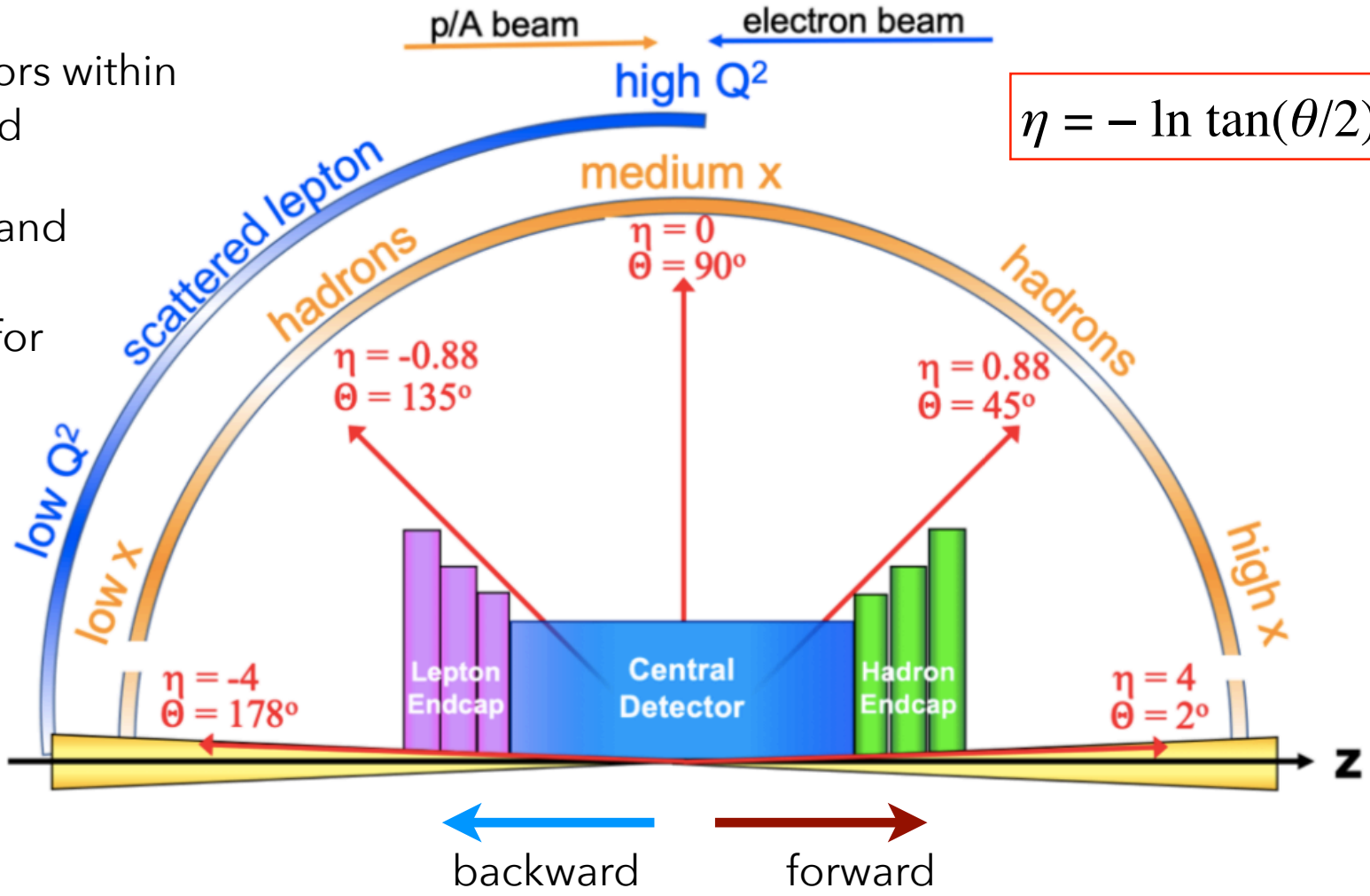

$$\eta = -\ln \tan(\theta/2)$$

The ePIC detector

Electron-Proton and -Ion Collider detector

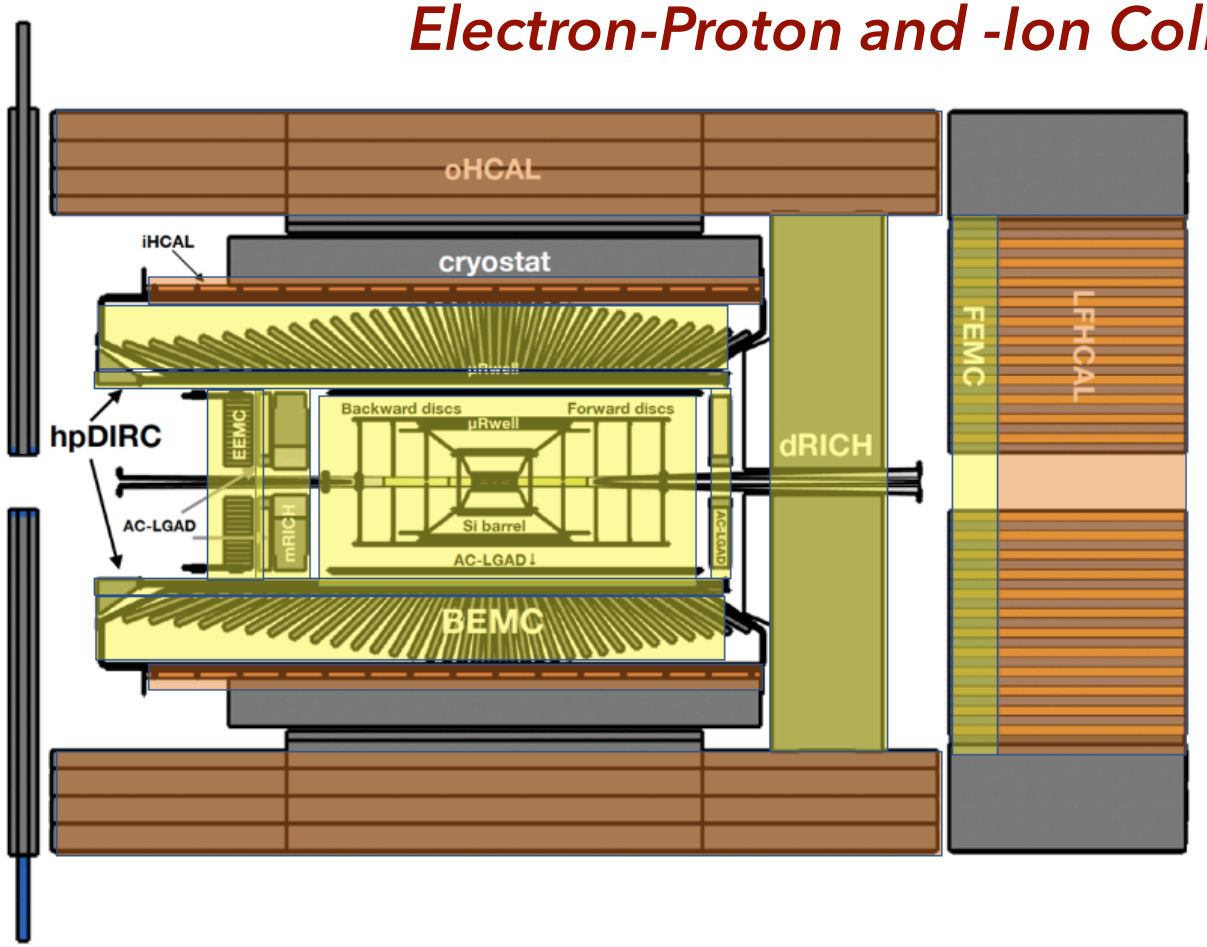

electron beam

hadron beam

Calorimetry:

Range of EM and hadron calorimeters.

Particle ID (PID):

High time-resolution Si (AC-LGAD), Cherenkov detectors: RICH, DIRC.

Tracking: New 1.7 T magnet (MARCO).

Light-weight Si tracking (65nm MAPS), micro-pattern gaseous detectors (MPGDs).

Win Lin, Wednesday, Rm 9

The ePIC detector

Electron-Proton and -Ion Collider detector

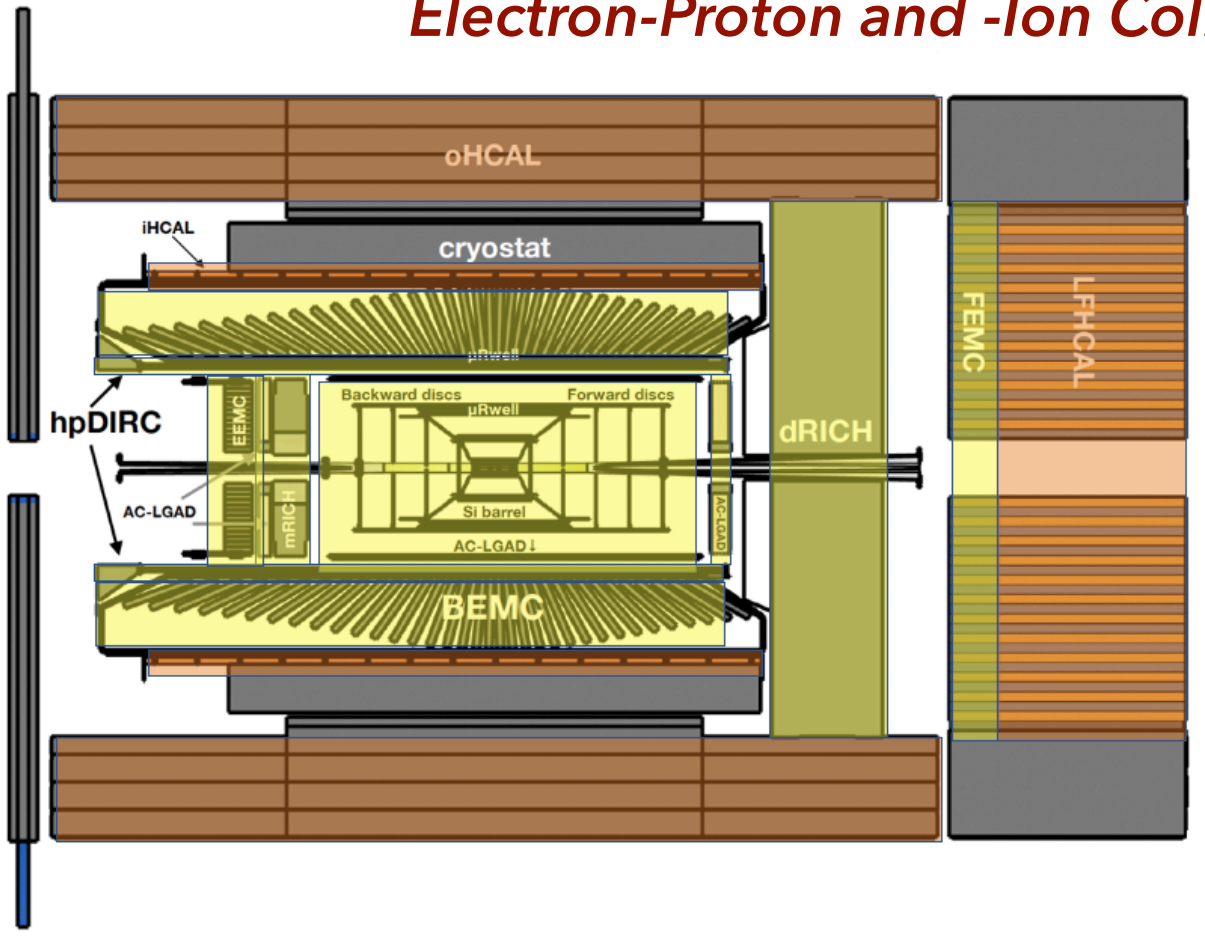

electron beam

hadron beam

Calorimetry:

Range of EM and hadron calorimeters.

Particle ID (PID):

High time-resolution Si (AC-LGAD), Cherenkov detectors: RICH, DIRC.

Tracking: New 1.7 T magnet (MARCO).

Light-weight Si tracking (65nm MAPS), micro-pattern gaseous detectors (MPGDs).

Recoil protons in *ep*

- The impact parameter information in many exclusive processes is encoded in *t*, via a Fourier Transform. Require accurate measurement of *t* from as close to zero as possible and across a wide range in *ep and e(light-A)* collisions.

- Scattered protons / light ions detected in Roman Pots (for the lowest values of *t*) and in the B0 spectrometers (for higher values).

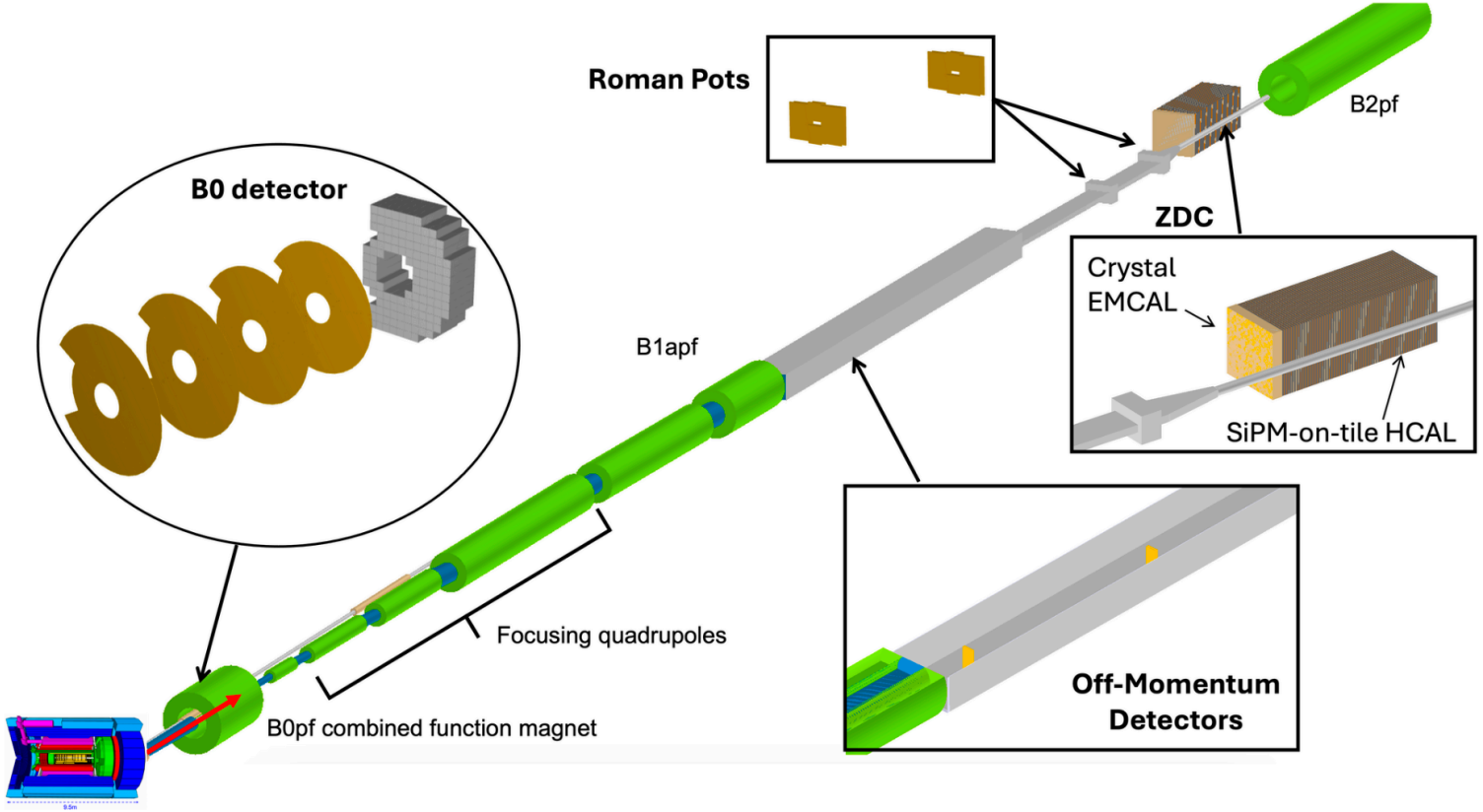

EIC kinematic reach: DVCS

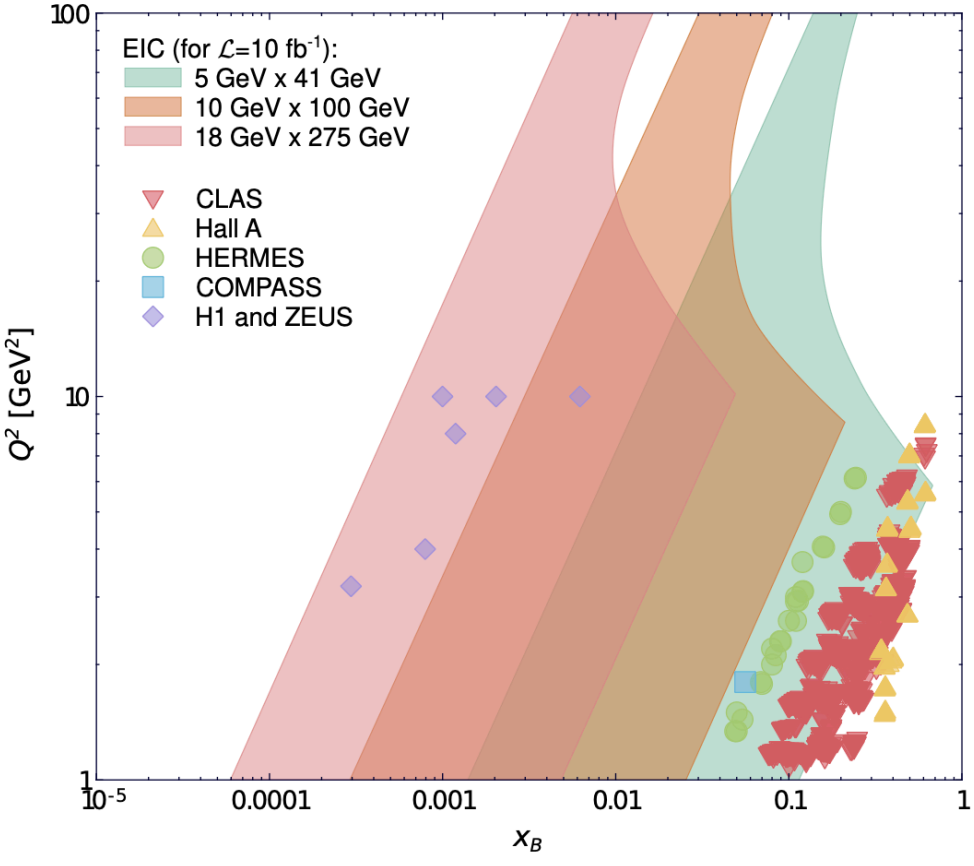

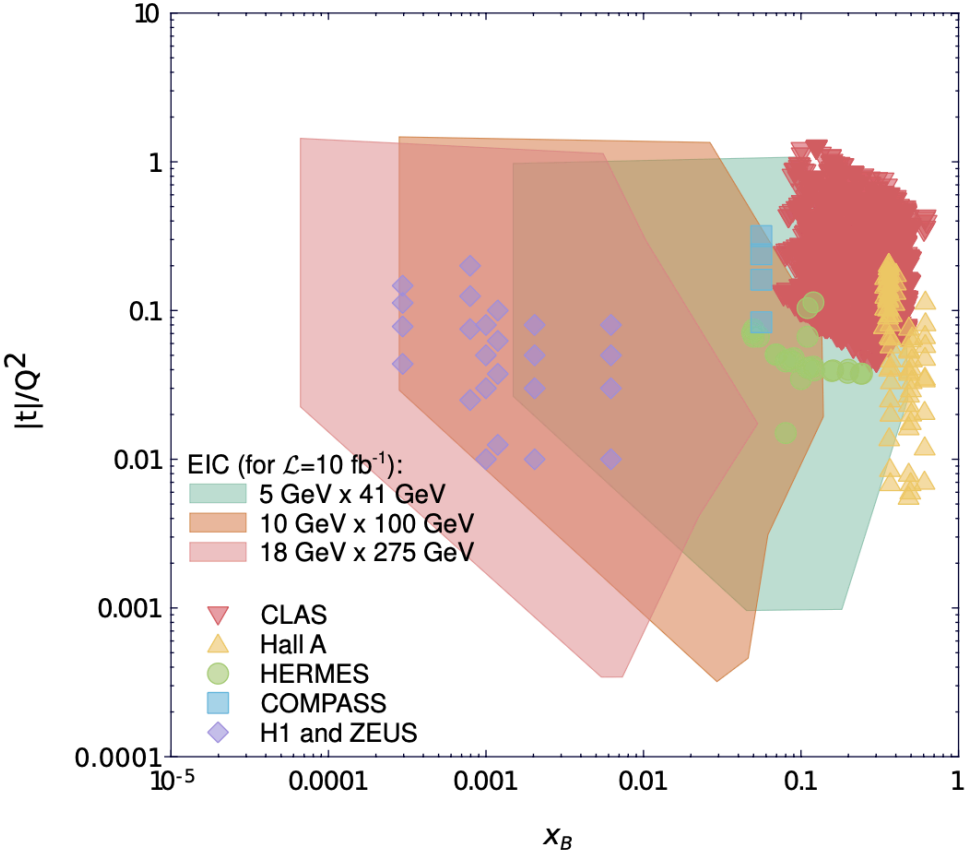

E. Aschenauer *et al.*, PRD 112, 036010 (2025)

DVCS final state reconstruction

electrons

protons

photons

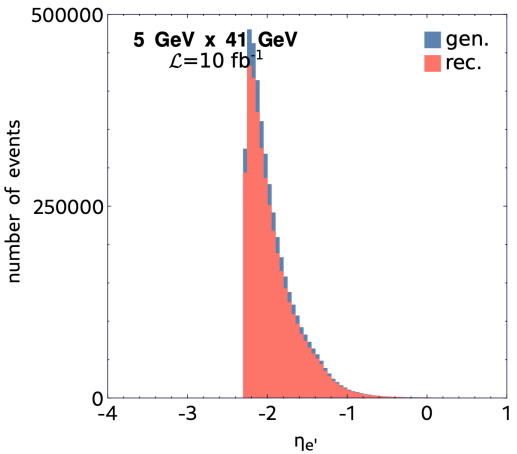

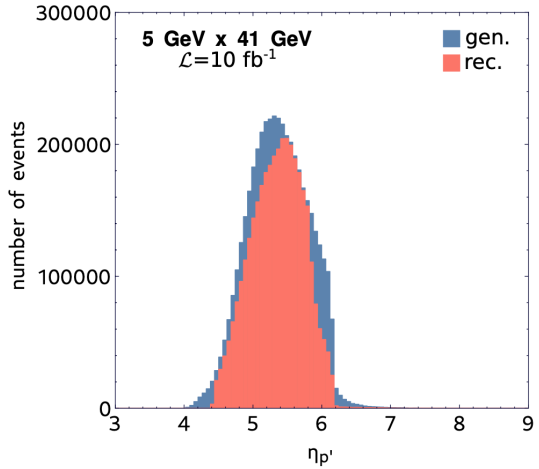

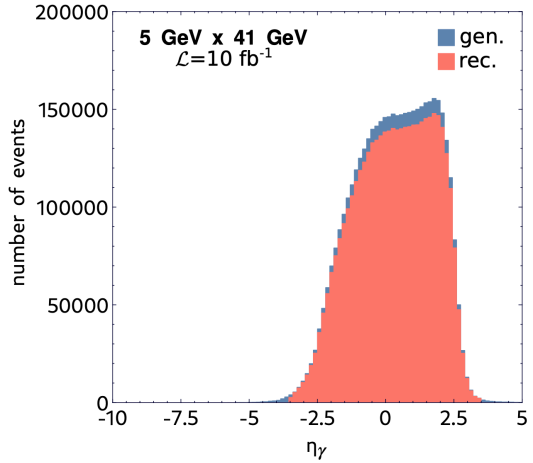

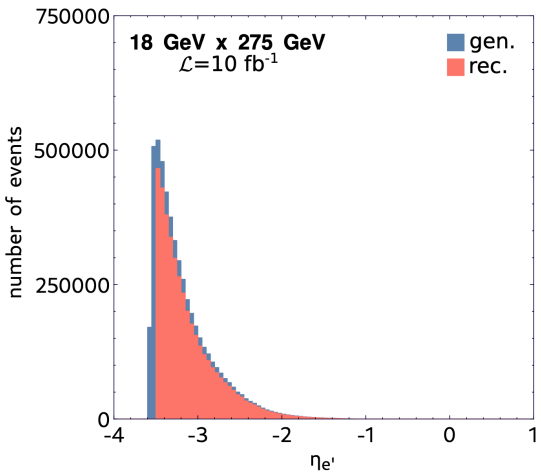

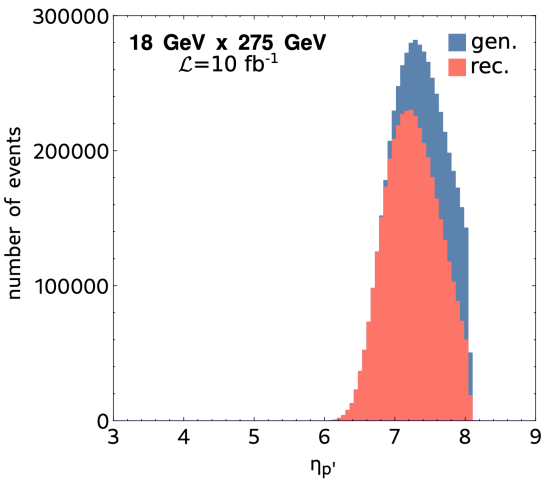

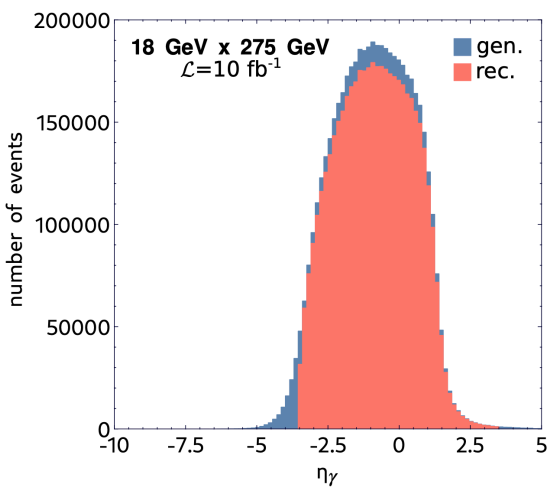

Excellent acceptance

E. Aschenauer *et al.*, PRD 112, 036010 (2025)

CFF constraints

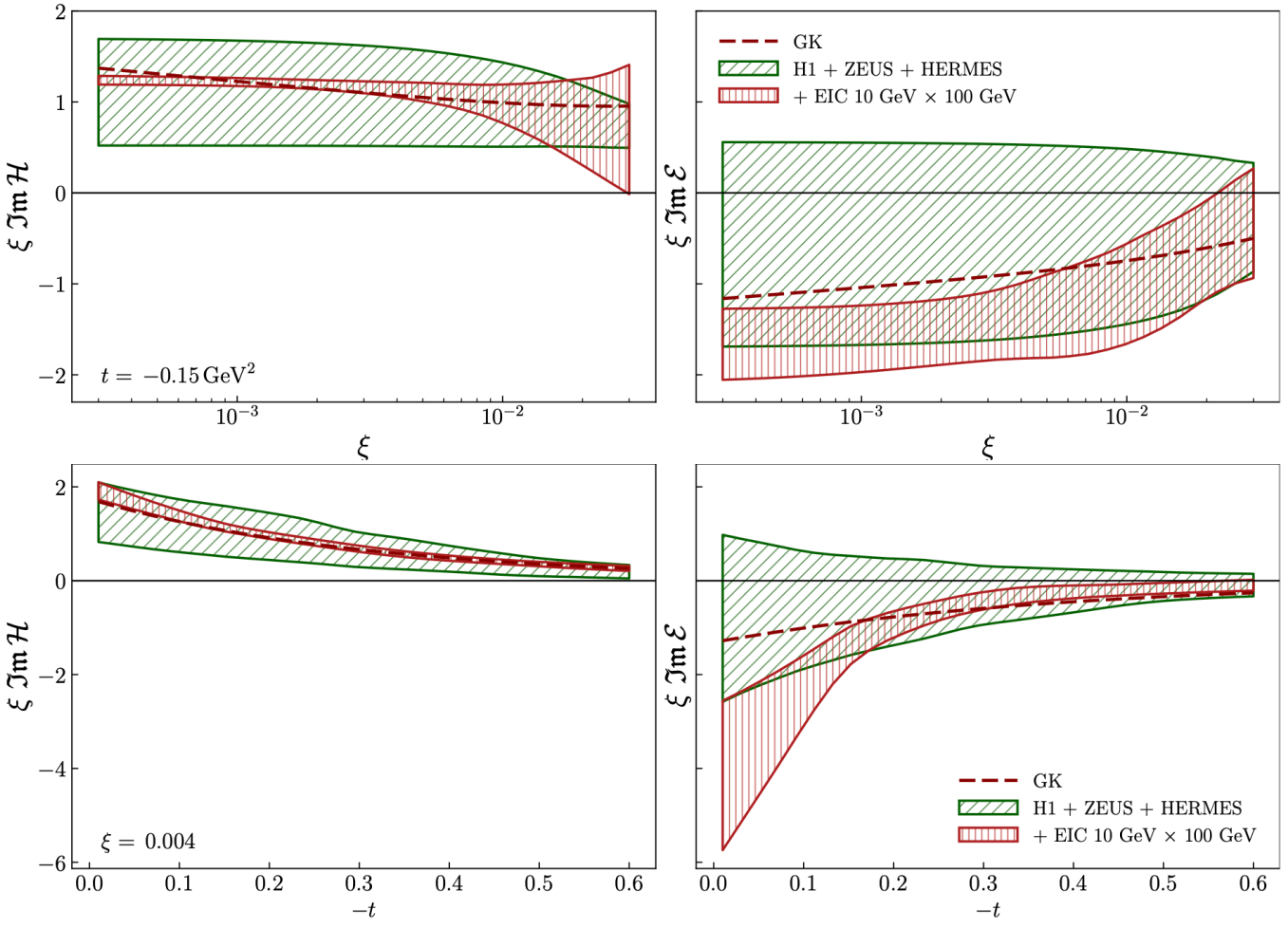

$Q^2 = 4\,\mathrm{GeV}^2$

Training a set of neural networks on world data with EIC pseudo-data shows a significant improvement on the current constraints.

E. Aschenauer *et al.*, PRD 112, 036010 (2025)

CFF constraints

Pawel Sznajder, Thursday

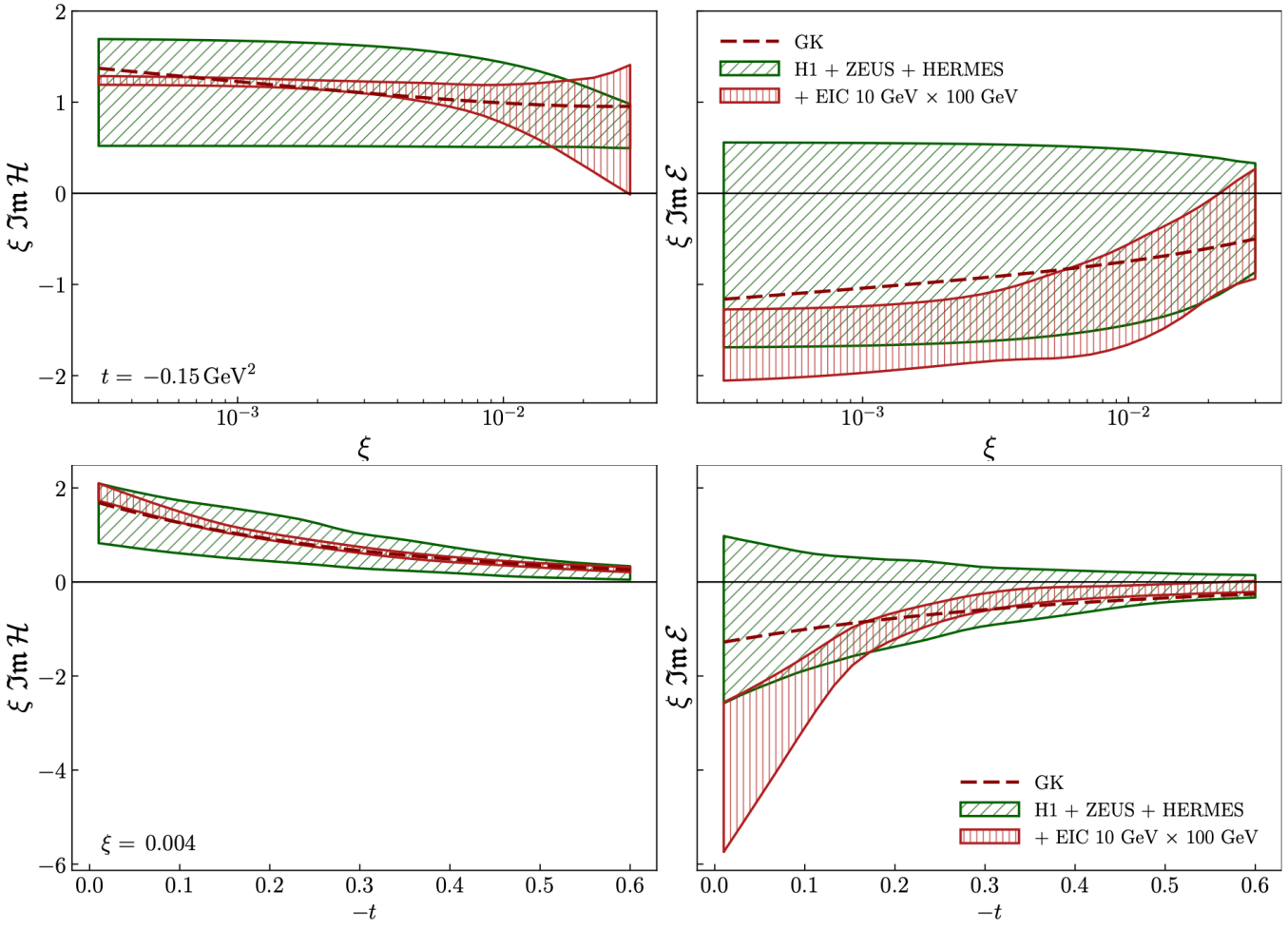

$Q^2 = 4\,\mathrm{GeV}^2$

Training a set of neural networks on world data with EIC pseudo-data shows a significant improvement on the current constraints.

E. Aschenauer *et al.*, PRD 112, 036010 (2025)

Nucleon tomography at EIC

DVCS pseudo-data $\mathcal{L}$=10 fb^{-1}

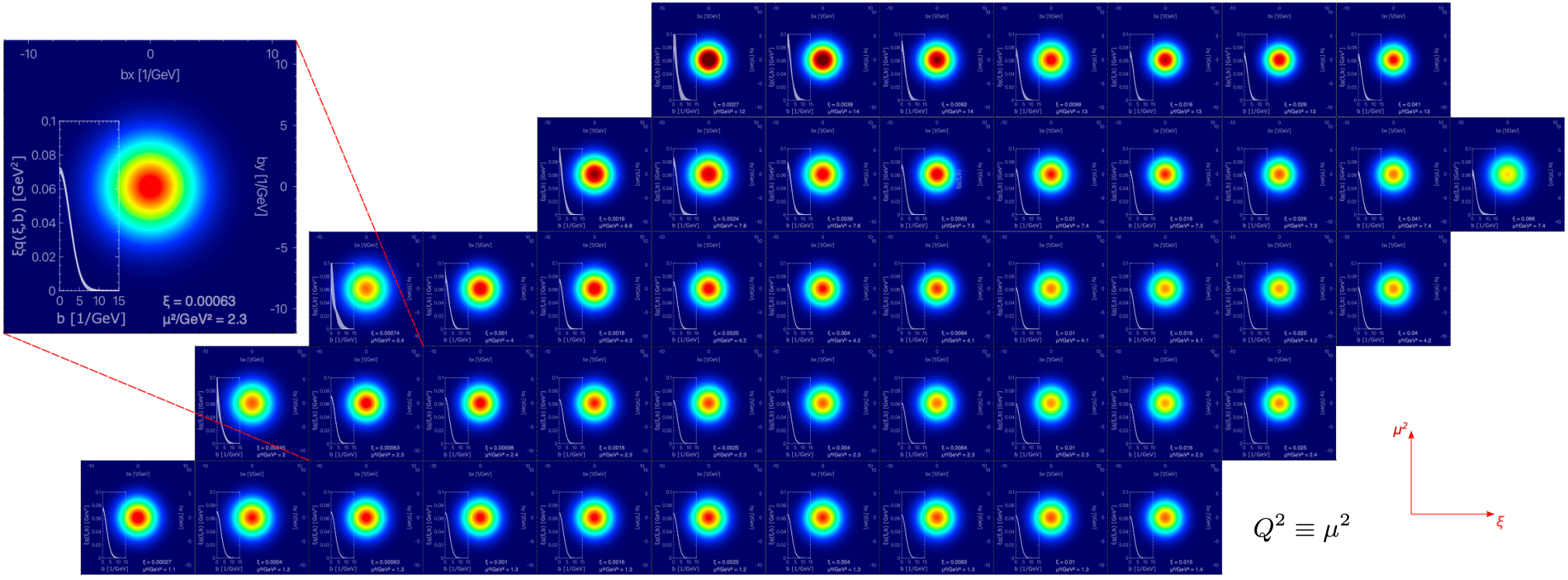

2D impact parameter distributions
obtained from DVCS pseudo-data at EIC

E. Aschenauer *et al.*, PRD 112, 036010 (2025)

Summary

- Generalised Parton Distributions contain information on orbital angular momentum contribution to nucleon spin, on mechanical properties of the nucleon and enable tomography of the nucleon.

- GPDs are accessible in exclusive processes, such as DVCS, TCS, hard exclusive meson production, Double DVCS, etc.

- A wealth of measurements in the valence region are coming from Jefferson Lab, while COMPASS at CERN is providing data in the sea-quark region.

- The Electron-Ion Collider will probe a wide range of phase space deep into the gluon sea.

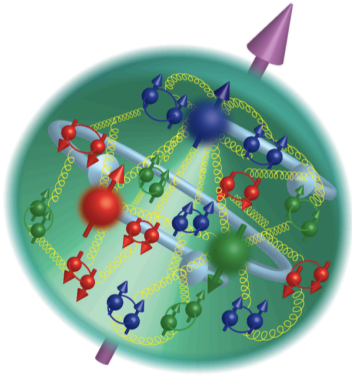

Many mysteries of nucleon structure are still to be revealed!


Thank you!
Any questions?


Back-up

The Interaction Region @ IP6

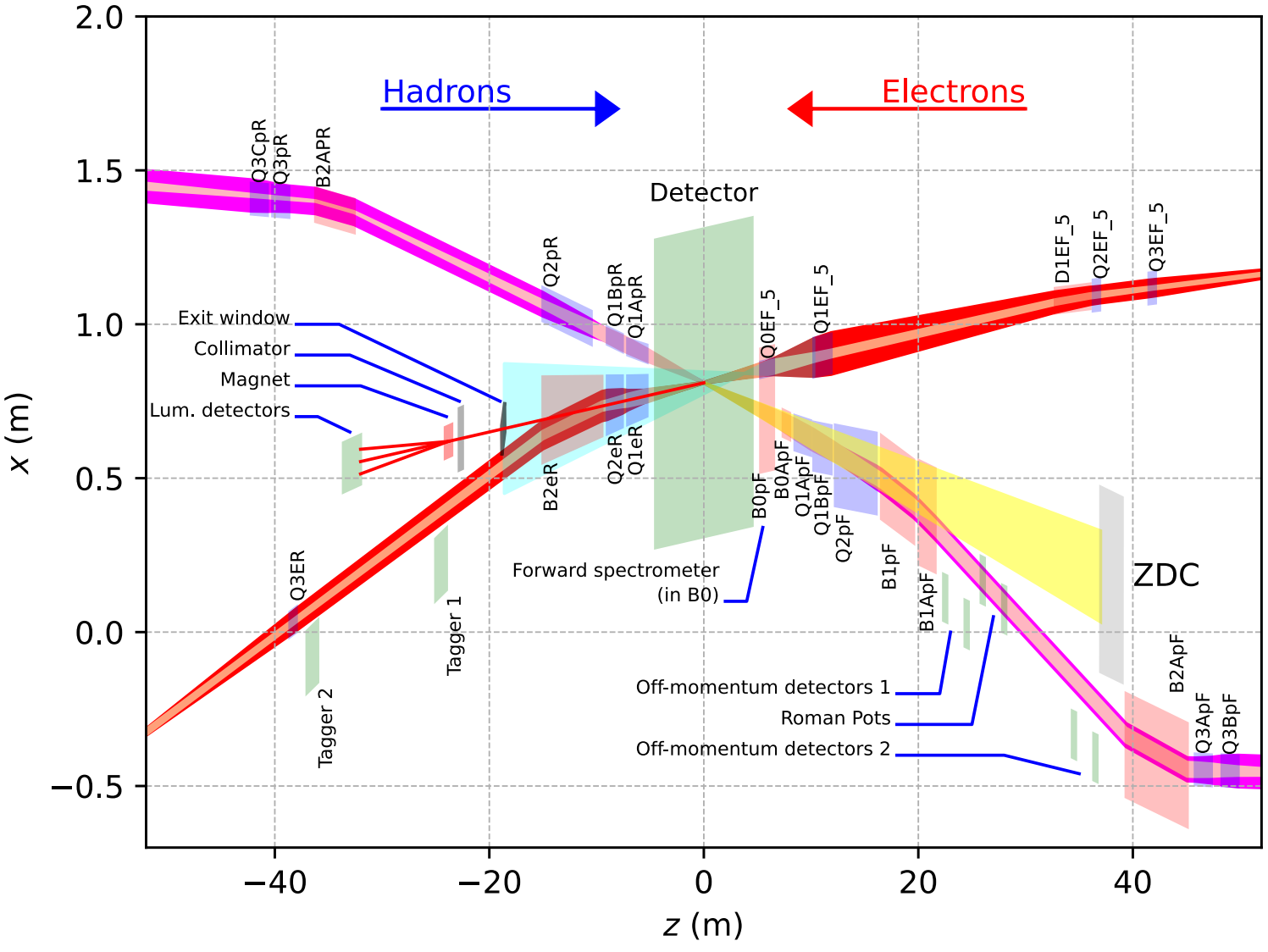

Crossing angle for the beams: 25 mrad.

Nucleon Tomography from GPDs

At a fixed Q^2, x_B and ξ=0 slope of GPD with t is related, via a Fourier Transform, to the transverse spatial distribution.

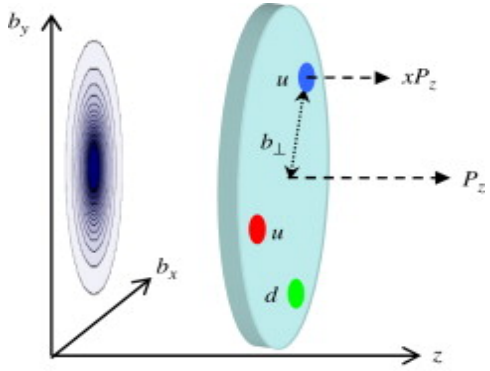

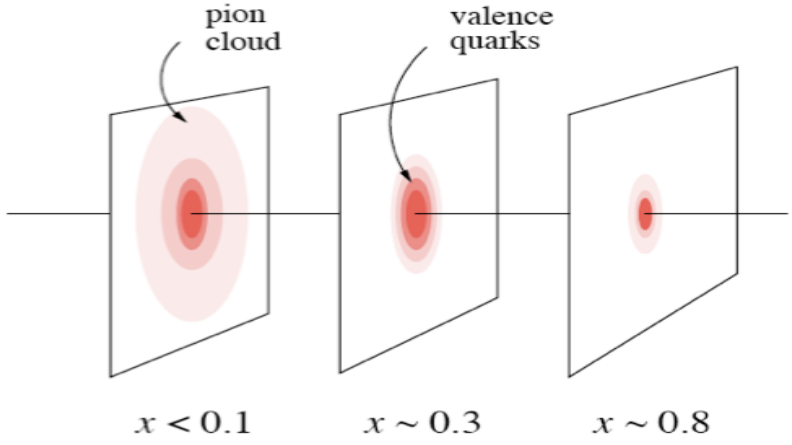

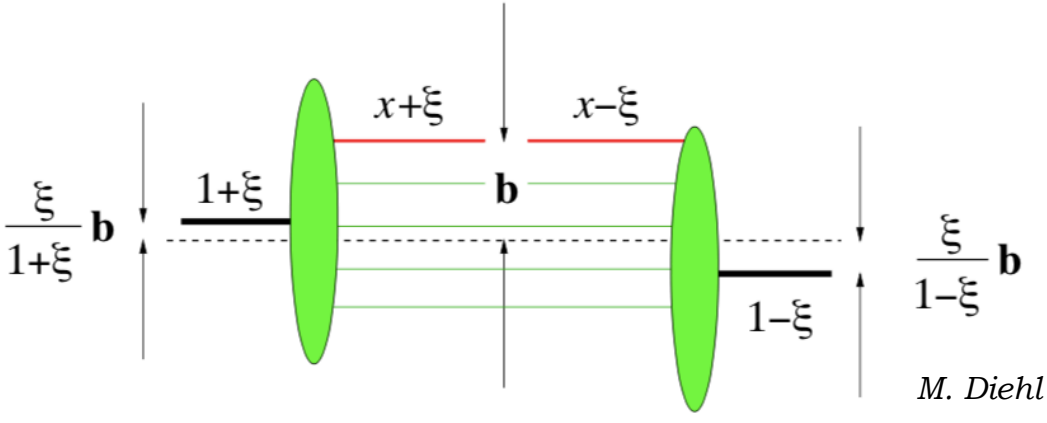

M. Diehl

Formally, the radial separation, **b**, *between the struck parton and the centre of momentum of the remaining spectators.*

Experimentally, can fit the t-dependence of structure functions (from meson-production) or Compton Form Factors (from DVCS/TCS) with an exponential:

$$eg: \quad \frac{d\sigma_U}{dt} = Ae^{Bt}$$

Towards nucleon tomography

- **Local fit** to extract CFFs: limits based on +/-5 * the VGG (Vanderhaeghen, Guichon, Guidal) model predictions using leading-twist amplitude based on Double Distributions.

- Assuming leading-twist and exponential dependence of GPD on t, using models to extrapolate to the zero skewness point $\xi = 0$ and assuming similar behaviour for u and d quarks there:

$$\langle b_\perp^2 \rangle^q(x) = -4 \frac{\partial}{\partial \boldsymbol{\Delta}_\perp^2} \ln H_-^q(x, 0, -\boldsymbol{\Delta}_\perp{}^2) \Big|_{\boldsymbol{\Delta}_\perp = 0}$$

$$H_-^q(x,0,t) \equiv H^q(x,0,t) + H^q(-x,0,t) \qquad t = \Delta^2$$

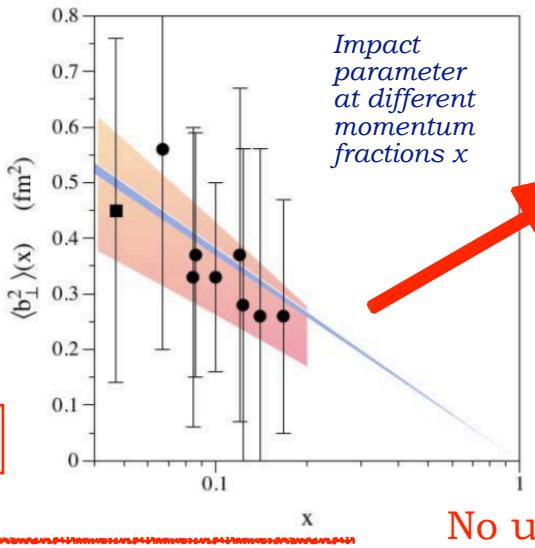

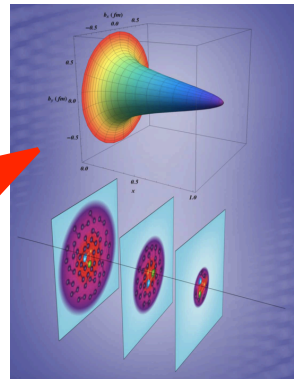

R. Dupré *et al.*, Eur. Phys. J **A 53,** (2017) 171

No uncertainties shown!

- **Global fits:** PARTONS framework using neural networks to minimise model-dependence in the extraction of CFFs.

We need more data from multiple channels and across a wide kinematic range!

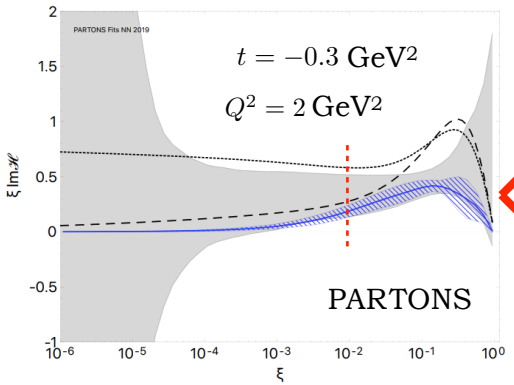

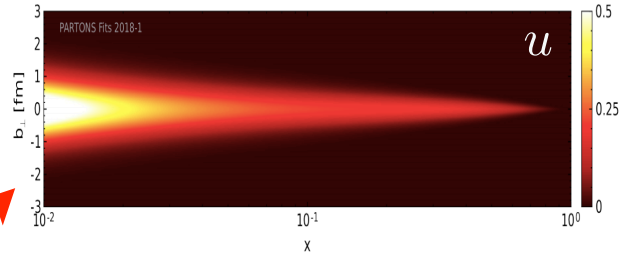

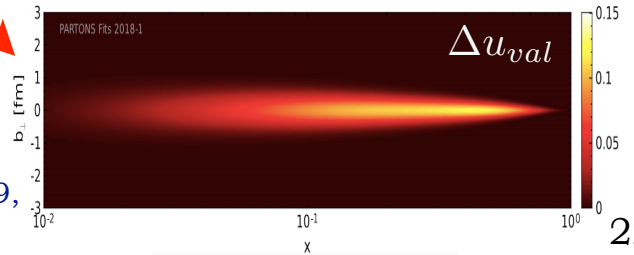

H. Moutarde *et al.*, Eur. Phys. J C79, 614 (2019)

Spin and pressure in the nucleon

- GPDs also provide indirect access to mechanical properties of the nucleon (encoded in the gravitational form factors, GFFs, of the energy-momentum tensor).

  X. D. Ji, PR**D 55**, 7114-7125 (1997)
  M. Polyakov, PL**B 555**, 57-62 (2016)

- Three scalar GFFs, functions of *t*: encode pressure and shear forces ($d_1(t)$), mass ($M_2(t)$) and angular momentum distributions ($J(t)$).

- Can be related to GPDs via sum rules: $\int x\,[H(x,\xi,t)+E(x,\xi,t)]\,\mathrm{d}x = 2J(t)$

$$\int xH(x,\xi,t)\mathrm{d}x = M_2(t) + \frac{4}{5}\xi^2 d_1(t)$$

(Ji's relation)

$$J_N = \frac{1}{2} = \frac{1}{2}\Sigma_q + L_q + J_g$$

- $d_1(t)$ (D-term) "last unknown global property of the nucleon" – can be accessed via the $\mathcal{R}e$ and $\mathcal{I}m\ \mathcal{H}$:

Dispersion relation: $\mathrm{Re}\mathcal{H}(\xi,t) = \int_{-1}^{1}\left(\frac{1}{\xi-x}-\frac{1}{\xi+x}\right)\mathrm{Im}\mathcal{H}(\xi,t)\ dx + \Delta(t).$

Assuming double-distribution parametrisation: $\Delta(t) \propto d_1(t)$

Spin and pressure

- GPDs provide indirect access to mechanical properties of the nucleon (encoded in the gravitational form factors, GFFs, of the energy-momentum tensor).

X. D. Ji, PR**D 55**, 7114-7125 (1997) M. Polyakov, PL**B 555**, 57-62 (2003)

- Four GFFs, functions of *t*, of which three are related to moments of GPDs: they encode pressure and shear forces ($d_1(t)$), mass ($M_2(t)$) and angular momentum distributions ($J(t)$):

$$\int x\,[H(x,\xi,t)+E(x,\xi,t)]\,\mathrm{d}x = 2J(t)$$

$$\int xH(x,\xi,t)\mathrm{d}x = M_2(t)+\frac{4}{5}\xi^2 d_1(t)$$

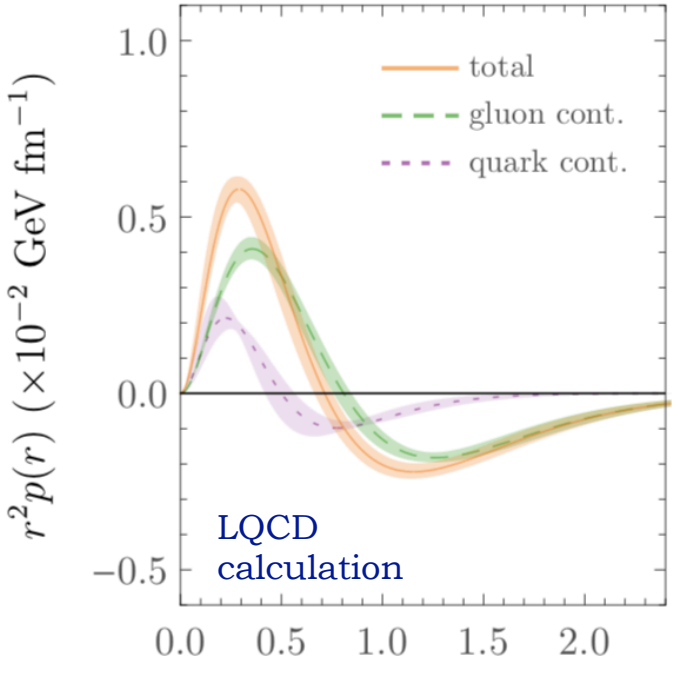

P. Shanahan, W. Detmold, PRL 122,072003 (2019)

- The D-term: "last unknown global property of the nucleon" -- can be related to spatial distribution of shear forces and pressure within the nucleon.

- Possibilities of "imaging" spatial distributions of angular momentum: C. Lorcé, M. Montovani, B. Pasquini, PL**B 776**, 38-47 (2018)

Imaging pressure within the nucleon

- Information on pressure and shear forces contained in *d*-term:

$$\int xH(x,\xi,t)\mathrm{d}x = M_2(t) + \frac{4}{5}\xi^2 d_1(t)$$

- Model-dependent extraction

V. Burkert, L. Elouadrhiri, F.-X. Girod, Nature **557**, 396-399 (2018)

- Neural net analysis, however: d-term almost unconstrained and consistent with zero

K. Kumerički, Nature **570**, E1-E2 (2019)

Possibility of extracting pressure distributions! But more data needed.

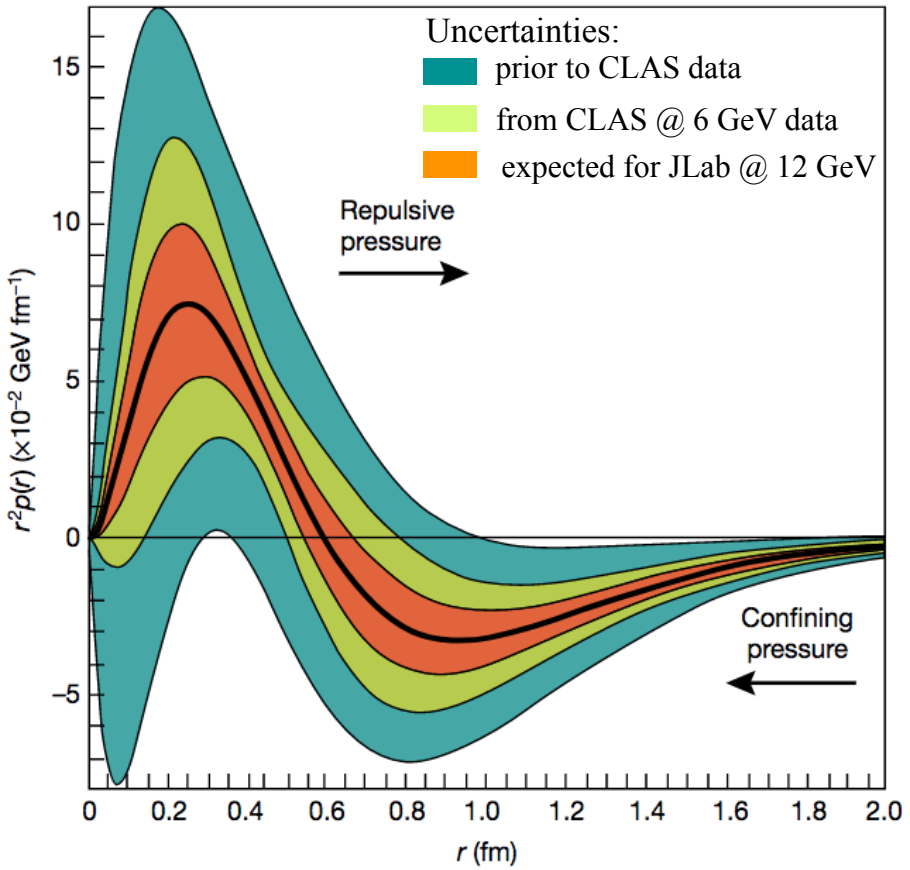

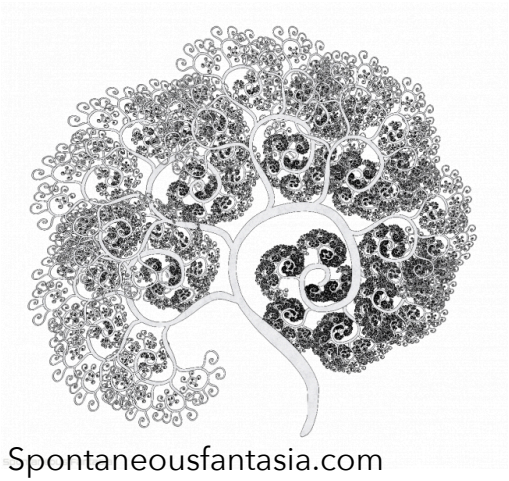
Spontaneousfantasia.com

Order and Twist

Leading order (LO)

Next-to-leading order (NLO)

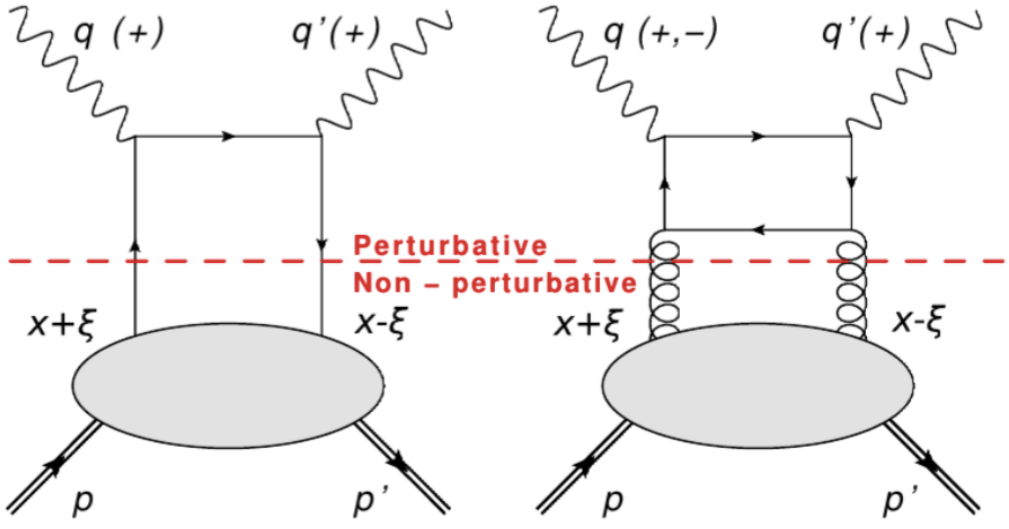

- Twist: powers of $\frac{1}{\sqrt{Q^2}}$ in the DVCS amplitude. Leading-twist (LT) is twist-2.

- Order: introduces powers of α_s

- Leading Order (LO) requires $Q^2 >> M^2$ (M: target mass)

GPDs through meson-production

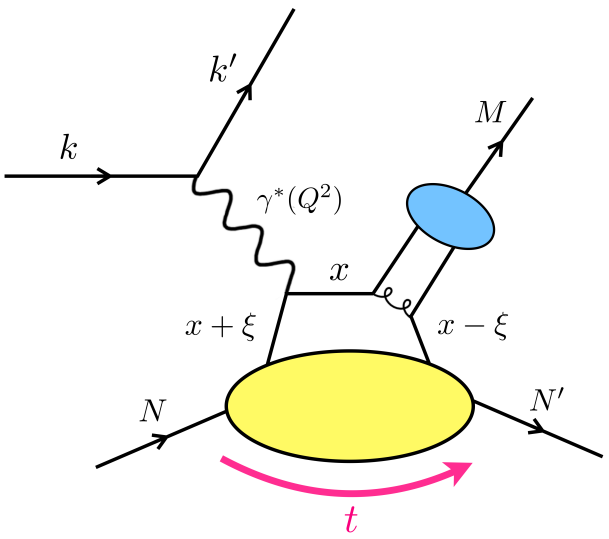

- Hard exclusive electro-production of vector mesons gives access to gluon GPDs, particularly clean in heavy mesons: J/Ψ and Υ

Hard scale in the scattering given by: $Q^2 + M_v^2$

Hence: $x_v = \frac{Q^2+M_v^2}{2\mathbf{p}\cdot\mathbf{q}}$

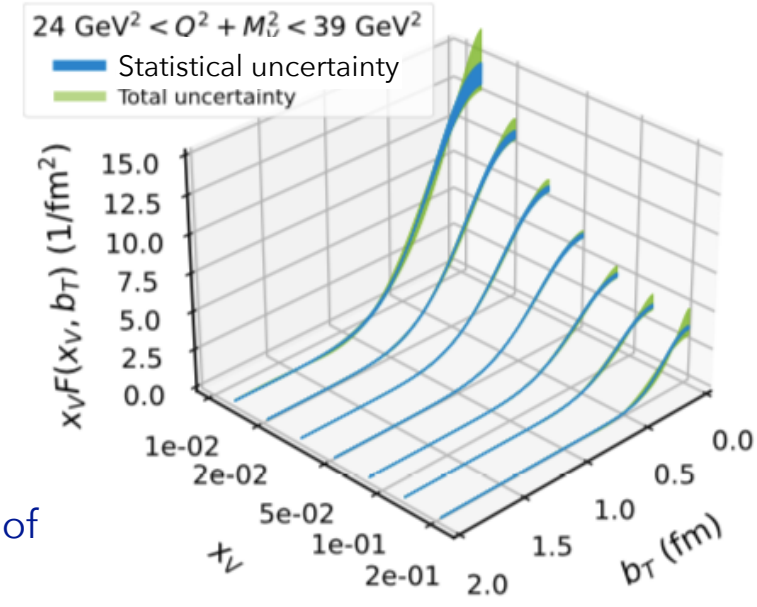

- Light vector-meson production additionally enables flavour-decomposition of GPDs.

Fourier transform of J/Psi-production cross-section

- Light pseudo-scalar meson production gives, at high Q^2, access to parity-odd GPDs: $\tilde{H}, \tilde{E}$ and at low Q^2 to chiral-odd, transversity GPDs which are not accessible at leading-twist in DVCS processes.

Timelike Compton Scattering

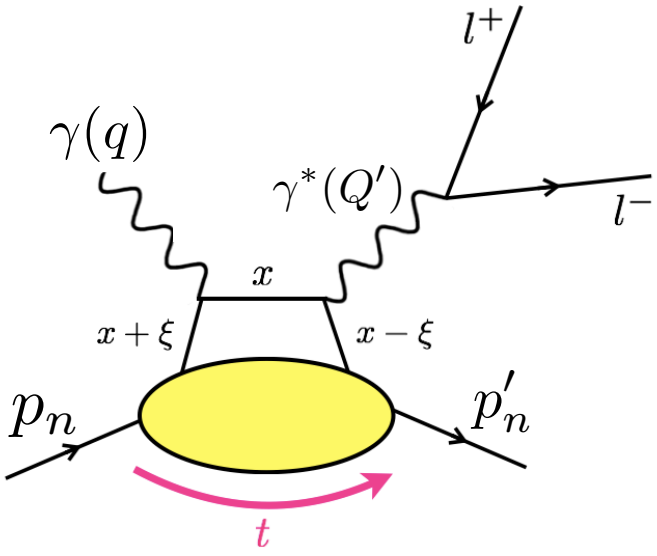

- Time-reversal process of DVCS: parametrised in terms of same Compton Form Factors (their complex conjugates).
  - Verification of GPD universality.
  - Another route to access the D-term.

- Factorisation ensured by hard scale of γ* virtuality:

$$\frac{t}{Q'^2} << 1$$

$$Q' = l^+ + l^- \qquad \xi = \frac{\tau}{2-\tau}$$

$$s = (q + p_n)^2$$

$$\tau = \frac{Q'^2}{s - m_p^2}$$

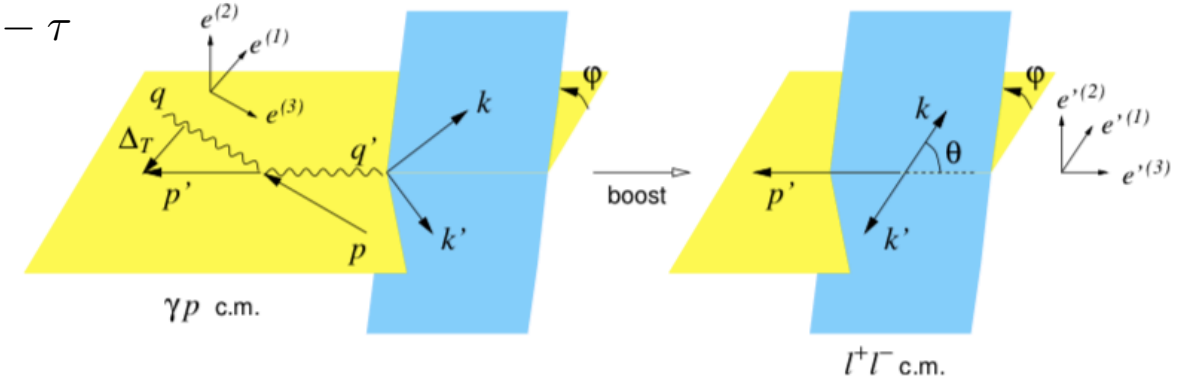

θ: angle between l^+ and scattered proton in lepton CMS

Bethe-Heitler in TCS

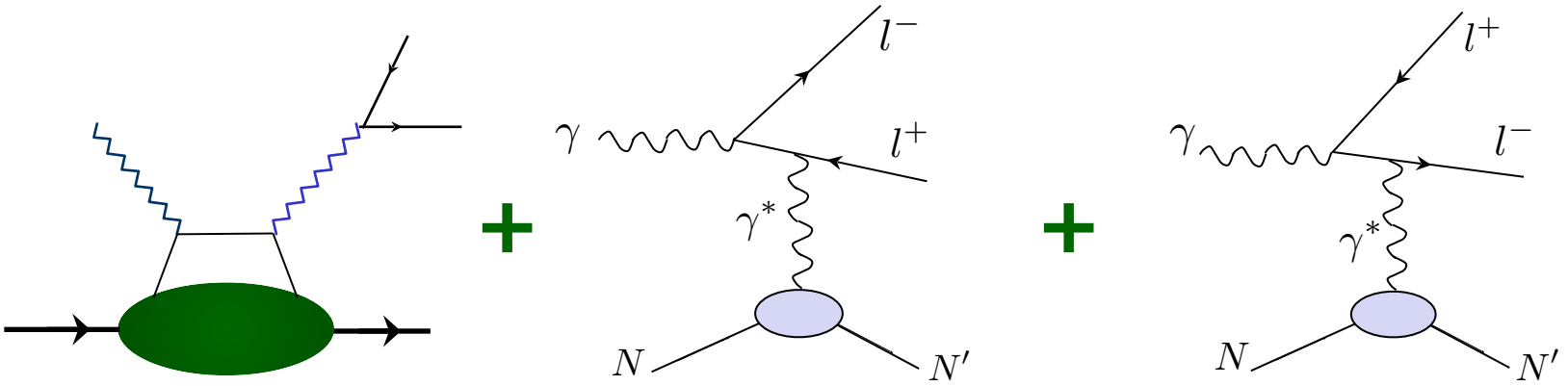

- Similarly to DVCS, TCS process interferes with Bethe-Heitler at the amplitude level.

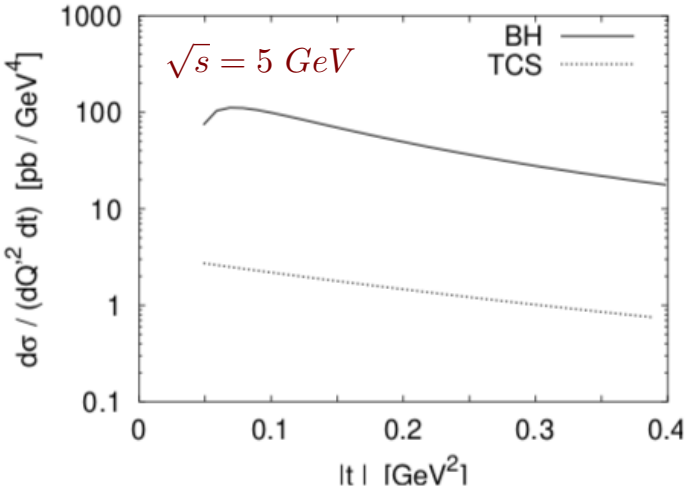

$$\sigma(\gamma p \to p' e^+ e^-) = \sigma_{BH} + \sigma_{TCS} + \sigma_{INT}$$

- Cross-sections hard to obtain! Suppressed by factor of 100 wrt BH.
- Look to other observables.

E.R. Berger, M. Diehl, B. Pire. EPJ C, 23(4):675?689 (2002)

TCS observables

- Unpolarised cross-sections:

  sensitive to $\mathcal{Re}\ \mathcal{H}$.

$$\frac{d^4\sigma_{INT}}{dQ'^2 dt d\Omega} = A\frac{1+\cos^2\theta}{\sin\theta}[\cos\phi\ \mathrm{Re}\tilde{M}^{--} - \nu\cdot\sin\phi\ \mathrm{Im}\tilde{M}^{--}]$$

$$\tilde{M}^{--} = \left[F_1\mathcal{H} - \xi(F_1+F_2)\tilde{\mathcal{H}} - \frac{t}{4m_p^2}F_2\mathcal{E}\right]$$

suppressed

- Circularly-polarised photon cross-section: access to $\mathcal{Im}\ \mathcal{H}$.
- More promising observables: asymmetries and cross-section ratios.
- Photon-polarisation (beam-spin) asymmetry:

$$A_{\odot U} = \frac{d\sigma^+ - d\sigma^-}{d\sigma^+ + d\sigma^-}$$

access to $\mathcal{Im}\ \mathcal{H}$

- Forward - backward asymmetry:

$$A_{FB}(\theta,\phi) = \frac{d\sigma(\theta,\phi) - d\sigma(180^\circ-\theta, 180^\circ+\phi)}{d\sigma(\theta,\phi) + d\sigma(180^\circ-\theta, 180^\circ+\phi)}$$

access to $\mathcal{Re}\ \mathcal{H}$

P. Chatagnon et al. (CLAS): arXiv:2108.11746 [hep-ex], *accepted (PRL)*

TCS observables

- The *R* ratio of integrated cross-sections:

Integrated cross-section over θ and φ

$$R(\sqrt{s}, Q'^2, t) = \frac{\int_0^{2\pi} d\phi \cos(\phi) \frac{dS}{dQ'^2 dt d\phi}}{\int_0^{2\pi} d\phi \frac{dS}{dQ'^2 dt d\phi}}$$

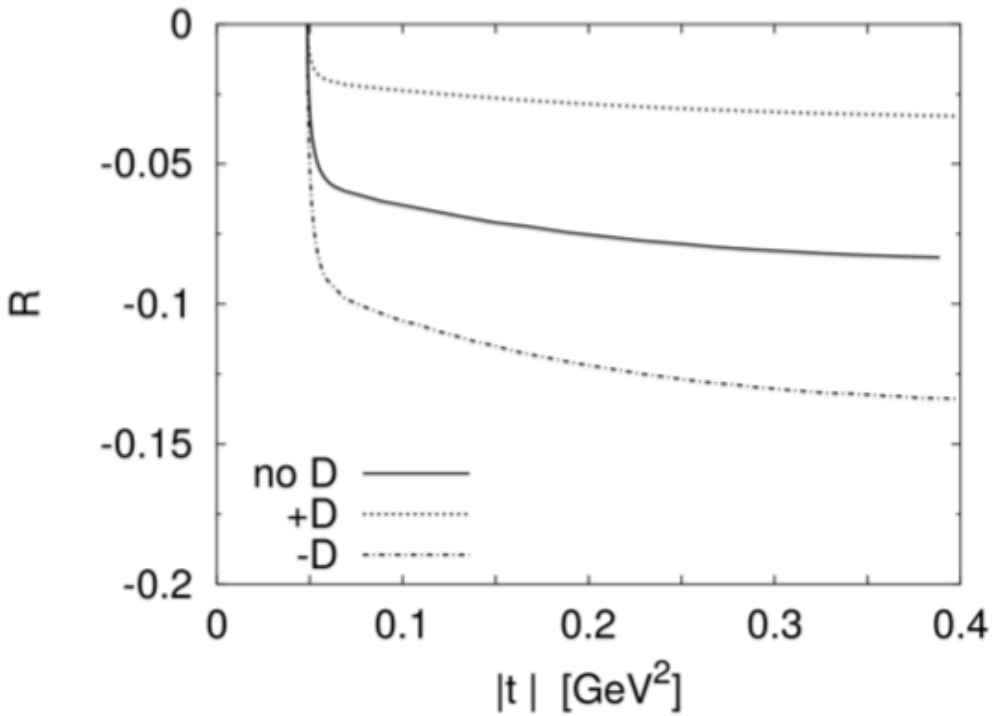

Sensitivity to $\mathcal{Re}\,\mathcal{H}$ and the D-term, but integrated over some of the phase-space: susceptible to detector acceptance effects.

E.R. Berger, M. Diehl, B. Pire. EPJ C, 23(4):675–689 (2002).

Jefferson Lab: 6 GeV era

CEBAF: Continuous Electron Beam Accelerator Facility.

- Energy up to ~6 GeV
- Energy resolution $\delta E/E_e \sim 10^{-5}$
- Electron polarisation up to ~85%

Hall A:

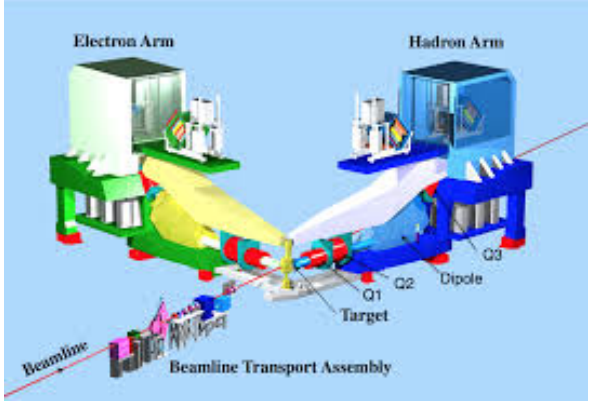

- High resolution($\delta p/p = 10^{-4}$) spectrometers, very high luminosity.

Hall B: CLAS

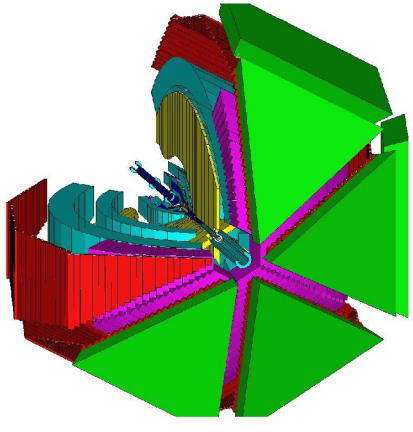

- Very large acceptance, detector array for multi-particle final states.

Hall C:

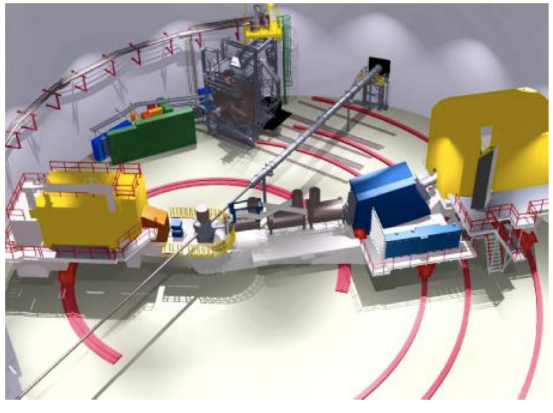

- Two movable spectrometer arms, well-defined acceptance, high luminosity

DVCS in Hall C

Detect electron with (Super) High Momentum Spectrometer, (S)HMS.

Detect photon in $PbWO_4$ calorimeter.

Sweeping magnet to reduce backgrounds in calorimeter.

Reconstruct recoiling proton through missing mass.

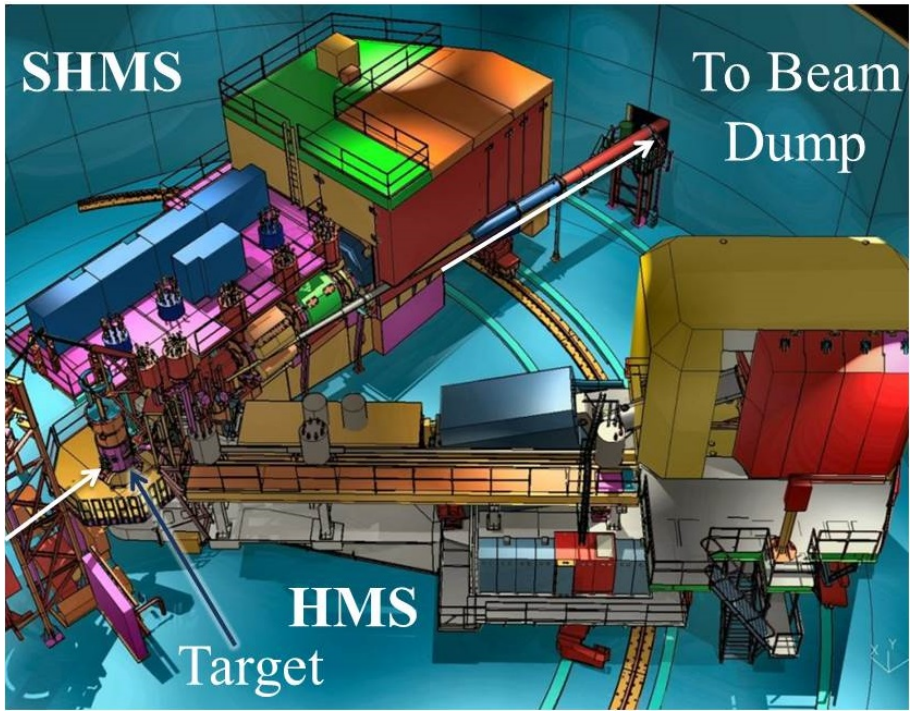

Similar principle applied in Hall A

DVCS in Hall A

* 15 cm long liquid H_2 target
* Luminosity =10^{37} cm^{-2}s^{-1}

$$ep \rightarrow e'\gamma(p')$$

Reconstructed through missing mass

Detected in High Resolution Spectrometer (SRS)

Detected in PbF_2 Calorimeter

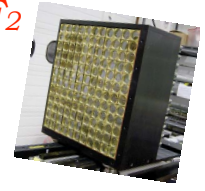

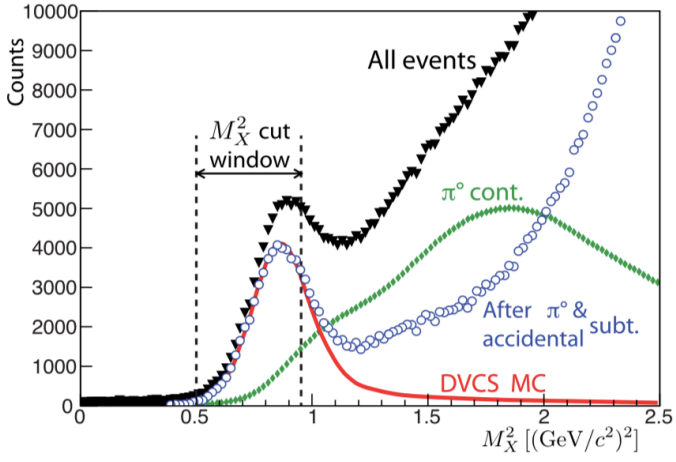

M. Defurne *et al*, ***PRC* 92** (2015) 055202.

* **E00-110 experiment** (2004): 5.75 GeV polarised electron beam
* Measure Q^2-dependence (Q^2: 1.5, 1.9, 2.3 GeV^2) of DVCS-BH cross-sections at fixed x_B (0.36) and x_B dependence at constant Q^2.

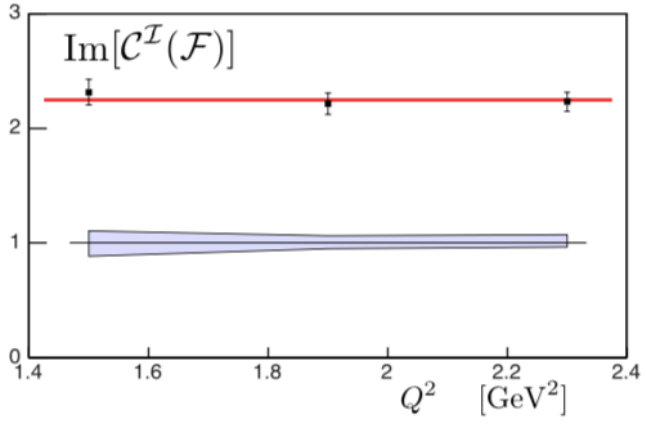

* **E07-004 experiment** (2010): Energy scan for fixed x_B, Q^2:

Q^2 (GeV^2)	x_B	E^{beam} (GeV)	$-t$ (GeV^2)
1.50	0.36	3.355 5.55	0.18, 0.24, 0.30
1.75	0.36	4.455 5.55	0.18, 0.24, 0.30, 0.36
2.00	0.36	4.455 5.55	0.18, 0.24, 0.30, 0.36

M. Defurne *et al*, ***PRC* 92** (2015) 055202.

High-precision cross-sections: Hall A

* High precision cross-section measurement in a small kinematic region: Generalised Rosenbluth separation of the DVCS^2 (scales as E_e^2) and the BH-DVCS interference (scales as E_e^3) terms. Addition of NLO and/or higher-twist improve model agreement.

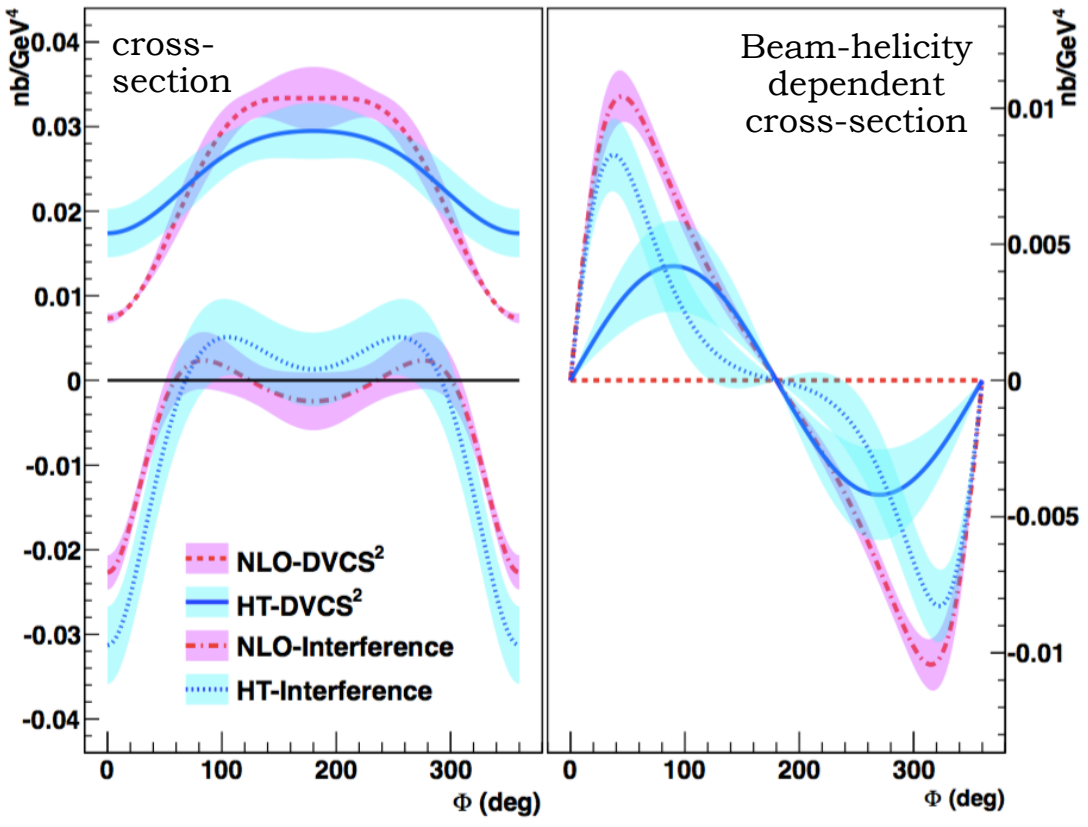

Q^2: 1.5, 1.9, 2.3 GeV^2 at fixed x_B 0.36
-t: 0.18, 0.24, 0.30

E_e: 4.5, 5.6 GeV.

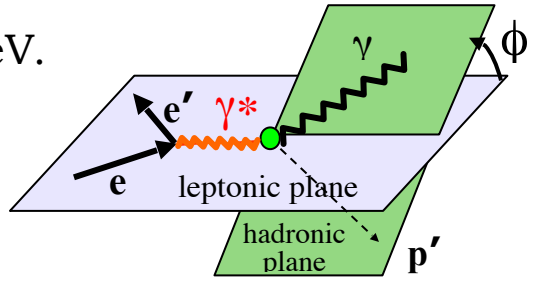

* Significant differences between pure DVCS and interference contributions.

* If NLO: sensitivity to gluons.

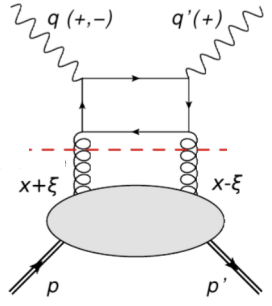

* Separation of HT and NLO effects requires scans across wider ranges of Q^2 and beam energy: JLab12.

M. Defurne *et al*, ***Nature Communications 8*** (2017) 1408.

Large kinematic coverage: CLAS

- Unpolarised DVCS cross-sections and helicity-dependent cross-section differences in a wide kinematic range:

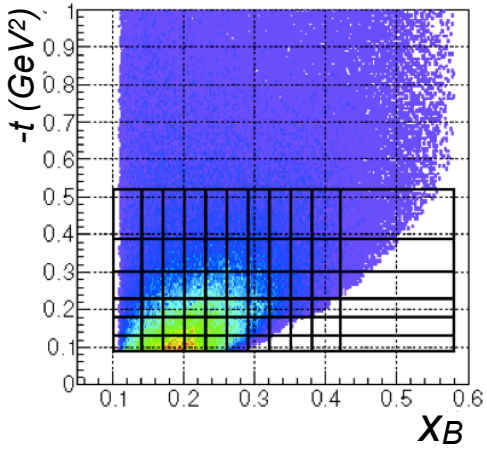

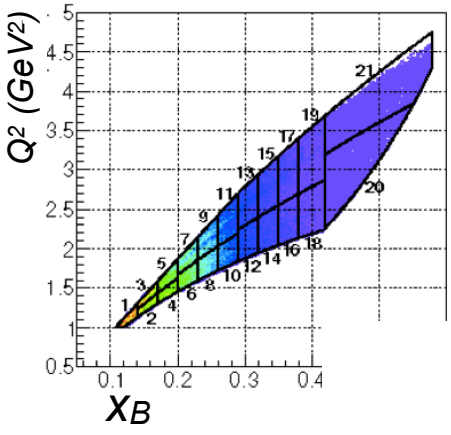

BH only
VGG *(Vanderhaeghen, Guichon, Guidal) - H only*
KM10 (Kumericki, Mueller) *includes strong* $\tilde{H}$
KM10a *(sets* $\tilde{H}$ *to zero)*
KMS *(Kroll, Moutarde, Sabatié, tuned on low* x_B *meson-production data)*

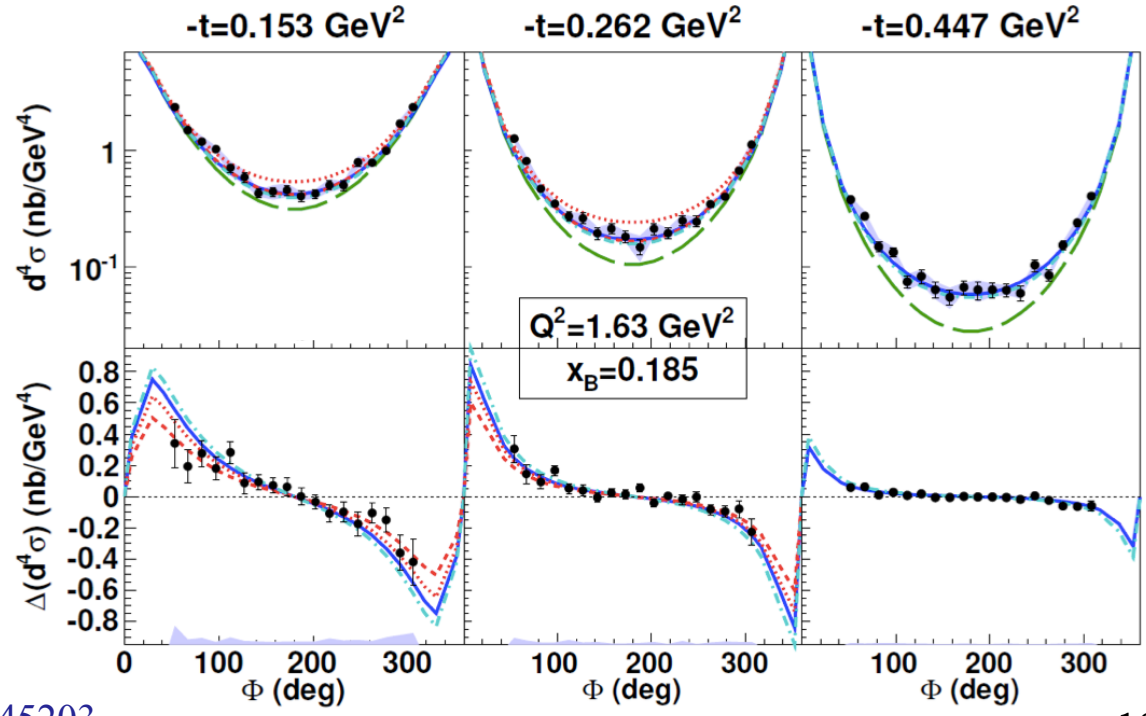

- Widest phase space coverage in valence quark region: CFF constraints.

- Dominance of GPD *H* in unpolarised cross-section.

H.-S. Jo *et al* (CLAS), ***PRL* 115** (2015) 212003
N. Hirlinger Saylor *et al* (CLAS), ***PRC* 98** (2018) 045203

DVCS asymmetries @ CLAS

High statistics, large kinematic coverage, strong constraints on fits, simultaneous fit of BSA, TSA and DSA at common kinematics from the same dataset:

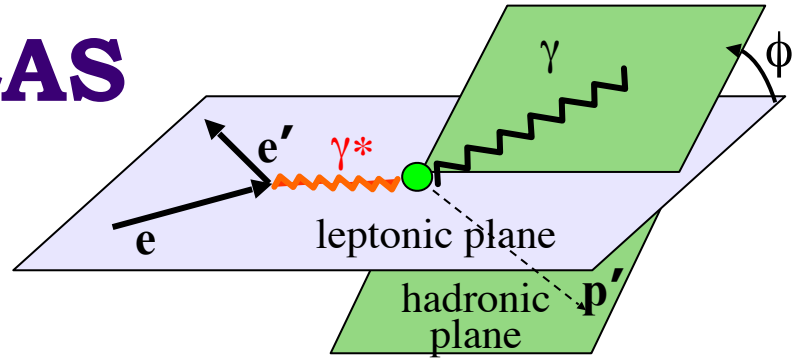

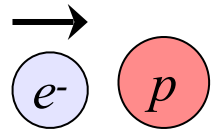

Beam-spin asymmetry (BSA):

$$\Delta\sigma_{LU} \sim \sin\phi\, \Im(F_1 H + \xi G_M \tilde{H} - \frac{t}{4M^2} F_2 E)\, d\phi$$

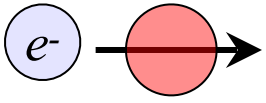

Target-spin asymmetry:

$$\Delta\sigma_{UL} \sim \sin\phi\, \Im(F_1 \tilde{H} + \xi G_M (H + \frac{x_B}{2} E) - \xi \frac{t}{4M^2} F_2 \tilde{E} + ...)\, d\phi$$

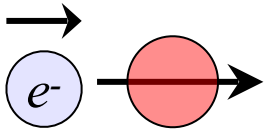

Double-spin asymmetry:

$$\Delta\sigma_{LL} \sim (A + B\cos\phi)\, \Re(F_1 \tilde{H} + \xi G_M (H + \frac{x_B}{2} E) + ...) d\phi$$

F_1, F_2: Dirac, Pauli form factors

→ Constraints on CFFs H and $\tilde{H}$

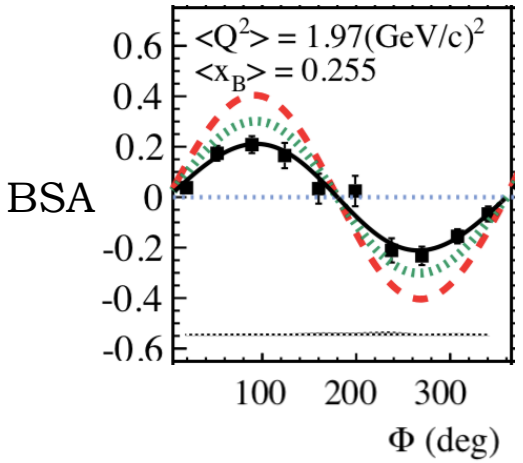

E. Seder *et al* (CLAS), ***PRL* 114** (2015) 032001

S. Pisano *et al* (CLAS), ***PRD* 91** (2015) 052014

F.-X. Girod *et al* (CLAS), ***PRL* 100** (2008) 162002

Beam- and target-spin asymmetries

CLAS

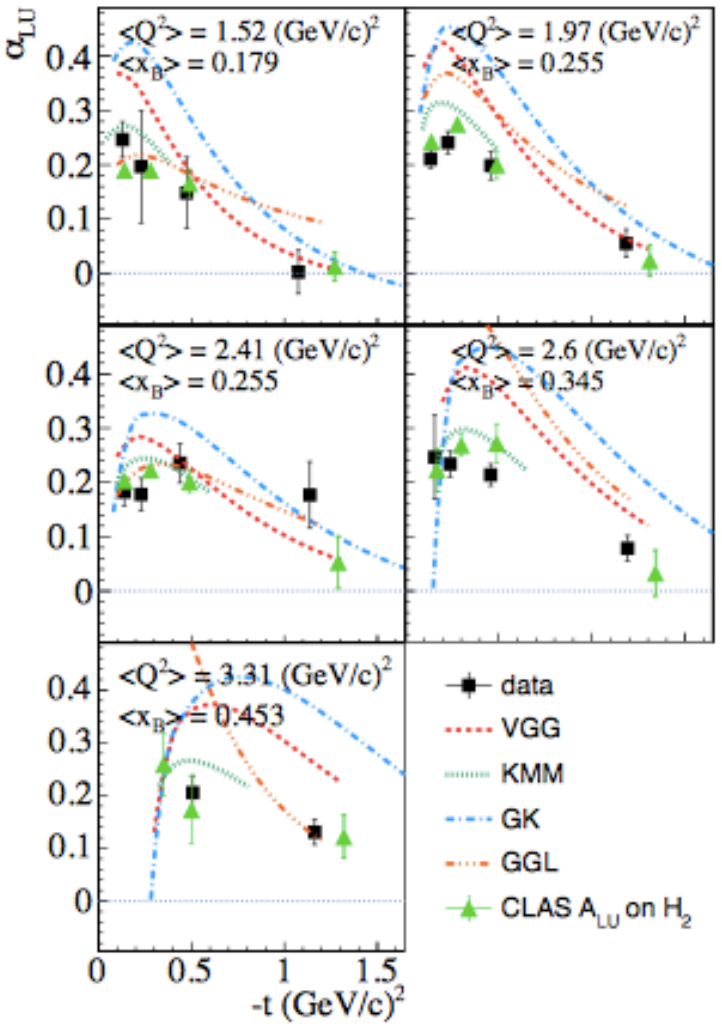

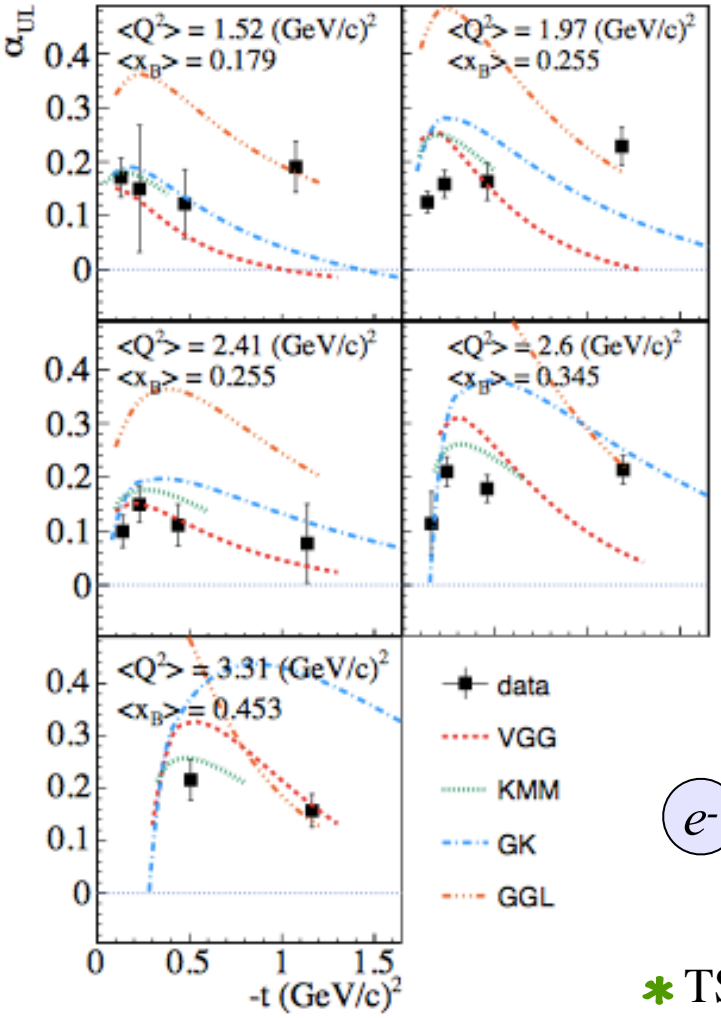

$$A = \frac{\alpha sin\phi}{1+\beta cos\phi}$$

GGL: Goldstein, Gonzalez, Liuti

GK: Kroll, Moutarde, Sabatié

KMM: Kumericki, Mueller, Murray

VGG: Vanderhaeghen, Guichon, Guidal

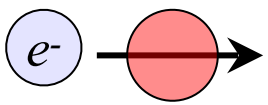

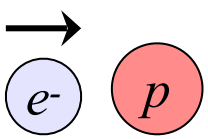

S. Pisano *et al* (CLAS), ***PRD* 91** (2015) 052014

E. Seder *et al* (CLAS), ***PRL* 114** (2015) 032001

* TSA shows a flatter distribution in *t* than BSA.

Compton Form Factors from CLAS data

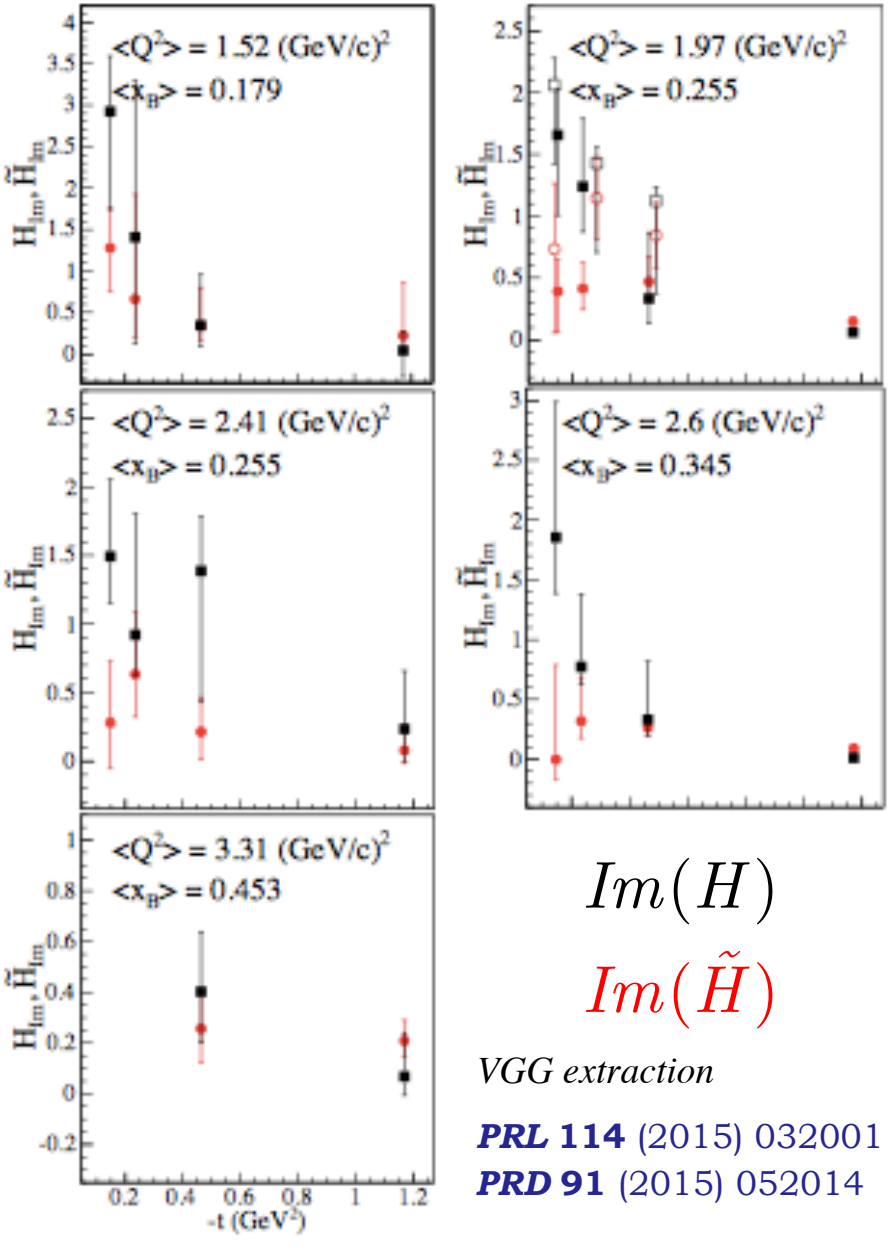

$Im(H)$

$Im(\tilde{H})$

VGG extraction

***PRL* 114** (2015) 032001
***PRD* 91** (2015) 052014

- Extracted using local fits to cross-sections and asymmetries, constrained by the VGG (Vanderhaeghen, Guichon, Guidal) model.
- Information on relative distributions of quark momenta (PDFs) and quark helicity, $\Delta q(x)$

$$H(x,0,0) = q(x) \quad \tilde{H}(x,0,0) = \Delta q(x)$$

- Indications that axial charge is more concentrated than electromagnetic charge.

$$\int_{-1}^{+1} H dx = F_1 \quad \int_{-1}^{+1} \tilde{H}\, dx = G_A$$

- Slope flatter towards higher-*x*: valence quarks are at centre, lower-*x* quarks at periphery.

Global analysis of all available data needed.

DVCS on the neutron: Hall A

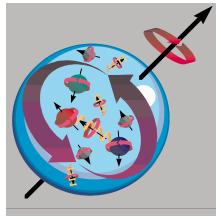

$$J_N = \frac{1}{2} = \frac{1}{2}\Sigma_q + L_q + J_g$$

* Ji's relation: $J^q = \frac{1}{2} - J^g = \frac{1}{2}\int_{-1}^{1} x dx \left\{ H^q(x,\xi,0) + E^q(x,\xi,0) \right\}$

* H^q in DVCS off the proton, first experimental constraint on E^q from neutron-DVCS beam-spin asymmetry.

$$\Delta\sigma_{LU} \sim \sin\phi\ \mathbf{Im}\{F_1 H + \xi(F_1+F_2)H - kF_2 E\}d\phi$$

M. Mazouz et al, PRL 99 (2007) 242501

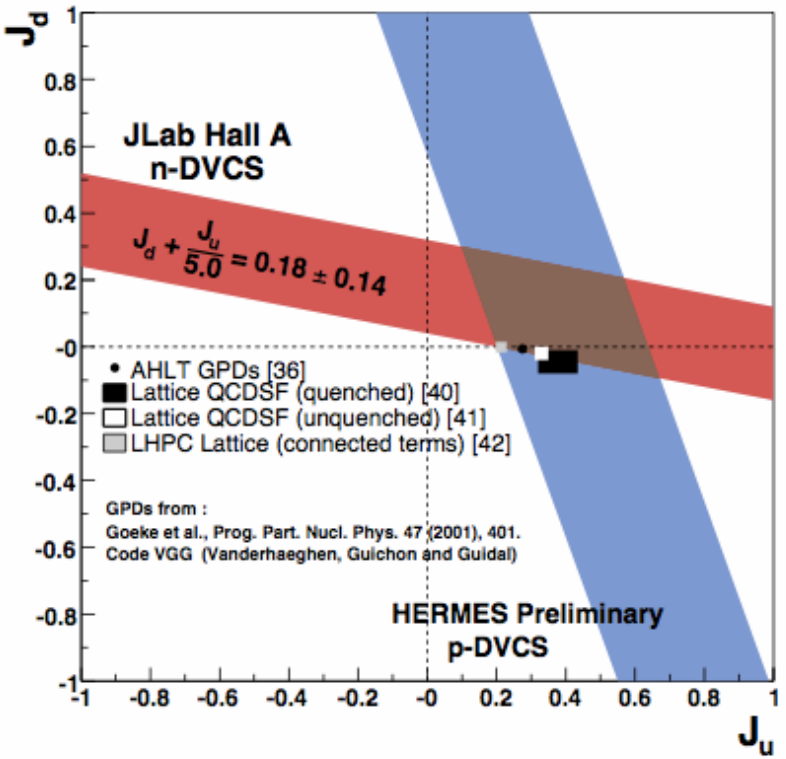

* Gives constraints on orbital angular momentum of quarks: the spin puzzle.

* Rosenbluth separation of interference & DVCS terms underway in neutron-DVCS cross-sections: E_e = 4.5 and 5.5 GeV (experiment E08-025).

LD_2 target $\langle Q^2 \rangle$ = 1.75 GeV^2 $\langle x_B \rangle$ = 0.36

DVCS on the bound proton

CLAS

- Beam spin asymmetry in DVCS from bound protons in ^{4}He (gas target).

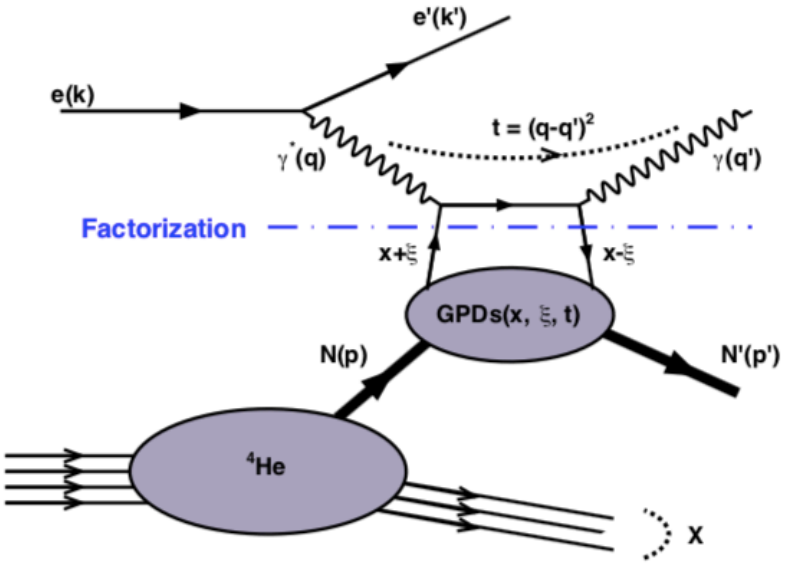

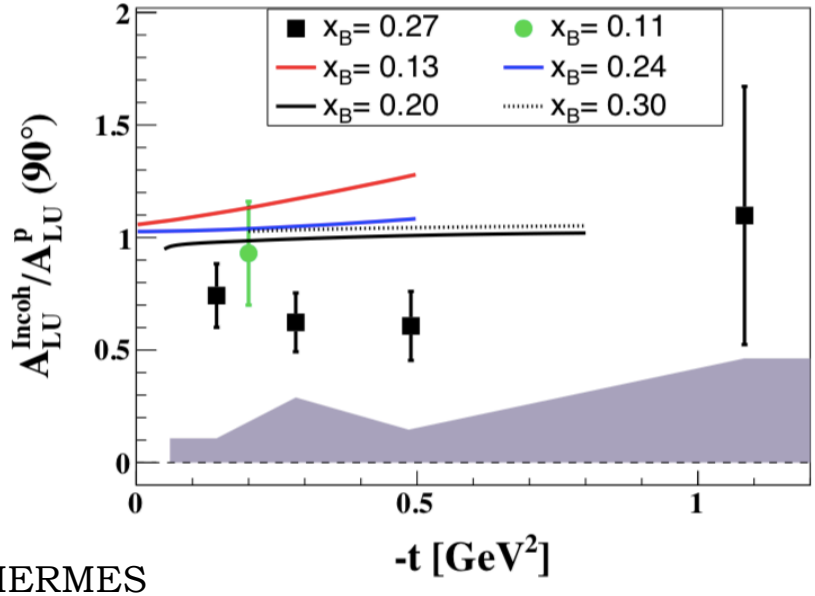

HERMES

Off-shell: S. Liuti, K. Taneja, PRC72, 032201 (2005)

On-shell: V. Guzey, A. Thomas, K. Tsushima, PLB673, 9 (2009)

- 25% - 40% lower asymmetries for bound proton compared to free, no strong dependence on *t*.
- Medium-modification effects, initial/final state interactions?

M. Hattawy *et al*, PRL **123**, 032502 (2019)

11 GeV era DVCS Cross-sections: Halls A and C

Experiments:
E12-06-114 (Hall A, 100 days),
E12-13-010 (Hall C, 53 days)

Unpolarised liquid H_2 target:

- Beam energies: 6.6, 8.8, 11 GeV
- Scans of Q^2 at fixed x_B.
- Hall A: aim for absolute cross-sections with 4% relative precision.

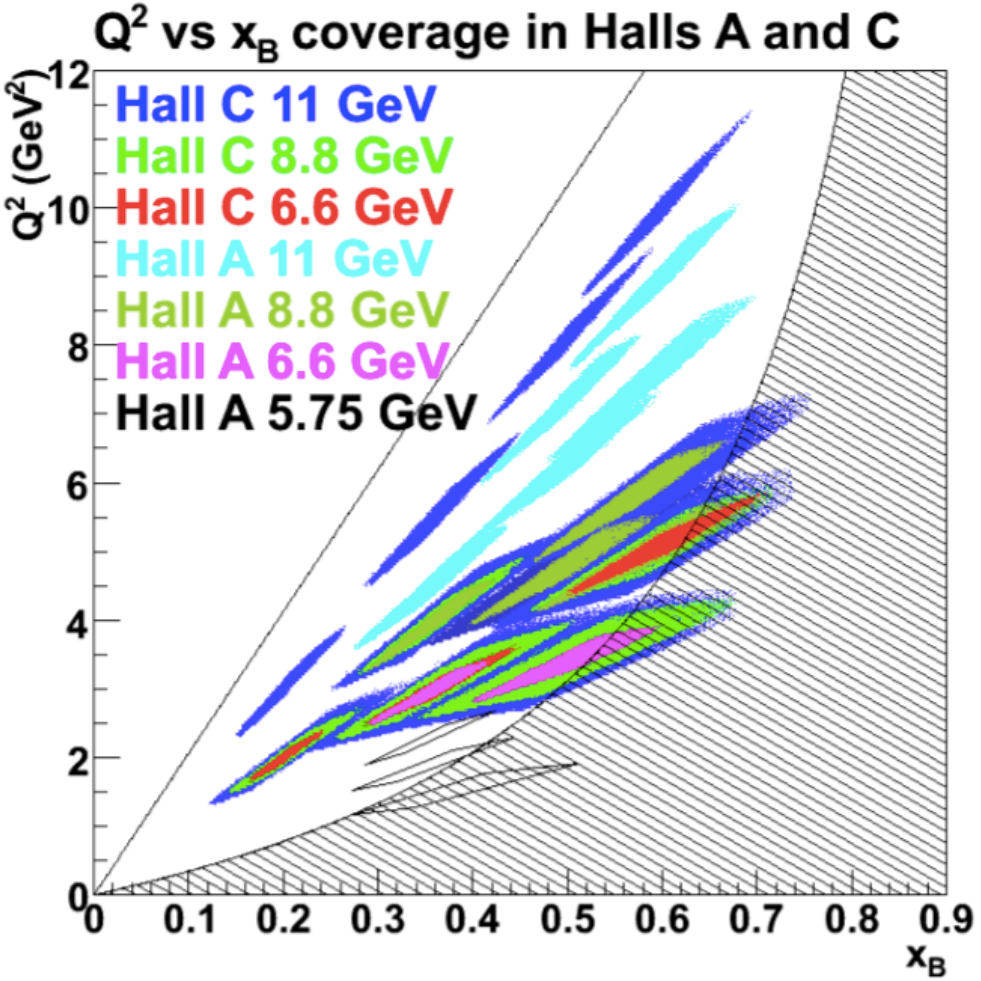

DVCS in Hall A: first experiment after upgrade. 50% of data taken!

✱ Azimuthal, energy and helicity dependencies of cross-section to separate $|T_{DVCS}|^2$ and interference contributions in a wide kinematic coverage.

✱ Separate *Re* and *Im* parts of the DVCS amplitude.

CLAS12

Design luminosity

$L \sim 10^{35}\ cm^{-2}\ s^{-1}$

High luminosity & large acceptance:
Concurrent measurement of exclusive, semi-inclusive, and inclusive processes

Acceptance for photons and electrons:
- $2.5^o < \theta < 125^o$

Acceptance for all charged particles:
- $5^o < \theta < 125^o$

Acceptance for neutrons:
- $5^o < \theta < 120^o$

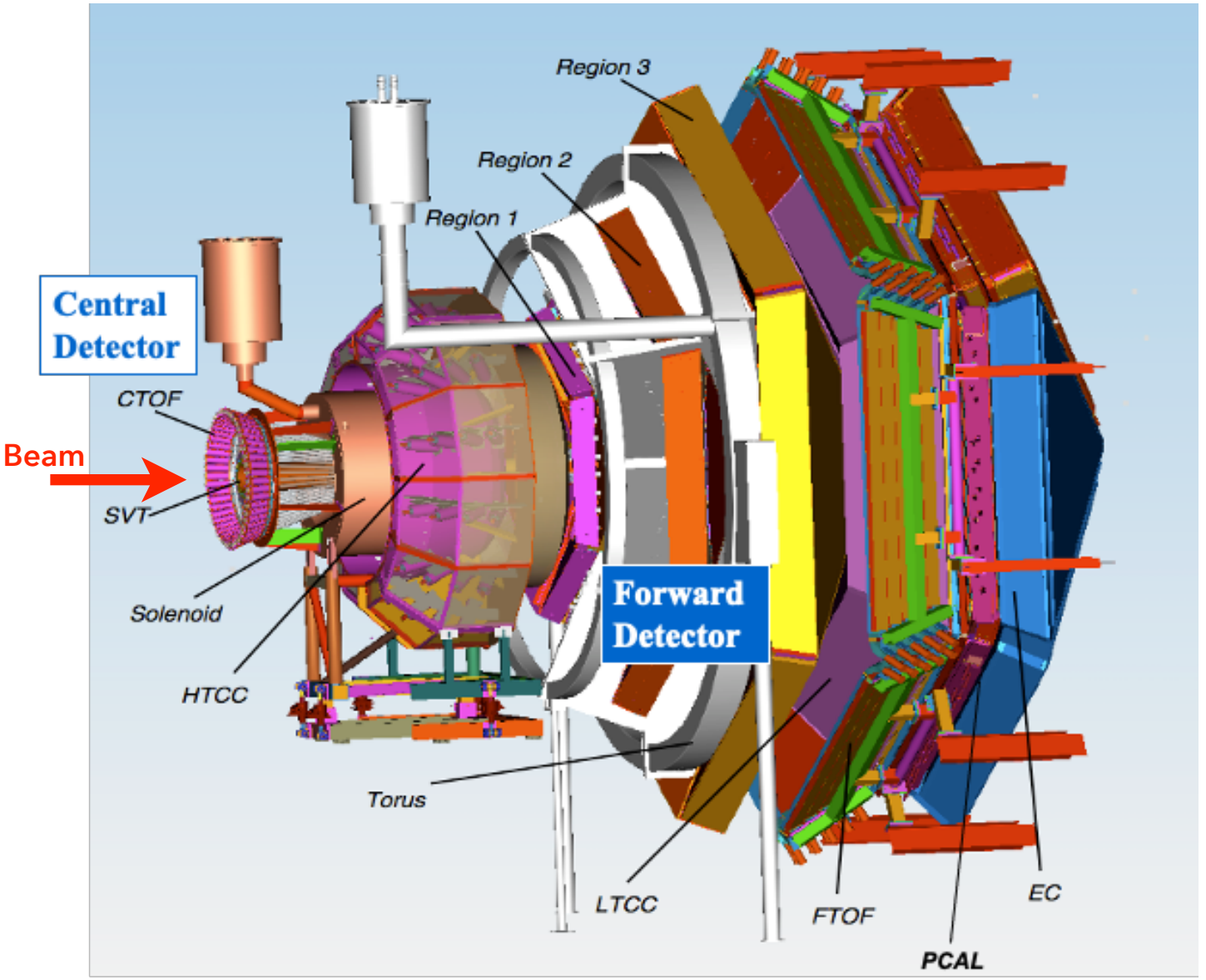

Data taking since 2018 with a max 10.6 GeV beam.

DVCS at lower energies with CLAS12

Experiment E12-16-010B

Unpolarised liquid H_2 target:

- Beam energies: 6.6, 8.8 GeV
- Simultaneous fit to beam-spin and total cross-sections.

* Rosenbluth separation of interference and $|T_{DVCS}|^2$ terms in the cross-section

* Scaling tests of the extracted CFFs

Compare with measurements from Halls A and C: cross-check model and systematic uncertainties.

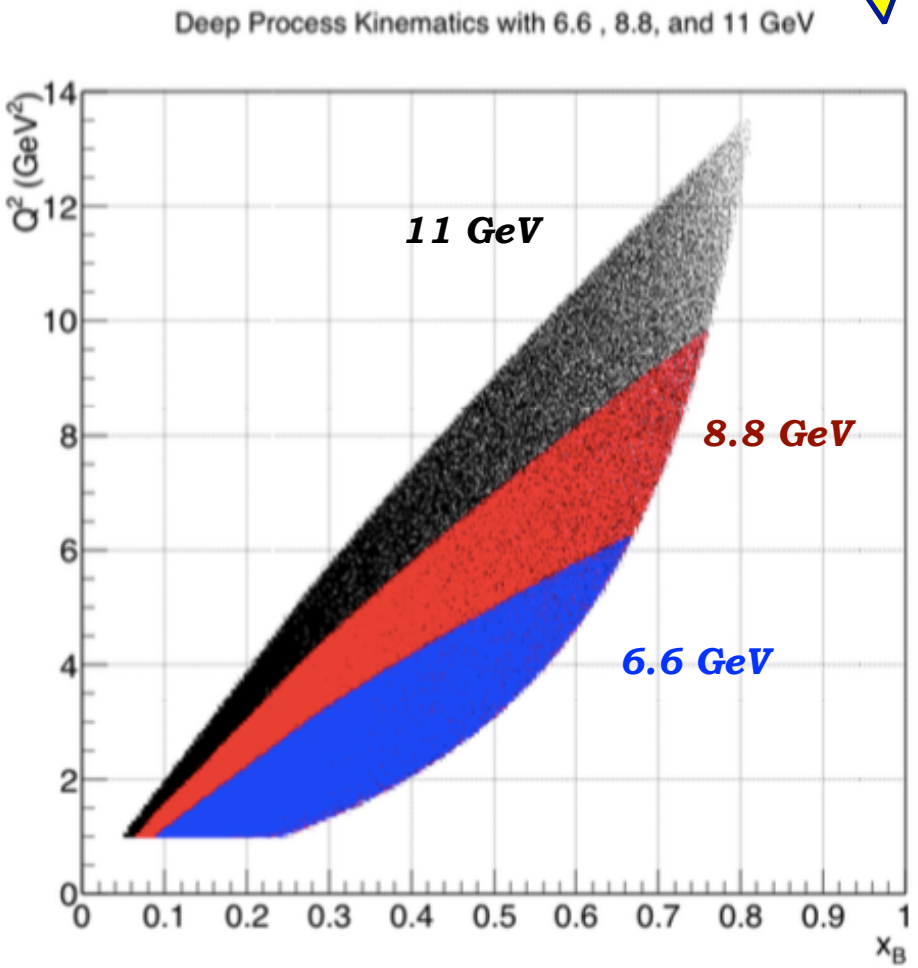

Data currently under analysis